QUANTITATIVE DIFFERENTIAL THERMAL ANALYSIS; AN EXPERIMENTAL ASSESSMENT

QUANTITATIVE DIFFERENTIAL THERMAL ANALYSIS; AN EXPERIMENTAL ASSESSMENT

by

VIWEK V. VAIDYA

A Thesis

Submitted to the School of Graduate Studies

in Partial Fulfilment of the Requirements

for the Degree

Master of Engineering

McMaster University

MASTER OF ENGINEERING
(Metallurgy)

McMASTER UNIVERSITY
Hamilton, Ontario

TITLE: Quantitative Differential Thermal Analysis; An Experimental Assessment

AUTHOR: Viwek V. Vaidya, B.Tech. (Indian Institute of Technology)

SUPERVISOR: Dr. P. S. Nicholson

NUMBER OF PAGES: 85, v

SCOPE AND CONTENTS:

The principle of quantitative differential thermal analysis is based on the fundamental principles of calorimetry. These principles cannot be rigorously applied while performing differential thermal analysis due to the complexities in the design, which lead to erroneous results.

A modified DTA apparatus was built to take into account some of the errors neglected in the present day apparatii. The heat transfer characteristics of the apparatus were found to limit in situ measurements of powder thermal conductivity. It was also demonstrated that the negligence of heat lost to the DTA block from the sample cell during an exothermic reaction and heat gained from the DTA block by the sample cell during endothermic reactions lead to large errors in quantitative estimations.

A modified apparatus was designed to take the aforementioned heat losses into account. The apparatus was calibrated with $CaCO_3$ endotherm and kaolinite exotherm and tested on the $SrCO_3$ rhombic $\rightleftharpoons$ trigonal inversion endotherm. The result was found to be in good agreement with accepted literature values.

ACKNOWLEDGMENTS

The author wishes to thank Dr. P. S. Nicholson for his invaluable help and guidance in conducting this work. The author also wishes to thank Dr. W-K. Lu and Dr. A. Hamielec for their help and stimulating discussions. Thanks are due to Mr. H. Neumayer and Mr. M. vanOosten for their advice and help during various stages of this work. Finally, acknowledgment is made to Miss Lydea de Jong for her expert and rapid typing of this thesis.

TABLE OF CONTENTS

CHAPTER I

INTRODUCTION AND LITERATURE SURVEY

I.1 Historical Development

The observation of the thermoelectric effect by Seebeck[1] in 1821 and its application to the measurement of high temperatures accurately by Becquerel[2] and Le Chatelier[3] in 1880, marked a major achievement in temperature measurement during the 19th century. At the same time the study of clay minerology was fast advancing but these minerals posed many identification problems. Their small particle size rendered normal mineralogical techniques of relatively little value. The possibility of application of thermal methods to such problems was suggested by Ramsay[4] and for the first time in 1887 Le Chatelier[5] produced heating curves for some clay minerals using thermocouples and automatic photographic recording instruments. The major advance came when Roberts-Austen[6] conceived the idea of measuring the temperature difference between a reacting sample and a thermally inert material so establishing the differential method.

In the U.S.S.R. the technique was developed by Kurnakov[7] and his pupils, particularly L.G. Berg[8]. The first quantitative application of differential thermal analysis seems to have been undertaken by Kracek[9] in 1929 and the next general upsurge of interest in this aspect followed the work of Norton[10] and of Berg et al[11]. In 1945, Speil[12] developed the first

theoretical treatment capable of explaining quantitative relationships between the measured and calculated variables associated with Differential Thermal Analysis (DTA). These efforts transformed the method from a purely empirical technique to one with a theoretical background and brought it to the attention of the chemists.

I.2 The Principle of Differential Thermal Analysis (DTA)

The present day differential thermal analysis technique is no different in principle from that suggested by Roberts-Austen[6] except for an increased sophistication of instrumentation. The method consists of heating a sample substance (S) and a thermally inert reference (R) at a given rate by an external furnace (F) as shown in Figure I.1. The sample and reference substances are placed symmetrically within the furnace by means of a suitably supported sample holder (H). The junctions of a differential thermocouple are embedded in or near the sample and inert substances symmetrically. The electromotive forces developed by these junctions are amplified and their differential displayed on a recorder. A linear heating rate is monitored by a suitable controller. In the absence of a heat effect the D.C. differential signal is ideally zero, thus producing a steady base line. Exothermic or endothermic changes that occur in the sample as the furnace temperature is raised at a linear rate are, therefore, recorded as deviations from the base line and appear as peaks on one side or the other of the base line. The positions of such deviations from the base line can be correlated with the temperature of onset of the enthalpic effect knowing the recorder chart speed

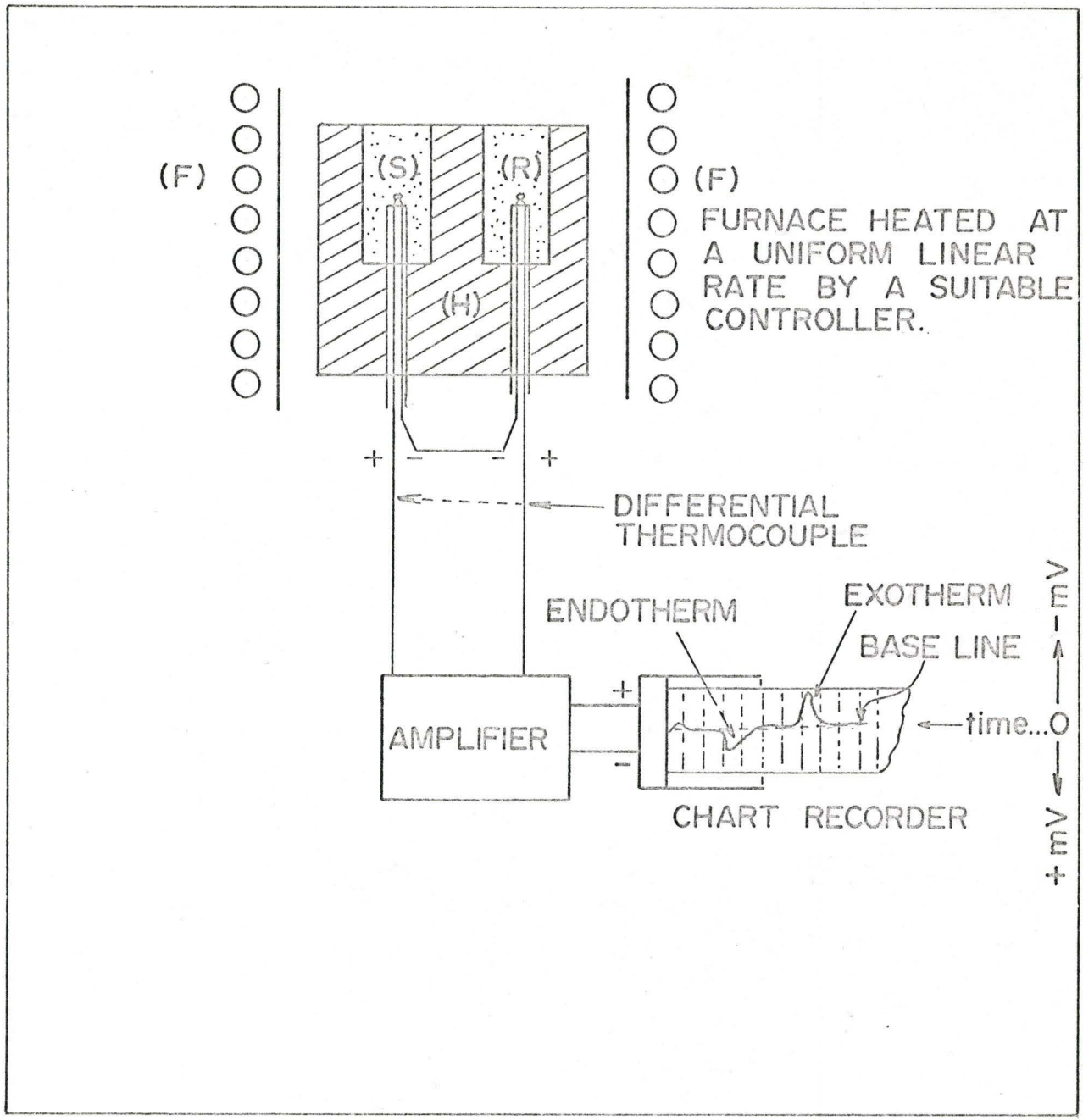

Figure I,1 The Principle of Differential Thermal Analysis

and the heating rate employed. The areas under the peaks are proportional to the enthalpic effects and this correlation forms the basis for quantitative DTA[12].

DTA is extensively used in qualitative investigations but quantitative applications have not been fully exploited owing to the errors introduced by the complexity of operating parameters. This facet of DTA will be reviewed later.

I.3 Merits, Limitations and Uses of DTA

The merit of a DTA curve is that all energy changes occurring in the sample during its heating or cooling are clearly observable. Because of this, each substance gives a characteristic DTA curve peculiar to itself. This forms the basis of DTA as a diagnostic method.

One of the limitations of the applicability of DTA to the diagnostic area is the dependence of the DTA curve or the thermogram on factors relating to equipment and experimental technique. This reliance is such that two DTA curves for the same material determined in different laboratories may differ markedly, thus rendering recognition difficult. Even with these difficulties, DTA can be effectively used in conjunction with other investigative methods such as chemical analysis, X-ray diffraction, infra-red absorption spectroscopy, electronoptical methods, thermogravimetry and evolved gas analysis. There is a large published collection of DTA curves for various minerals[13], a punched card index for minerals and inorganic and organic compounds[14,15], and a

library of standard reference curves for organic materials[16].

DTA can sometimes reveal minor structural changes, e.g., the clay mineral montmorillonite can give three different types of curves indicating differences in bonding energy of its structural $(OH)^{-1}$ groups[17], although all the samples give the same X-ray diffraction patterns. DTA can also detect very finely divided minerals which may not appear on an X-ray diffraction pattern.

A distinct advantage of the DTA method is the rapidity with which a curve can be determined. At a heating rate of $10^{o}C$/min a temperature range between $0^{o}C$ and $1200^{o}C$ can be spanned in two hours. Some industrial applications use heating rates of $50^{o}C$/min so making the method very flexible. The method can be used to check the identity of two samples, i.e., using the curve for "finger printing".

The technique finds wide application in polymer chemistry[18,19] to define the glass transition temperature, Tg[20], which is usually manifested by a drastic change in the base line, the degree of crystallinity[21], of cross-linking and temperatures of depolymerization[22]. Thompson[23] has used DTA to show the dependence of Tg on the molecular weight of the polymer. The application of DTA to polymerization studies has been far from extensive. The method appears to offer the investigator a convenient means of determining heats of polymerization[24], degree of curing and the effects of various catalysts on the polymerization reactions[25].

Glass is formed by melting selected ingredients, shaping and then cooling the melt under controlled conditions. Many complex reactions occur during the heating of such raw materials and DTA is useful in studying batch materials[26]. DTA has also been used to study the devitrification temperatures of glass ceramics. While the mixtures of such glass-producing

materials are heated slowly, the crystallization of glass produces a peak in the thermogram and the peak temperature is an important process parameter which ensures production of uniform texture of microscopic crystals[27].

Soldering fluxes sometimes contain ammonium halides. The selection of a given halide for a flux is made with reference to its temperature of decomposition and the flux melting point. When the two are close together, the liberated acid from the flux removes the tarnish with the minimum time lag for surface oxidation to occur between the release of the acid and the soldering operation. Hill et al[28] determined DTA curves for ammonium halides and these aid the choice of the appropriate halide for a given solder. The rates of reduction of sixteen metallic oxides by hydrogen and carbon monoxide[29] have been studied by DTA. Dichtl[30] has applied the technique to measure the amount of austenite in steels and Spencer et al[31] have used it as a quality control test of brake-lining materials.

Grim and Johns[32] used a full sized clay brick as a sample to determine the firing reactions, so permitting the planning of proper firing schedules[33]. Ramachandran and Majumdar[34] applied DTA to predict thermal efficiency of kilns. A glassy phase is usually detrimental to the use of refractories and Kantzer[35] applied the technique to determine the amount of glassy phase in refractories.

In recent years, DTA has been applied extensively to the study of phase diagrams. It has proved to be a valuable accessory tool, although admittedly, in most cases, equilibrium conditions do not pertain during typical analyses. Where thermal effects indicative of a transformation are very small, DTA can provide useful information. Some phase diagrams constructed from DTA investigations are Fe-Pd, Si-C, Ni-S, Pu-Cu, CeO_2-SrO, NaCl-VCl_2, $BaCl_2$-$BaTiO_3$,

$PuCl_3$-LiCl, V_2O_5-Li_2O, Na_3AlF_6-Li_3AlF_6-Al_2O_3 and phenanthrene-anthracene[36].

Cements are prepared by heating selected mixtures of materials to produce compounds which on hydration, provide desirable cementing properties. The technique is useful, therefore, not only for studying reactions that occur during heating to form the desired compounds, but also to learn more about the hydration mechanism and the conditions under which these hydrates decompose[37]. Midgley[38] applied quantitative DTA to set portland cement, so determining the amounts of tobermorite, ettringite and calcium hydroxide in cements aged for periods up to 28 days.

Following dilution with inert materials such as Al_2O_3, explosive materials can be conveniently studied by thermal analysis. Rivette et al[39] have used the technique to characterize new propulsion systems. Explosive materials when stored in bulk sometimes detonate violently due to the presence of small impurities and Keenan[40] has used DTA to examine such hazardous impurities.

Soils are formed by the decomposition of rocks and by the decay of plant and animal life, and the minerals in soil play an important role in its engineering characteristics. Eades and Grim[41] have found DTA to be very useful in identifying these minerals.

Cr_2O_3-ZnO catalysts gradually deactivate on progressive use and Bhattacharrya and Ramachandran[42] postulate that this deactivation is due to the stepwise formation of the spinel and this is observed by DTA. Locke and Rase[43] point out that the optimum conditions of pretreatment and the effects of contaminants in reactor feed on catalyst operation could be determined by a series of thermal analyses.

Since the heat transfer rates encountered in the carbonization of coals

can be closely duplicated in a DTA apparatus, the technique has been used to study the carbonization of coals. Stephens[44] has developed fluidized bed DTA to simulate the conditions more realistically. Warne[45] found that the technique was sensitive enough to determine quantitatively the minerals present in any coal of sub-bituminous or higher rank. King and Whitehead[46] have used DTA to correlate the rank of various coals.

In the field of radiation damage the technique has been applied to measure the life time of metamict minerals. Due to α-bombardment, a material is transformed into the disordered state. By heating this mineral in a DTA apparatus the exothermic effect associated with the mineral reversing to its natural state can be defined. The area under the peak thus obtained is proportional to the amount of disorder originally present, which in turn is a measure of the α-activity which induced it. In this fashion, the age of a rock can be estimated[47]. DTA has been applied to irradiation studies involving copolymerization of formaldehyde and styrene[48] and to radiation induced polymerization in the solid state by Hardy et al[49]. It has been suggested by Murphy and Hill[50] that quantitative applications of the technique in such studies could lead to the development of dosimeters applicable over a wide range of energy levels.

Krawetz[51] has used DTA to determine the relative stability of lubricants. Recent applications to pharmaceuticals[52,53] show DTA to be a valuable tool for purity evaluation, polymorphism and solvation of these complex organic materials. Mitchell et al[54] have applied the technique to experimental botany and Liptay et al[55] utilized the technique for examination of stones of urological origin.

A summary of pertinent industrial applications of DTA technique is shown in Table I.1.

TABLE I.1

To determine or evaluate \ DTA is vital in the study of	Ceramics	Cements	Chemicals	Elastomers	Explosives	Forensic Chemistry	Fuels	Glass	Inks	Metals	Minerals	Paints	Pharmaceuticals	Phosphors	Plastics	Propellants	Soaps	Soils	Textiles
Identification	x		x	x	x	x	x		x	x	x		x	x	x	x	x	x	x
Composition (Quantitative)	x	x	x	x	x	x			x	x	x	x	x	x	x	x	x	x	x
Phase Diagrams	x	x	x					x		x	x			x	x	x	x		
Solvent Retention			x	x	x	x			x			x	x	x	x	x	x		x
Hydration - Dehydration	x		x			x					x		x	x				x	x
Thermal Stability			x	x	x		x		x		x	x	x	x	x	x	x		x
Oxidative Stability			x	x	x		x		x	x		x	x	x	x	x	x		x
Polymerization				x			x		x			x			x				
Curing				x	x	x						x			x	x			
Purity			x			x							x				x		
Reactivity		x	x					x		x	x	x	x	x	x	x	x		
Catalytic Activity	x	x	x				x	x		x	x								
Glass Transitions				x	x										x	x			x
Radiation Effects	x	x				x	x	x		x	x	x		x	x	x			x
Thermochemical Constants	x	x	x	x	x	x	x	x	x	x	x	x	x	x	x	x	x	x	x

I.4 Quantitative DTA Theory

In Figure I.2, a cylindrical DTA block (A) is mounted coaxially in a cylindrical furnace tube (B). This block contains two cylindrical cavities, one for the sample (S) and the other for the reference material (R). Two identical thermocouples are mounted symmetrically within the cavities or wells and are connected differentially. The differential signal is amplified and fed into a recorder. The temperature of the furnace is raised linearly by a temperature monitor.

When the sample and the reference, contained in the geometrically and thermally symmetrical cells, are heated uniformly points a and b should be at the same temperature at a given instant, because heat arriving at these points is the same, assuming that the DTA block material has uniform thermal properties. The temperature of the sample and reference thermocouples is the same if heat arrives at these two points at the same rate and this is possible only if the thermal diffusivities of the reference and the sample material are the same. Furthermore, the temperatures of the two materials will rise at the same rate only if the sample and reference specific heats are identical.

Consider the heat balance of the sample and reference cells, when an endothermic peak, such as that shown in Figure I.3, occurs:-

At point p, the sample and the reference temperatures are increasing at the same rate, assuming that the rate of heating is uniform and linear, there is no reaction occurring in the sample and quasi-steady state conditions have been established. As the temperature increases, an endothermic reaction occurs (point a) in the sample. The sample absorbs heat and as a result

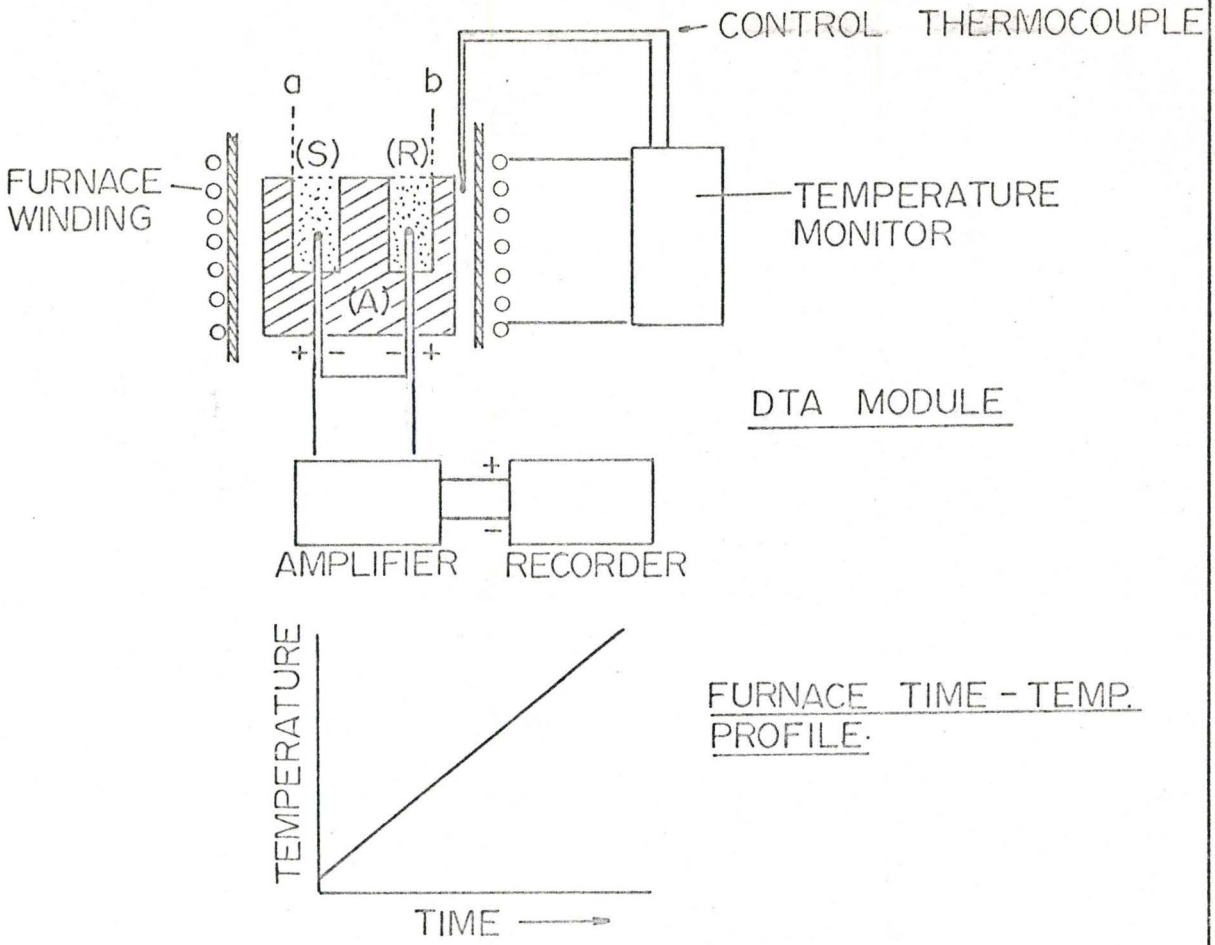

FIGURE 1.2 DTA SCHEMATIC

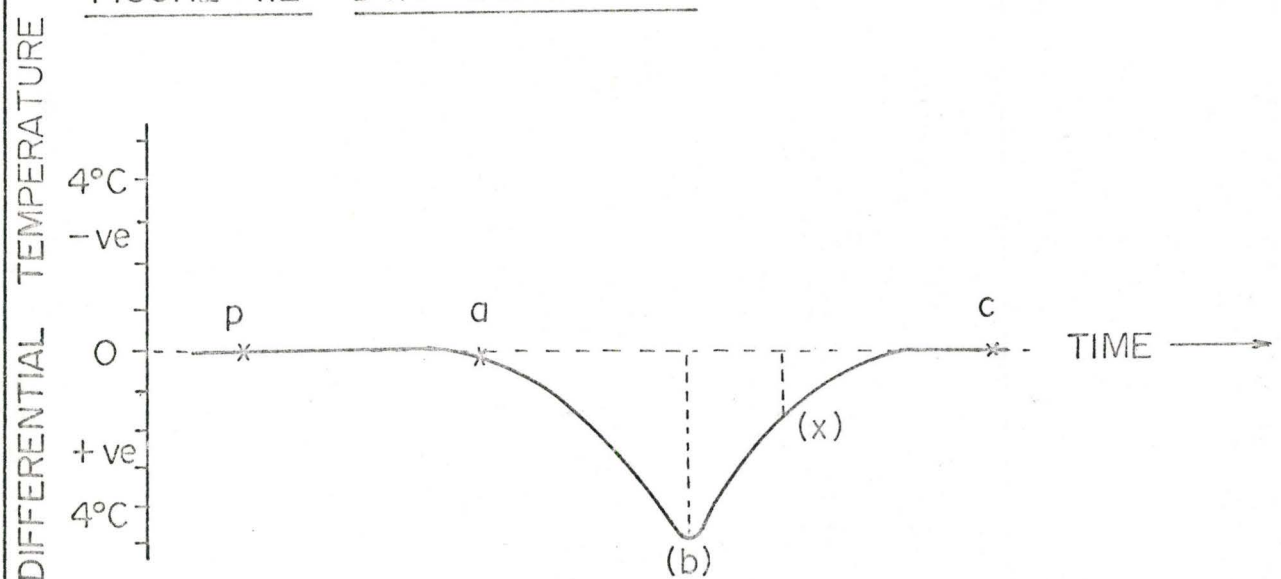

FIGURE 1.3 A THERMOGRAM

its temperature lags behind that of the reference. At point b, the rate at which the source is supplying the heat equals the rate of sample heat absorption. Point b, therefore, does not mark the end of the enthalpic effect but marks the point of equilibrium between the source and sink of heat. Along bc, the sample still absorbs heat but to a lesser and lesser degree. Thus, over the whole process, the sample has absorbed more heat than the reference, and this heat is equal to the total enthalpic effect. It is immediately evident that the area under such a peak should be related to the total enthalpic effect.

The above phenomenon can be expressed mathematically by comparing total heat contents of the sample and reference cells. The difference should give an analytical expression for the heat of the reaction. The simplest derivation was proposed by Speil[12] and is considered here. The more sophisticated derivations give essentially the same answer[56,57,58].

For any point between a and c in Figure I.3, (x), the heat balance for the sample and reference cell may be written as follows:

$$\underbrace{m \int_a^x \frac{dH}{dt} \cdot dt}_{\text{(sample reaction)}} + \underbrace{gK_s \int_a^x (T_W - T_S) \cdot dt}_{\text{(heat content increase for sample due to temperature)}} = \underbrace{m_s c_s (T_s - T_o)}_{\text{(total increase in heat content of the sample)}} \qquad (1)$$

A B C

and for the reference cell:

$$\underbrace{gK_r \int_a^x (T_w - T_r) \cdot dt}_{B'} = \underbrace{m_r c_r (T_r - T_o)}_{C'} \qquad (2)$$

(heat content increase for reference due to temperature)

(total increase in heat content of the reference)

where t = time

m = mass of reactive component in the sample

m_s = total mass of sample

m_r = total mass of reference material

dH = the decrement of heat absorbed from the sample by the endothermic reaction in time interval dt

g = geometrical shape factor, experimentally made equal for sample and inert cavities through symmetric geometry of the cavities in the block

K_s = effective thermal conductivity of the sample

K_r = effective thermal conductivity of the reference

T_w = temperature of DTA block at $t = x$

T_s = temperature at centre of sample at $t = x$

T_r = temperature of center of reference or sample at $t = a$

C_s = mean specific heat of sample between $t = a$ and $t = x$

C_r = mean specific heat of reference material between $t = a$ and $t = x$

These heat balance equations neglect the mode of variation of T_r, thus imposing the condition that $C_r - C_s$ is negligible relative to C_s[7].

The factor A in equation (1) defines the quantity of heat added to or subtracted from the sample due to the reaction. Factor B defines the

quantity of heat absorbed by the sample. (Speil assumes that there is no effective temperature gradient between the outside of the sample and outside of the reference material or around the perimeter of the sample walls since the heat flow in a metallic holder is much more rapid as compared to the sample or reference materials if they are ceramic powders). A + B = C because at any time x, along the DTA curve (Figure I.3), the amount of heat utilized to raise the temperature of the sample must equal that flowing from the sample block plus the amount added or subtracted by the reaction.

For the reference material, factor A does not exist, hence B' in equation (2) must equal the heat to raise the temperature of the reference material C'.

Assuming:

$$C_r = C_s + \delta C \tag{3}$$

$$K_r = K_s + \delta K \tag{4}$$

and, experimentally within the error of measurement,

$$m_r = m_s \tag{5}$$

then subtracting equation (2) from (1), rearranging and using relations (3), (4) and (5) gives:

$$m \int_a^x \frac{dH}{dt} \cdot dt - gK_s \int_a^x (T_r - T_s) \cdot dt - g\delta K \int_a^x (T_w - T_r) \cdot dt \tag{6}$$

$$= m_s \left[C_s (T_s - T_r) - \delta C (T_r - T_o)\right] .$$

Let $T_r - T_s = y$, the temperature indicated by the differential thermocouple and equation (6) be simplified by assuming that the terms containing $(T_w - T_r)$ and either δC and δk are small in comparison with other terms then using a and c as the integration limits:

$$m \int_a^c \frac{dH}{dt} \cdot dt - gK_s \int_a^c y.dt = m_s C_s (T_s - T_r) \tag{7}$$

In most cases:

$$(T_s - T_r) = 0 \text{ at } c \tag{8}$$

As, to a close approximation, the total heat of reaction is given by:

$$m \int_a^c \frac{dH}{dt} \cdot dt = m \Delta H \tag{9}$$

and

$$\therefore \quad \Delta H = \frac{gK_s}{m} \int_a^c y.dt \tag{10}$$

Thus peak area =

$$\frac{m \Delta H}{g K_s} \tag{11}$$

If β is the uniform heating rate, then,

$$t = T/\beta = T_r/\beta \tag{12}$$

$$dt = dT_r/\beta \tag{13}$$

substituting (12) in (10) and rearranging:

$$\int_a^c y \, dT_r = \frac{m \, \Delta H}{g \, K_s} \cdot \beta \qquad (14)$$

Thus the area under the differential temperature peak is directly proportional to the mass of the active component, the heating rate and inversely proportional to the thermal conductivity of the sample for a given heat-transfer configuration, i.e., a given furnace, DTA block, thermocouple assembly and method of loading the DTA cells. It is self-evident, that changing the furnace, DTA block or any other factors mentioned above would change the geometric factor, which is determined by the heat-transfer characteristics of the DTA block and furnace assembly heating rate.

A similar expression has been derived by Boersma[57], i.e.,

$$\int_{t_1}^{t_2} y \cdot dt = \frac{m \, \Delta H}{G} \qquad (15)$$

where:

$y = T_r - T_s$

m = mass of sample

ΔH = heat of reaction

G = heat transfer coefficient

t_1 to t_2 = time interval of reaction.

L. G. Berg et al[11] also derived a similar relationship:

$$S = K \, \Delta H \qquad (16)$$

where: S = peak area

ΔH = the heat absorbed or liberated by the sample

K = coefficient of proportionality.

Berg notes[59]:

> "Owing to the extremely high number of factors determining the value of the coefficient K, it is practically impossible -- at least at present -- to give a full mathematical interpretation of K."

Sewell and Honeybourne[58] have studied the theory of quantitative DTA and obtained a mathematical expression for the peak area, i.e.:

$$\text{Peak area} = [\omega_o \, a^2 \, \rho_s] \, \frac{\Delta H}{K_s} \qquad (17)$$

where $(\omega_o \, a^2)$ is a factor determined by the shape of the test sample, ρ_s the sample bulk density determined by the method of packing, and K_s the sample heat transfer coefficient.

It should be noted, however, that in deriving these formulae all authors assume the reference material and the sample to have identical thermal conductivities, specific heats and bulk densities. Furthermore, no account is taken of the variation of the heat of reaction and the change of heat transfer coefficients with temperature.

The factors that influence equation (11) are heating rate, choice of DTA block material, type of thermocouple wires, thermal conductivity of the sample and the relative amount of heat actually sensed by the sample thermocouple during various reactions. These parameters will now be considered

individually in more detail.

I.4(a) The Heating Rate

The heating rate affects peak height, peak width and, for decomposition reactions, the peak temperatures[12,60,8,61,62]. The general effects of slow and fast heating rates are listed in Table I.2.

Slow heating rates require more sensitive recording systems to obtain comparative accuracy, whereas with fast heating rates a lower sensitivity can be used but neighbouring peaks tend to coalesce. For calorimetric and thermodynamic studies slow heating rates are desirable, since conditions more nearly approach equilibrium.

I.4(b) The Thermal Conductivity

The derivation of the peak area relationship (11) assumes that over the entire temperature range the thermal conductivities, masses and specific heats of the reference and the sample remain constant. These assumptions however, are far from reality. In a decomposition reaction such as dehydration, where one of the reaction products is gaseous and therefore lost during the reaction, the bulk density of the sample may change during the reaction. This introduces a drift in the base line due to the changing thermal diffusivity of the sample. Generally the specific heat remains constant throughout the reaction[63] unless the sample undergoes a second order

TABLE I.2

EFFECTS OF SLOW AND FAST HEATING RATES

Heating Rate	Effect
Slow	Little base line drift. Near equilibrium conditions. Broad shallow peaks on $\Delta T/t$ curves. Sharp small peaks on $\Delta T/T$ curves. Long time per determination.
Fast	Base line drift may be appreciable. Conditions far from equilibrium. Large narrow peaks on $\Delta T/t$ curves. Large broad peaks on $\Delta T/T$ curves. Short time per determination

transformation.

It is well known that thermal conductivities of solids decrease with temperature. Heat transfer through a particulate medium, however, is highly complex. In most applications the sample and reference materials are in the powdered form and heat is therefore not only transferred by conduction through particle point contacts but also by gaseous conduction and radiation across the pores. Above moderate temperatures, radiation plays a predominant role in the heat transfer. As a result, the overall heat transfer coefficient increases with temperature for particulate media[64]. Thus, the evolution of a gas, during a reaction, can change the heat transfer coefficient of the sample. Furthermore, sintering and consequent shrinkage at higher temperatures produces an air gap between the sample and the container walls which completely upsets the heat transfer conditions.

Often, in quantitative analysis, dilution techniques are employed to circumvent these difficulties. Normally the samples are diluted up to 70% by the reference material. This, however, only reduces the disparity of properties between the reference and the sample, but the actual values of the overall sample thermal conductivity remain unknown. The total heat effect is also considerably reduced with the consequent loss of accuracy.

Most attempts at quantitative analysis stem from calibration procedures, and absolute methods have not yet been perfected. In a calibration method a DTA is made of a sample with a known enthalpic effect. Then under the same experimental conditions, a DTA is performed on the unknown sample. The heat of reaction of the unknown sample is then calculated from a proportionality equation such as:

$$\Delta H_{unknown} = (\Delta H_{known}) \times \left(\frac{\text{area under the peak for unknown}}{\text{area under the peak for known}} \right) \qquad (18)$$

Using the relationship (18) involves the difficulty of preparing samples of the same thermal conductivity from different materials.

Vold[65] has suggested a method to eliminate the thermal conductivity, K_s, from the relationship between peak area and heat of reaction. The temperature distribution in a DTA type of an assembly is given by[66]

$$T(P,t) = \beta t - f(P) - \sum_{m=1}^{\infty} f_m(P) \exp(-B_m t) \qquad (19)$$

in which $f(P)$ and $f_m(P)$ are functions of position (P) only, and the coefficients B_m are independent of P and time (t). β is the heating rate.

In the transient terms of the solution of a heat problem, B_1 is usually much smaller than other coefficients, so that the slope of the curve of $\ln(\Delta T - \Delta T_o)$ against t is practically equal to B_1.[58]. B_1 is proportional to $K_S/a^2 C_S P_S$[66] where a is determined by the shape of the test sample. Thus the product B_1 times the peak area (equation 17) is proportional to $\Delta H/C_S$ and if B_1 and C_S can be estimated, the heat of reaction can be found out from the peak area without the knowledge of sample thermal conductivity.

However, Vold's method depends on the practicability of measuring B_1. For phase transitions, the reaction is sensibly completed when the temperature difference is greatest, so that all the return curves may be used for evaluation of B_1. As pointed out earlier, all reactions do not reach com-

pletion at the peak temperatures. Murray and White[67] for instance, have shown that dehydroxylation reactions in clay minerals continue almost until the peak approaches the base line; consequently, there appears to be considerable danger of using the wrong part of the curve to estimate the B_1 value. The use of this method is limited to certain classes of reactions, and wrong interpretation can result in gross errors.

The other approach to this problem would be to measure the thermal conductivity of the DTA sample and apply a correction factor to relation (18). Berg et al[63] and Yagfarov[68] suggest a method of measuring the effective thermal conductivity "by placing thermosensing elements behind the sample". Yagfarov uses an apparatus shown in Figure I.4, and suggests that the effective thermal conductivity may be calculated by the formula:

$$k = C_{p_1} \times \gamma_1 \times \frac{v}{\Delta t_2 - \Delta t_1 \times K_2} \times K_3 \qquad (20)$$

where: k = effective thermal conductivity

C_{p_1} = the heat capacity of the standard

γ_1 = the density of the standard

v = the heating rate

K_2, K_3 = constants determined by block dimensions

Δt_1 = temperature differential measured by the differential thermocouple with the junctions at 1-1 and 1-2

Δt_2 = temperature differential measured by the differential thermocouple with the beads at 2-1 and 2-2

There is, however, no experimental data to supplement the above relationship (20).

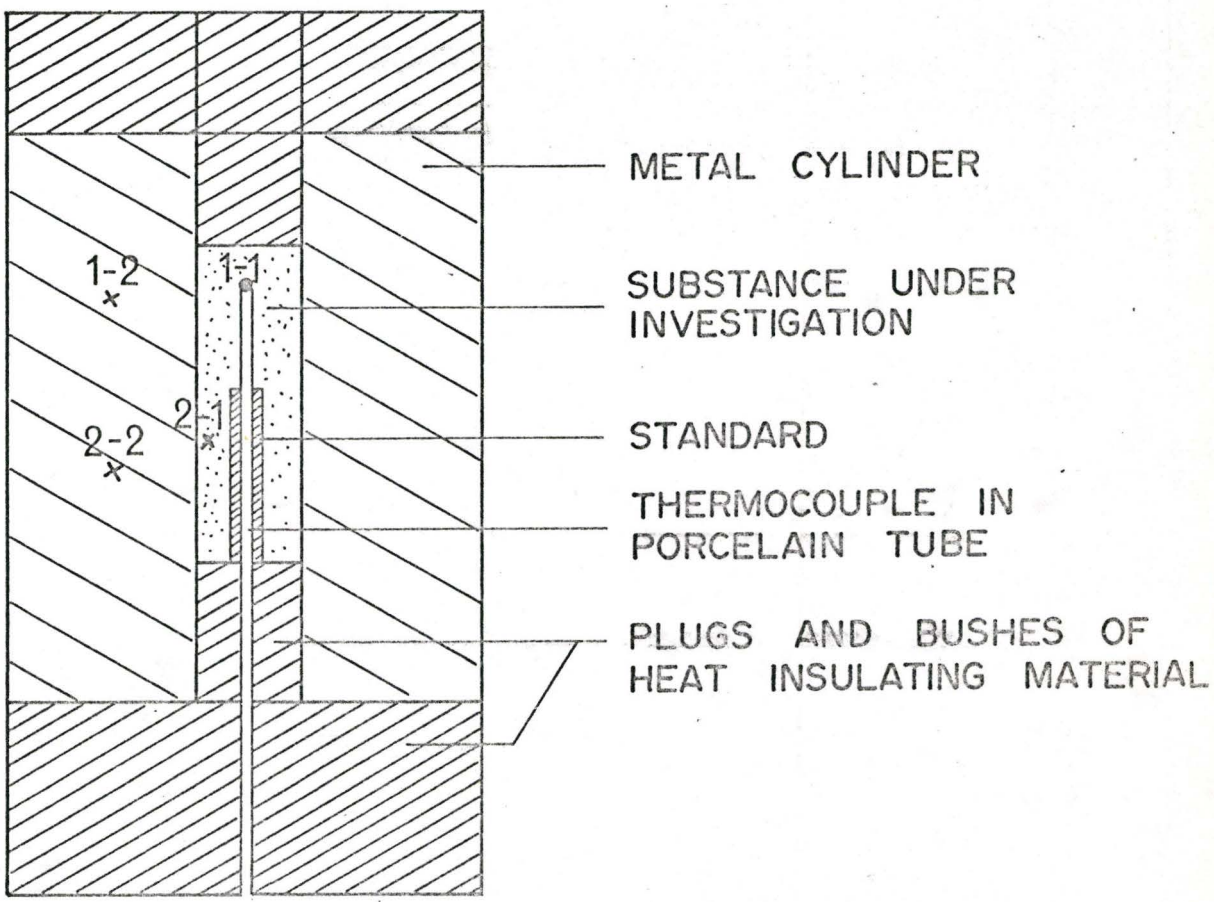

Figure I.4 Apparatus Used by Yagfarov

I.4(c) The Geometric Factor

The geometric factor which appears in equation (11) accounts for temperature gradient distribution in the sample. The heat transfer conditions of the system can change by changing the block material or the geometry of the sample and reference cells and the positioning of the thermocouples in the cells.

The effect of holder design on the shape and size of DTA peaks has been studied. Wilburn et al[69], using electrical analogues, have considered the cumulative effect of heat leakage between the sample and reference cells, and the diffusivity of the block on the shape of the DTA peak. They have shown that the heat leakage between the sample and reference materials should be kept to a minimum whilst the heat transfer to the sample and reference should be maximised. These last two requirements are conflicting as a high diffusivity block, which is necessary for rapid heat transfer to the sample and reference, will allow heat transfer to take place fairly easily between the sample and the reference. They have also shown that the DTA peak can off-shoot the base line if the block diffusivity is very low.

deJong[70], following the dehydration reaction of $CuSO_4.5H_2O$, studied the effect of sample and reference cell dimensions on the peak areas for the two endotherms which correspond to the loss of four molecules of water. His results are shown in Figure I.5 and the influence of sample geometry on the peak areas is evident.

A part of the heat generated in the sample cell is carried away by the sensing thermocouple wires. Boersma[57] mathematically calculated the approximate amount of heat that could be lost through the thermocouple wires and he suggests that heat leakage through the thermocouple leads reduces the peak area to less than 50%. A difference of 15 to 30% in the peak area

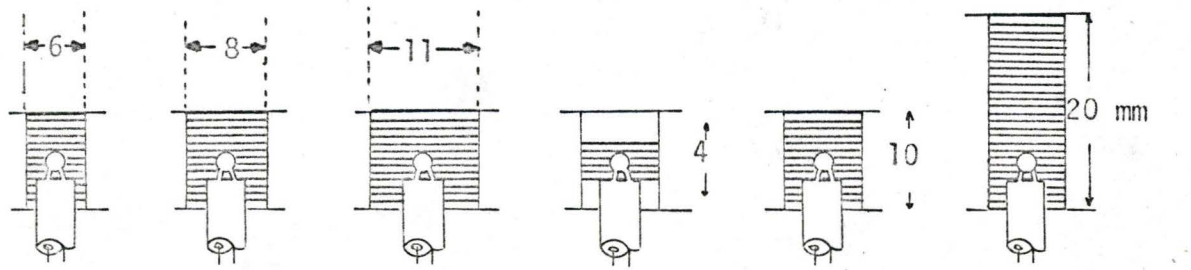

Peak area	314	496	930	338	496	550	
at 150°C	300	510	910	290	510	540	deg sec

Figure I.5 The Effect of Sample and Reference Cell Shape on the Peak Area.

measurement was observed between two Pt/Pt-Rh thermocouples by de Jong[70]. This error could possibly be overcome by the incorporation of guard heaters around the lower section of the existing thermocouple wires.

The effect of change in position of the thermocouple in the sample cell on the peak area has been considered by Sewell[58] and Berg[8]. In a ceramic block, ± 25% displacement of the thermocouple bead in the vertical plane can cause an error of ± 8% in the peak area, and 66% displacement from the centre of a cylindrical cell in the horizontal case can cause about 18% uncertainty in the peak area. Thus for quantitative analysis, the thermocouples must be rigidly fixed and in the same position as in the calibration runs.

I.4(d) Heat Losses (ΔT)

Kronig and Snoodijk[71] describe in detail how the heat dissipates out of a sample, using the theory of heat conduction. From this, they determine the differential temperature rise originating in the centre of the sample and brought about by the heat produced in various small zones within the sample. These individual contributions differ, depending on the place where they originate[57]. By dissipation, the differential temperature will decrease in the course of time and tend towards zero, giving an area in the temperature-time graph which contributes to the total peak area. The calibration technique thus assumes that the sample thermocouple senses the same percentage of heat evolved from the samples of known and unknown enthalpic effects. The technique does not take into account the possible loss of heat to the block during an exothermic reaction, or the gain of heat from the block during

an endothermic reaction in the sample.

The sensing thermocouple bead in the sample registers the flow of heat either to it or away from it. This is true whether the differential thermocouple bead is located inside the sample or on its perifery[72]. The hottest part of the sample will be its outer perifery and consequently the initial reaction will start at this surface. Considering the heat flow associated with the initial reaction, with the aid of Figure I.6, it can be seen that a temperature peak will be produced on the system temperature profile. This peak will either be positive or negative depending on whether the reaction is exo- or endothermic.

Considering the exotherm first, heat will flow towards the differential couple located in the sample and into the sample block. The outflowing heat (supplied to the DTA block) is not sensed by the differential thermocouple and therefore does not appear on the ΔT vs. time peak. With an endotherm, the flow of heat is reversed and now it flows from the sensing couple environment and the block. The heat supplied to the reaction by the DTA block is not sensed by the differential couple and therefore does not appear on the ΔT vs. time trace. Hence in both cases the ΔT vs. time peak does not indicate the entire heat effect involved in the reaction. Furthermore, depending upon the intensity of heat effect the amount of heat lost to or gained from the DTA block would differ due to the complicating factor of unknown thermal conductivities of the samples.

The error introduced by the above factor in quantitative analysis, has never been considered before. In the present work, a modified DTA design is proposed to take the above into account. The possibility of measuring sample thermal conductivity in situ, as proposed by some workers, is also

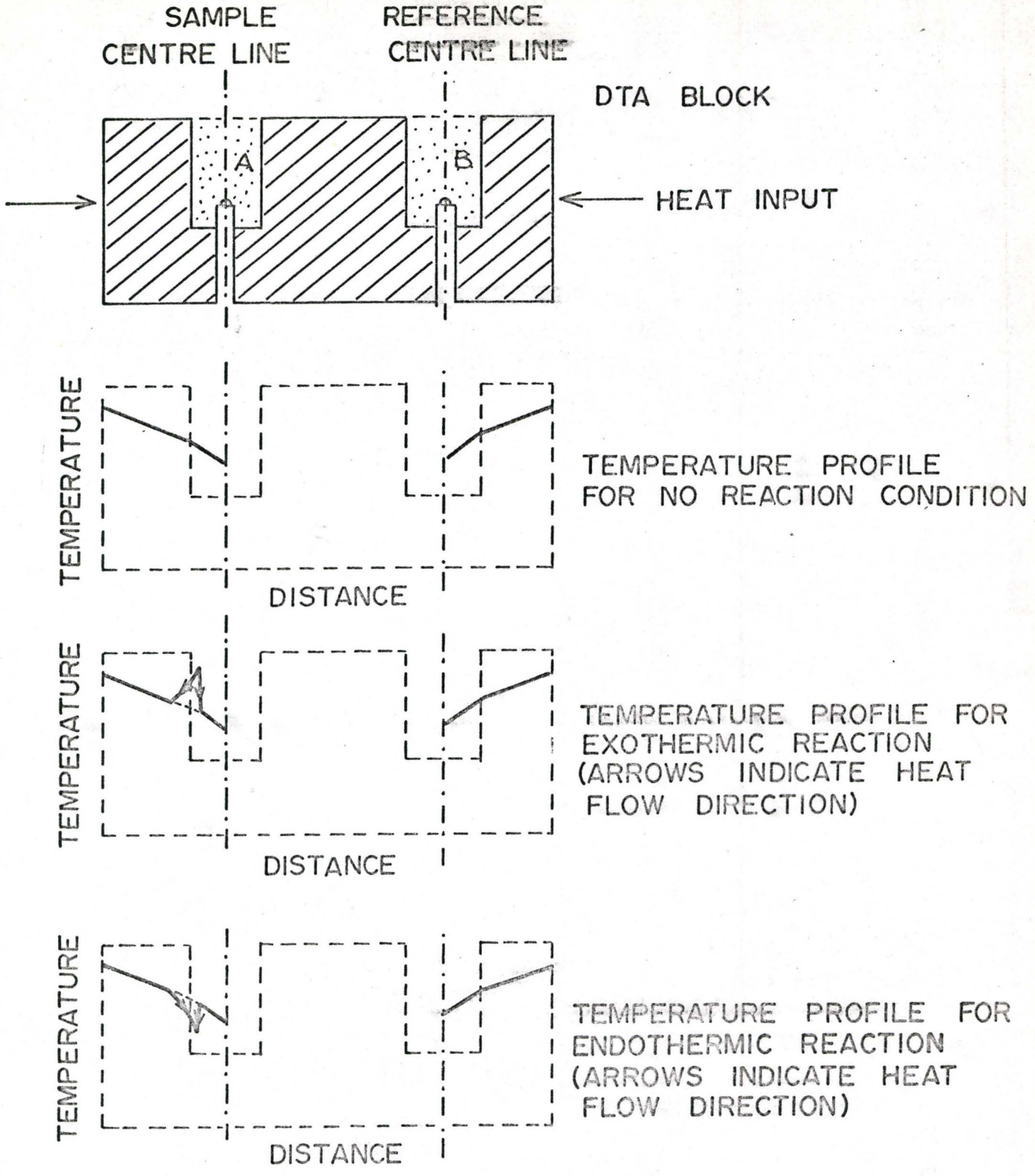

Figure I.6 Temperature Profiles Associated with Initial Sample Reaction.
(A - sample cell, B - reference cell)

investigated and the Herold-Planje[72] type of apparatus for quantitative measurements, suggested by Sewell and Honeybourne[58] is studied. Herold and Planje described an apparatus designed to generate differential temperature information based on the cell walls alone. Sewell et al suggest that such a design could give accurate quantitative data as the thermal conductivity of the reacting sample can be ignored.

The overall errors in quantitative DTA can be large as shown in Table I.3. The scope of use for a reliable absolute quantitative DTA technique is evident and it was to indicate possible modifications in present designs that the following investigations were undertaken.

TABLE I.3

TRANSFORMATION TEMPERATURE RANGES AND HEATS OF REACTIONS FOR SELECTED MINERALS AS DETERMINED BY DTA

Mineral	Temperature ^{o}C	Heat of Reaction cals/gm	%Error about the mean value cals/gm
Kaolinite	500-650	90-140	±21%
	925-1030	-(20-40)*	±33%
Halloysite	500-650	80-130	±28.3%
	970-1030	-(25-35)	±16.7%
Montmorillonite	125-260	0-40	±100%
	625-750	23-60	±80.5%
	800-925	10-20	±33%
	900-980	-(10-35)	±55.5%
Quartz	575-600	2-4	±33%
Talc	880-1050	50-80	±23.1%
Muscovite	800-950	10-25	±75%
Brucite	390-550	150-220	±18.8%
Gamma Fe_2O_3	700-800	-(22-28)	±12%

* Negative heat of reaction indicates exothermic transformations.

CHAPTER II

EQUIPMENT AND EXPERIMENTAL TECHNIQUE

II.1 Electronic Components

The apparatus consisted of various components as shown in Figures II.1 and II.2. The furnace (Figure II.1 - #14) and the DTA unit (# 8) were designed and built by the author. The differential signals from the thermocouple junction (# 8) were amplified by two D.C. amplifiers (# 1) capable of measuring D.C. signals in the 1000 V to 10 μV range. In most of the experimental runs the 300 μV scale was used. The amplified signals were fed into a two-pen recorder (# 6) with adjustable chart speed and range features. In all the DTA experiments a chart speed of 1" per 10 minutes was employed. In all the experiments the amplifiers measuring on the 300 μV scale were coupled with the recorder on the 100 mV scale, such that 100% of the microvoltmeter produced a pen deflection of 100% on the recorder chart scale.

The Thermac power and temperature controller (# 3) coupled with a Datatrak programmer (# 2) served as the temperature monitoring system. The controller (# 3) could be operated in manual, set-point or programme modes. The programmer (# 2) consisted of a rotating drum on which a conducting chart could be mounted. The drum was rotated by a time-base motor such that a rotation could be completed in 24 hours. A profile was inscribed on the drum chart, such that a non-contacting, movable sensing probe could electrostatically locate the line drawn on the chart. 100% of the chart scale corresponded to

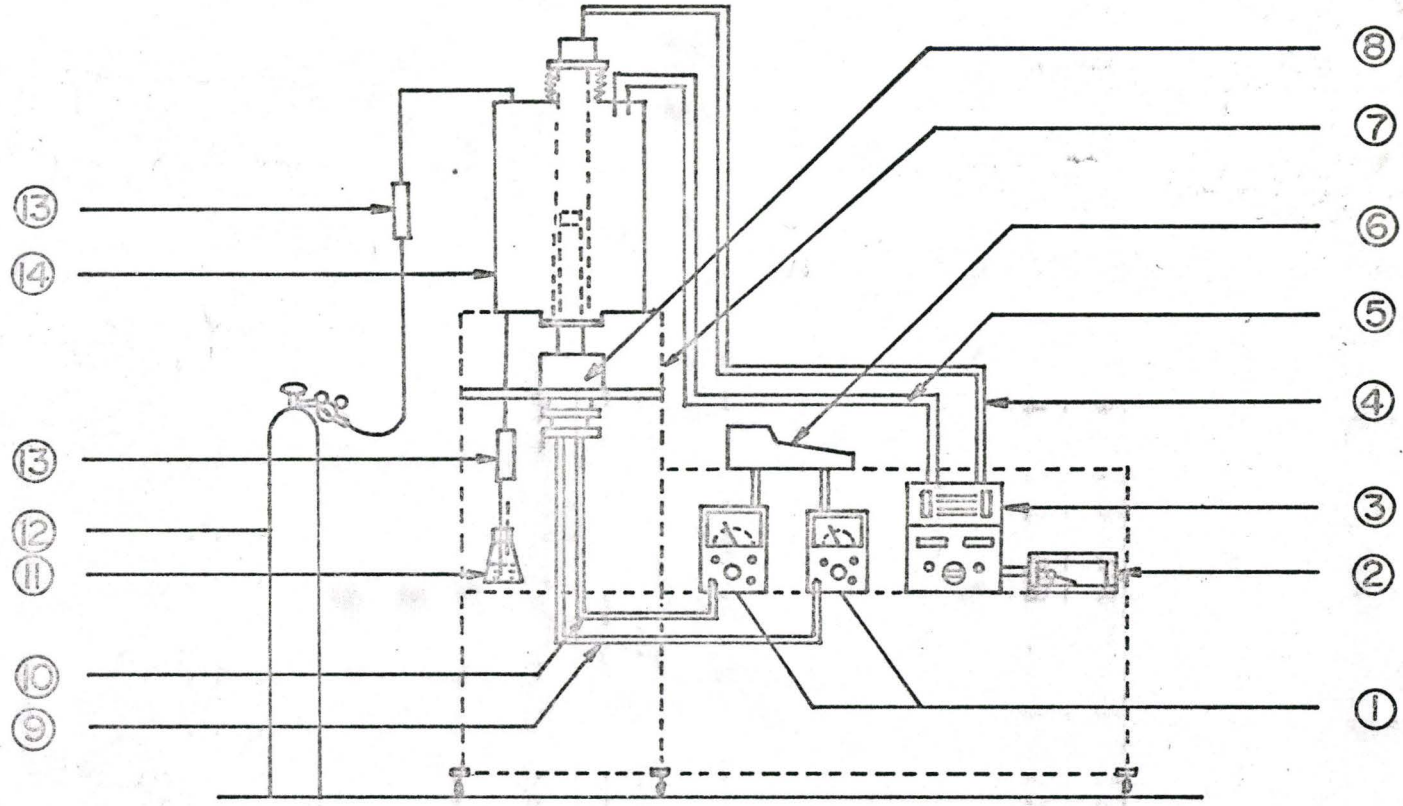

Figure II·1

Schematic Diagram of the Experimental Apparatus

Legend for Figure II.1

1. Keithley model 153 microvolt-ammeter.

2. R-1 control's Data-trak Model 5500 - line following programmer.

3. R-1 control's Thermac series 6000 temperature-power controller Model 625.

4. Control Pt/Pt-13% Rh control thermocouple extension leads.

5. Molybdenum furnace power leads.

6. Sargent 2 pen recorder Model DSRG S-72180-80.

7. Support trolley.

8. DTA unit.

9. Wall differential thermocouple leads.

10. Base differential thermocouple leads.

11. Gas bubbler.

12. 95/5:N_2/H_2 gas bottle.

13. Drierite container.

14. Molybdenum furnace.

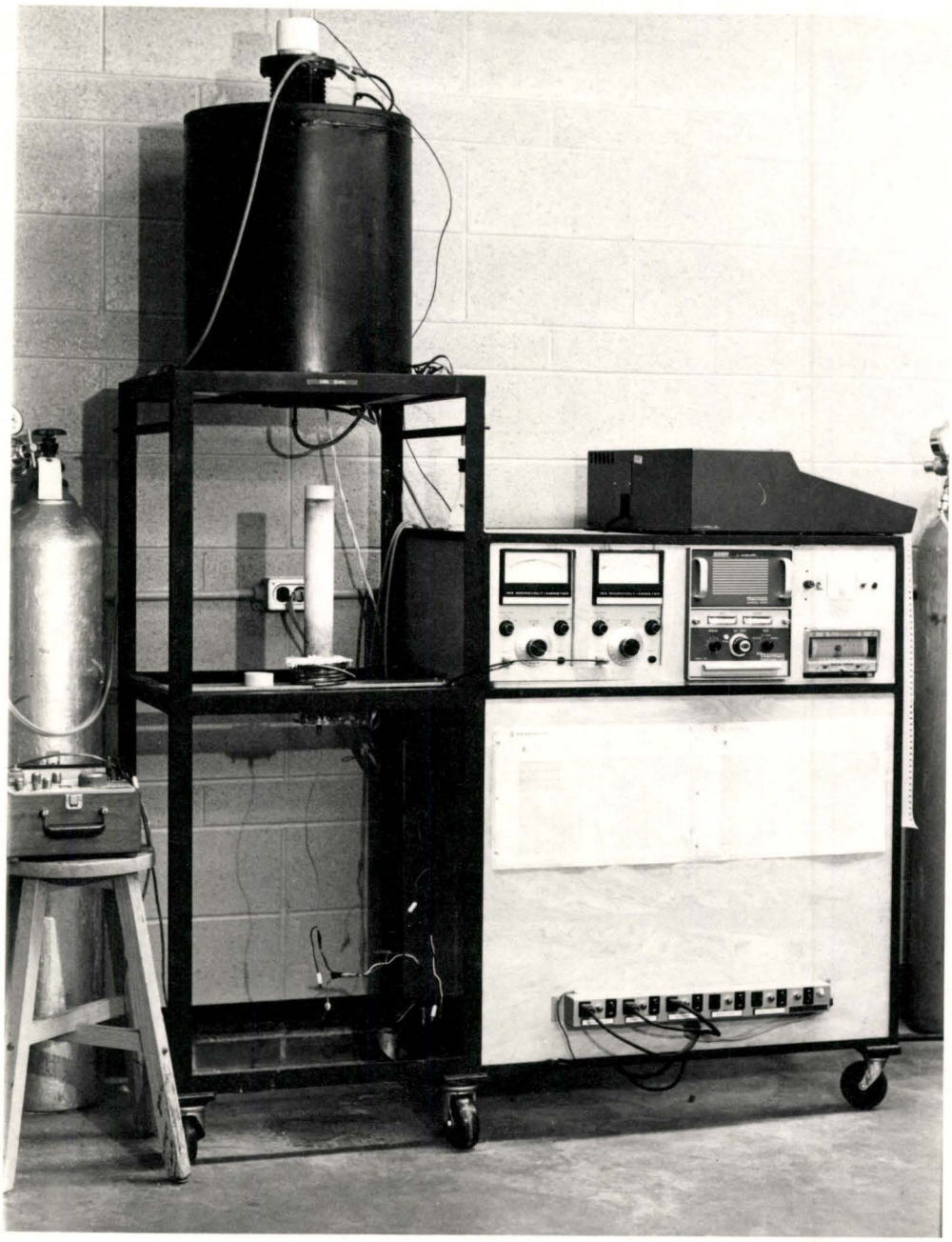

Figure II.2 The Experimental Apparatus

100% of the set point scale on the controller which in turn corresponded to 1700°C. A linear program was inscribed on the chart which heated the furnace up to 1260°C in 12 hours and cooled it to room temperature in the same time.

II.2 The Furnace

Figure II.3 shows the molybdenum furnace used in the experiments. Each winding required approximately 80 ft. of the 0.050" diameter wire. Along the length of the tube, an 11" winding was placed 5" from one end and 12" from the other, corresponding to the lower and the upper ends of the furnace. To help widen the constant temperature zone in the furnace, the winding was wound differentially. The first and the last 2½" of the 11" winding space, along the length of the furnace tube was wound with 10 turns per inch and the remaining 6" with 8 turns per inch.

The winding was covered with moist Alundum cement and allowed to dry for one day. The tube was installed in the furnace with its lower end in the lower 'O' ring seal. The space (# 12) around the winding was filled with Norton alumina bubbled grain. The twisted ends of the winding were the top plate (# 8) lowered into position. A protective N_2/H_2 (95%/5%) gas mixture was passed and its flow regulated by a two stage gas regulator. It was necessary to put a drierite tube (Figure II.1 - # 13) between the furnace gas outlet and the bubbler to act as a water trap as insufficient delivery pressure

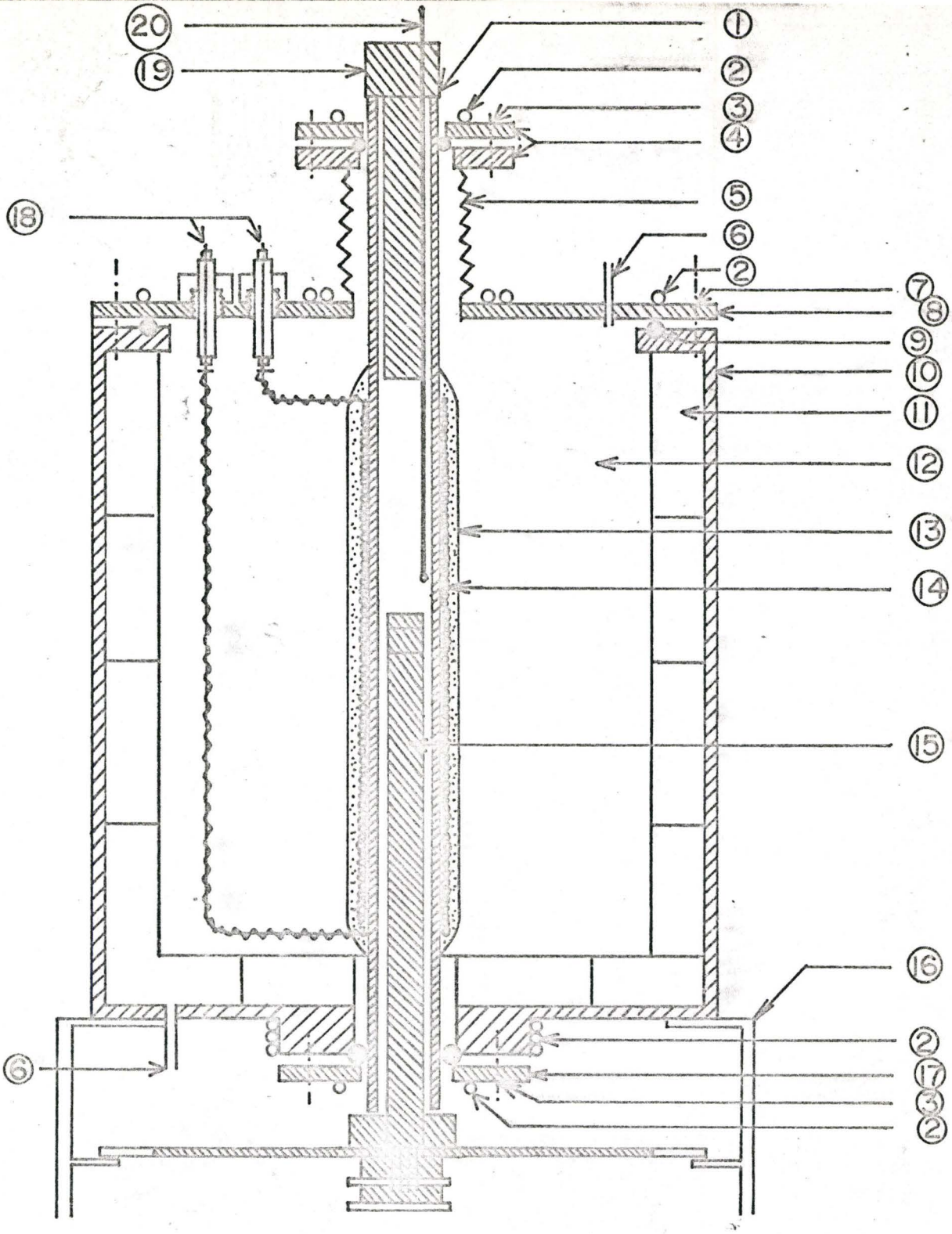

Figure II·3

Furnace Assembly with DTA unit

Legend for Figure II.3

1. Furnace tube.

2. Water cooling copper tubes.

3. Screws to hold the top end plates together.

4. Top end plates with an '0' ring.

5. Gas tight stainless steel bellows.

6. N_2/H_2 gas duct.

7. Screws to hold top plate in position.

8. Furnace top plate.

9. '0' ring.

10. Furnace shell.

11. Refractory brick lining.

12. Space filled with bubble-alumina.

13. Alundum cement.

14. Molybdenum winding.

15. DTA unit.

16. Steel support trolley.

17. Bottom end plate with '0' ring.

18. Gas tight teflon insulated, threaded brass studs held in position by brass swage locks brazed to the top plate.

19. Refractory furnace and plug.

20. Control thermocouple.

of the gas while the furnace cooled created sufficient suction to remove sizable quantities of water from the bubbler. After preheating the furnace to 200°C for a day, it was ready for use.

II.3 ZrO_2 Block Casting Technique

To cast the zirconia DTA block, a stabilized Zircoa-Cast 60D castable powder in conjunction with Zircoa Bond 6 vehicle was used. A ratio of 10 gms of powder to 1 cc of vehicle was found to be satisfactory. The resulting density of 3.6 gms/cc of the slurry served as an important design parameter for the different cast shapes fabricated.

To produce a casting such as the DTA block shown in Figure II.4 a metal die of the type shown in the figure was fabricated. Before casting, the different die components were coated with a thin, uniform layer of paraffin wax. The casting slurry was made in a separate beaker and poured into the die. The die was then manually vibrated for about 3 minutes to allow the slurry to fill the mold completely. Excessive vibration produced cracks in the upper surface of the casting after firing.

The cast mold was allowed to dry for about 4 hours and then placed in an oven at 180°C. After about five minutes the wax melted and the mold could be easily dissembled. The green casting was then carefully placed in an oven and dried at 90°C for 2 hours and 180°C for about 4 hours till the pink casting turned light yellow.

The casting was then carefully loaded in a gas furnace and fired

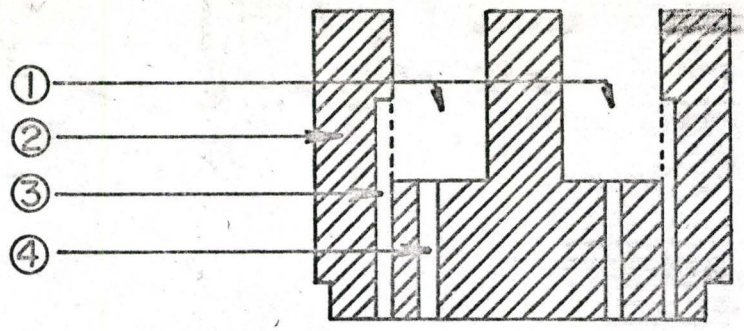

Zirconia DTA Block Casting

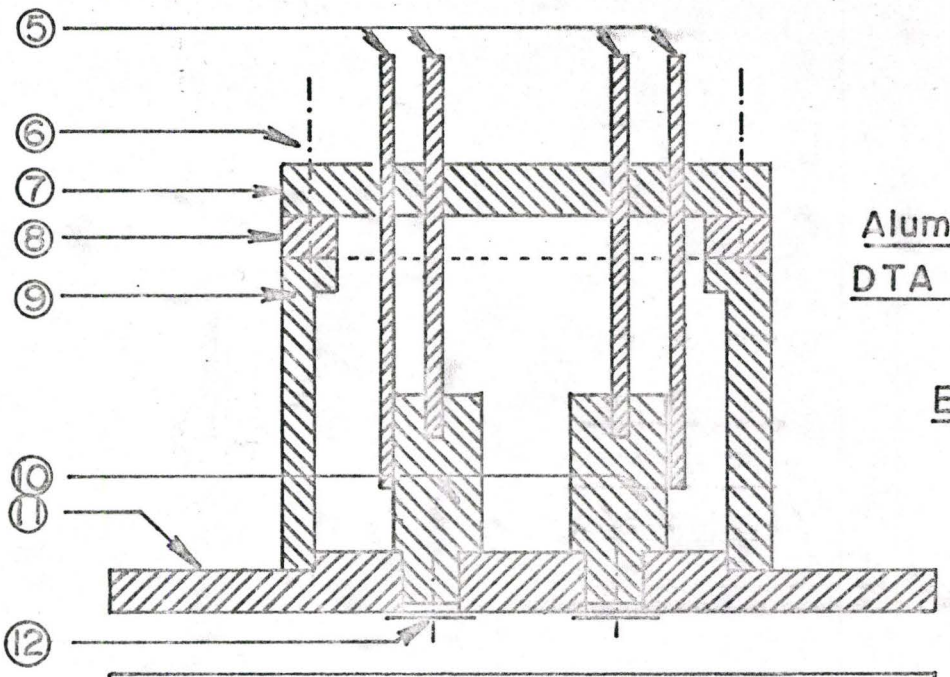

Aluminium Die for DTA Block. Casting

Elevation

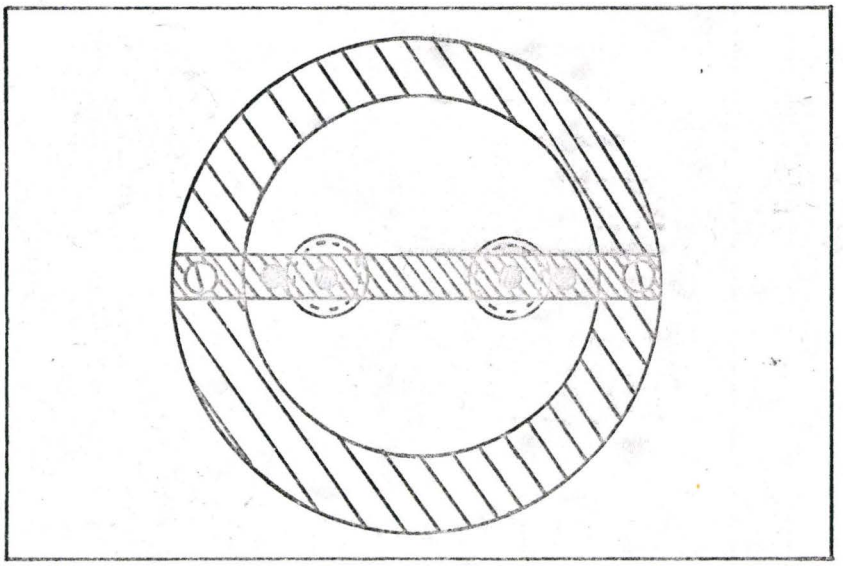

Plan

Figure II·4

Die Assembly for a DTA Block casting

Legend for Figure II.4

1. Reference or sample well.

2. ZrO_2 block.

3. Cylindrical cavity for the wall thermocouple sheathing.

4. Cylindrical cavity for the base thermocouple sheathing.

5. Steel drill rods with matched diameters to produce cylindrical cavities for the thermocouple sheathing.

6. Screw to hold lucite plate in position.

7. Lucite plate to hold drill rods in position.

8. Lucite washer.

9. Aluminum die wall.

10. Aluminum studs to produce reference and sample cell cavities.

11. Aluminum base plate.

12. Screw and washer to hold the aluminum studs tightly in position.

to 1350 to 1400°C for about seven hours. Some of the cast DTA blocks and dies are shown in Figure II.5.

II.4 DTA Unit Assembly

Conventional DTA systems in calorimetric work have never considered the heat lost to the DTA block or gained from it during exothermic or endothermic reactions. In an effort to estimate the magnitude of the errors entailed by this negligence, modifications were incorporated in the normal DTA design.

To minimize the heat loss to the DTA block and prevent heat leakage between the sample and reference cells, the low thermal conductivity ZrO_2 block material was selected. Several designs of block were made by the technique described in II.3. The block design shown in Figure II.4 was found the most satisfactory. The bottom and walls of each cavity were lined with 0.010" platinum foil and Pt/Pt-13% Rh thermocouples were spot welded to the wall platinum lining as illustrated in Figure II.6. The block was placed on the alumina support tube (Figure II.7 - # 4) and thermocouple sheaths passed upwards through the lucite plate (# 8) and the aluminum holder block (# 5) to the DTA block (# 2). All the thermocouple sheaths used were 1/8" double-bore mullite.

The Pt/Pt-13% Rh thermocouples were threaded through the sheaths and after setting up the wall thermocouple, the wires were pulled lightly to set the platinum wall foil properly in each well. The foil was then evened

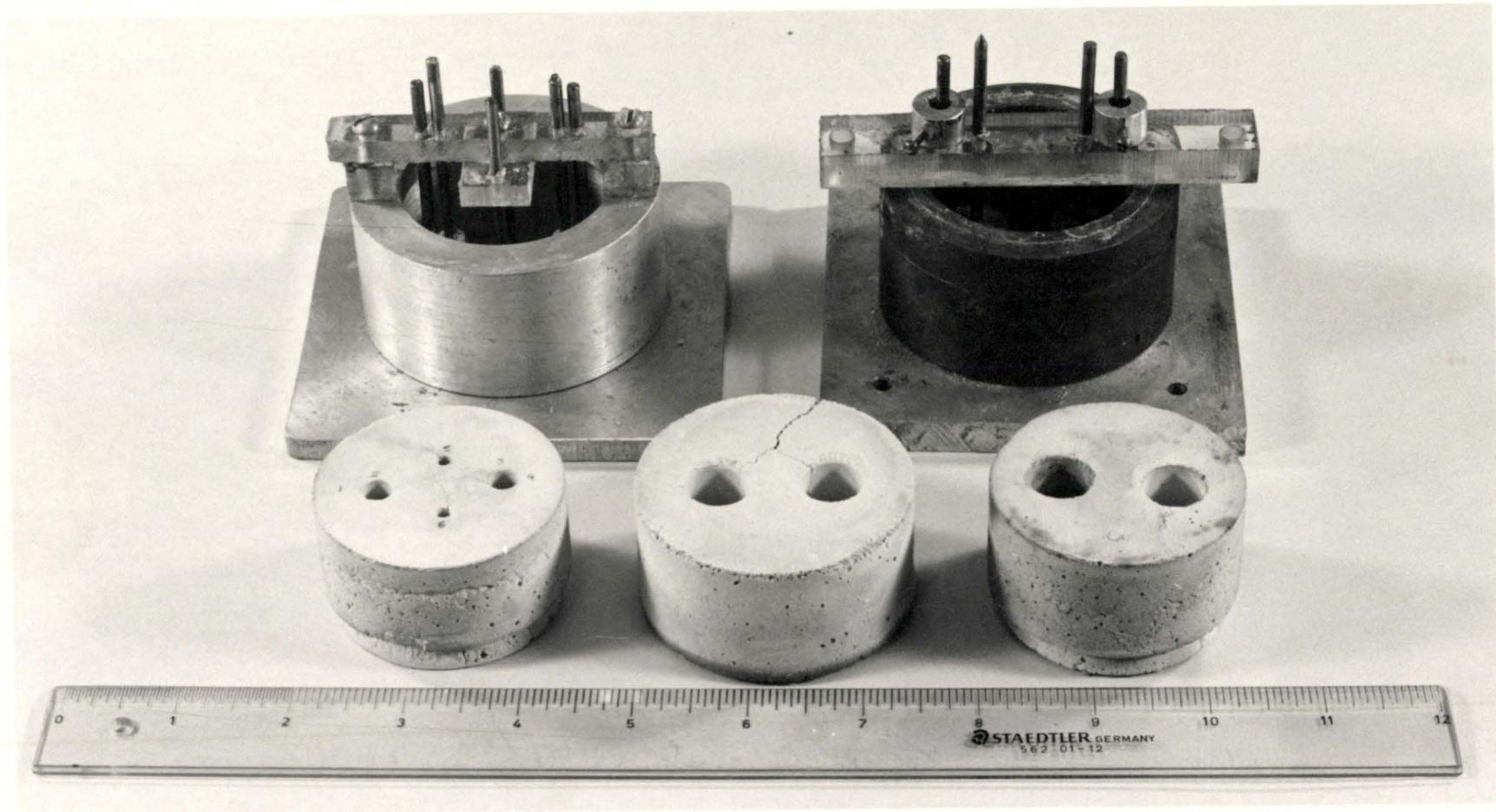

Figure 11.5 DTA zirconia block castings and metal dies.

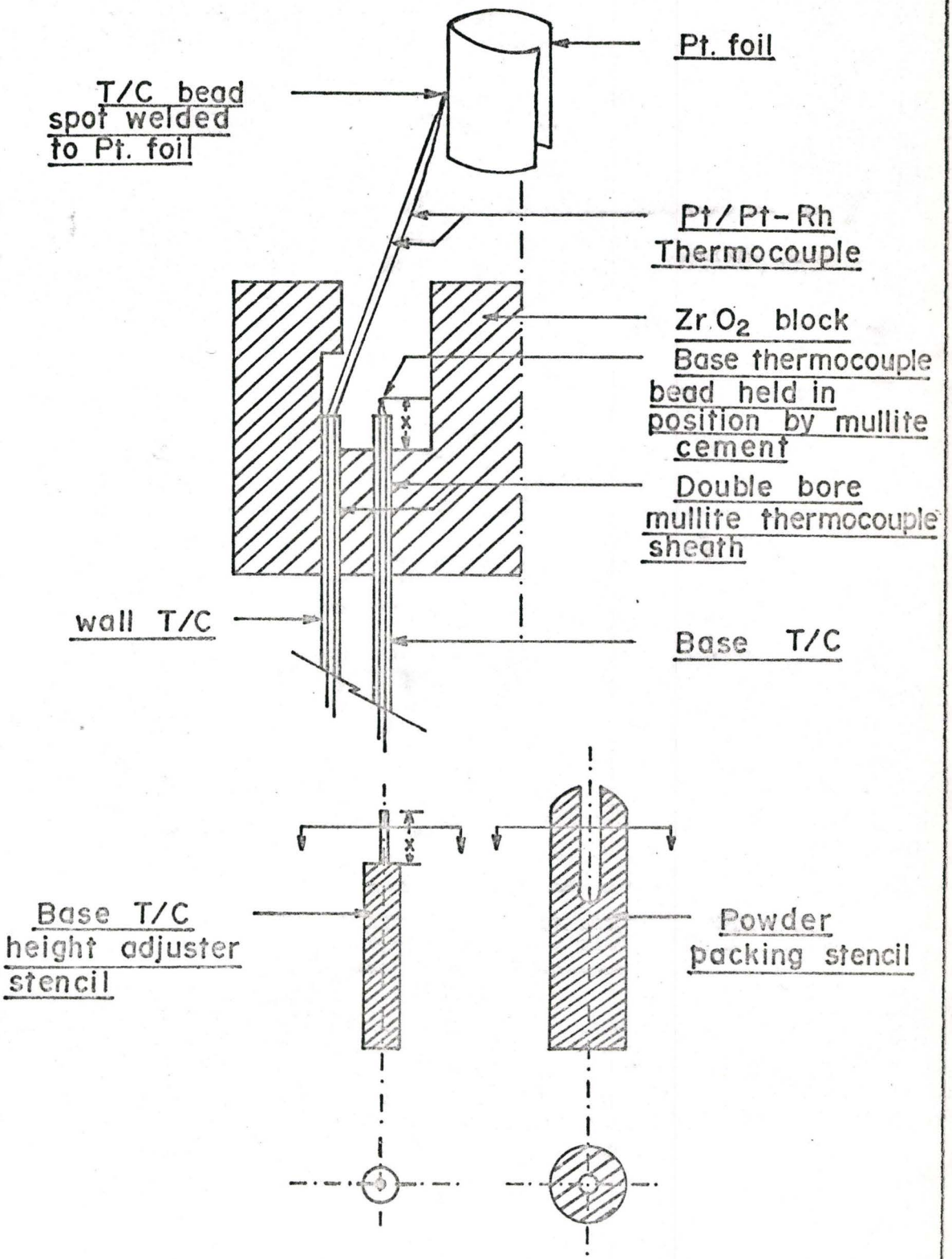

Figure II·6

DTA Block Assembly and Loading Kit

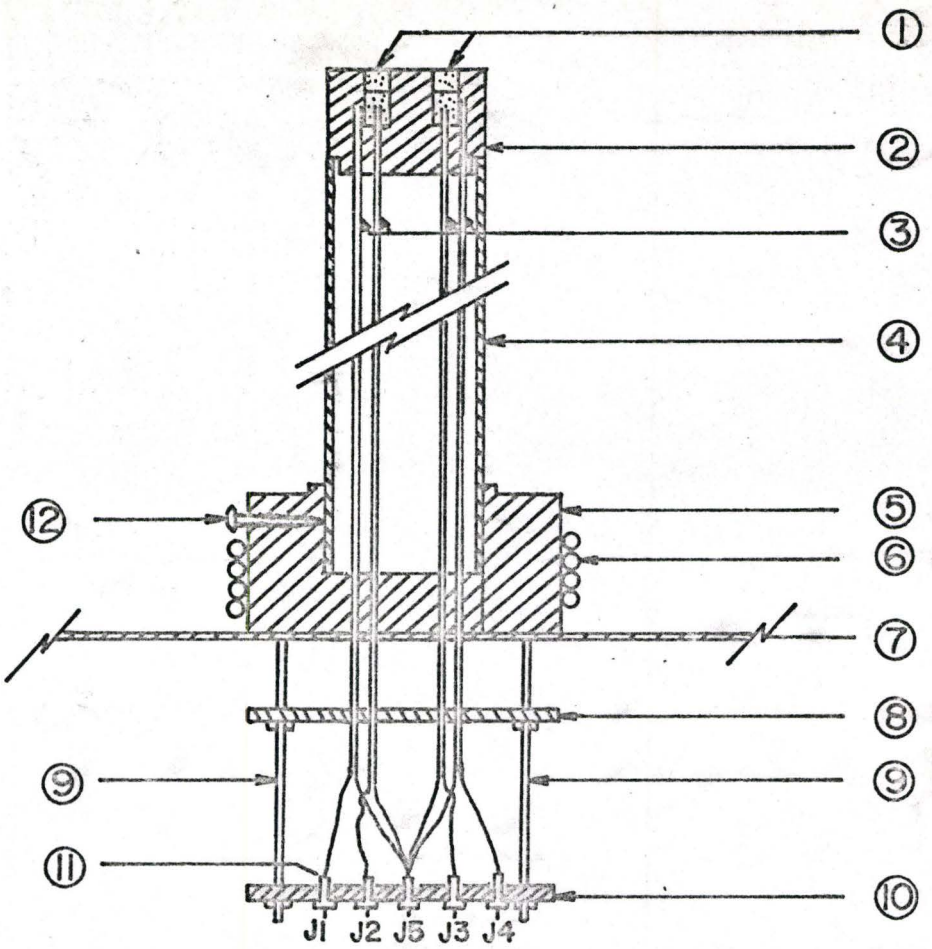

Figure II·7

DTA Block and Thermocouple Assembly

Legend

1. Platinum lined reference and sample cells.
2. ZrO_2 DTA block.
3. Thermocouple sheathing.
4. Al_2O_3 support tube.
5. Aluminum block.
6. Water cooling.
7. Aluminum support plate.
8. Lucite plate with set screws to hold T/C sheaths in position.
9. Brass screw rod.
10. Lucite plate with banana jacks.
11. Banana jacks.
12. Set screw to hold (# 4) in position.

out against the cell wall using the powder packing stencil shown in Figure II.6. The vertical heights of the thermocouples in the sample and reference walls were accurately adjusted using the height adjuster stencil shown in Figure II.6. It was observed that loose thermocouples gave rise to noise in the differential output signal and to minimize this and maintain reproducibility of the results, the thermocouple beads were cemented in position on top of the thermocouple sheaths with mullite cement.

The thermocouples were soldered to banana jacks by a low thermo-e.m.f., Cd-Sn solder. Since all the temperature measurements were differential, ice-water bath cold-junctions were unnecessary. Room temperature was measured by a mercury thermometer and it remained fairly constant during the experiments. The thermocouples were found to maintain their characteristics before and after the experiments.

II.5 Experimental Design

The experiments were divided into two parts:

I) assessment of the potential of the modified DTA for in situ measurement of sample thermal conductivity, and

II) measurement of the heat loss to the DTA block or heat gain from it during exothermic or endothermic reactions, respectively.

The influence of the following variables on these heat losses was also investigated:

a) the type of reaction, i.e., solid state polymorphic reactions (rhombic $\rightleftharpoons$ trigonal $SrCO_3$); solid state crystallization reactions (kaolinite exotherm $3(Al_2O_3\ 2SiO_2) \rightleftharpoons 3\ Al_2O_3\ .\ 2SiO_2 + 4SiO_2$ β-quartz); dehydroxylation reactions (kaolinite endotherm $Al_2(Si_2O_5)(OH)_4 \rightarrow Al_2Si_2O_7 + 2H_2O\uparrow$); and decomposition reactions ($CaCO_3 \rightarrow CaO + CO_2\uparrow$),

b) the degree of dilution of the sample, i.e., kaolinite diluted to different levels by Al_2O_3 and by dead-burnt kaolinite,

c) the change of reference substance from Al_2O_3 to dead burnt kaolinite for kaolinite DTA, and

d) the change of the block geometry.

Results obtained on a commercial and the constructed DTA units were also compared.

II.6 Assessment of the Modified DTA for Static Thermal Conductivity Measurements

Equation (4) of Chapter I implies that the thermal conductivities of the reference and the sample are assumed very nearly equal, i.e., under isothermal or dynamic conditions the temperature drop ΔT_r (Figure II.8) across the reference cell should be equal to the temperature drop ΔT_s across the sample cell for a uniform and equal heat influx to the two cells at a given temperature. This assumption was checked by comparing the ΔT's across the sample cell for live kaolinite, dead burnt kaolinite and montmorillonite over a range between room temperature and 1150°C.

The furnace was driven by a 4.4 Kw powerstat. The temperature gradients were measured on the Keithley microvolt ammeters on 300 μV, 100 μV

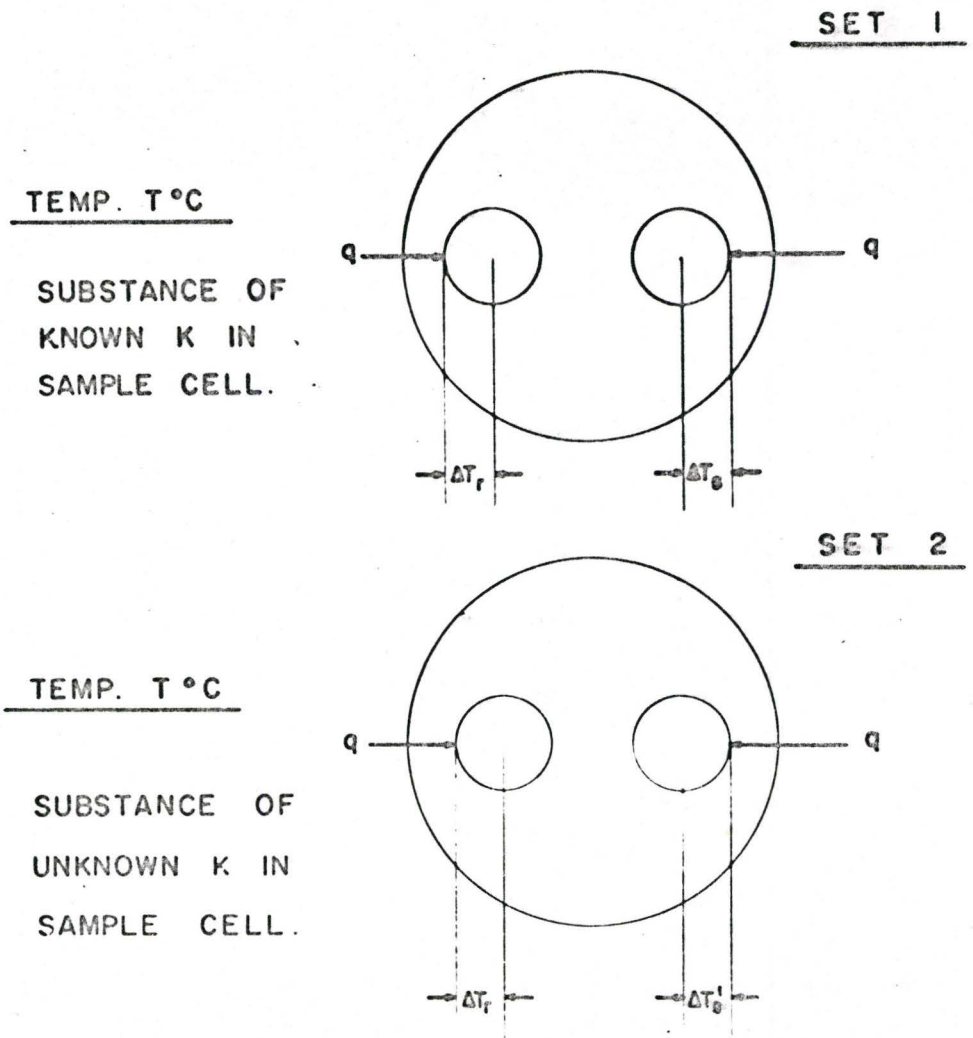

Figure II.8

Thermal Gradient Measurement Scheme

and 30 μV full scale ranges with ± 2% accuracy.

Isothermal observations were made as follows:

The reference cell was filled with (-325 mesh) Al_2O_3 powder and all the observations were referenced to the differential temperature across this cell. This cell was left intact during all the isothermal thermal conductivity experiments. The sample cell was filled with the (-325 mesh) test powder. The DTA column was then inserted into the furnace and visually aligned. An additional cylindrical nickel shield was interposed between the DTA column and the furnace tube and was electrically grounded to eliminate electronic noise (Figure II.9). The furnace was then heated to a temperature of 300°C and allowed to stabilize for about 8 to 10 hours to ensure steady state conditions. The DTA column was then electrically aligned by making sure ΔT_w (the temperature difference between the wall thermocouples of both cells) was 0 ± 3 μV. Once the column was thus aligned it required no further alignment during subsequent observations during a given experimental run. The ΔT_r and ΔT_s were measured for seven or eight different higher temperatures by increasing the power input to the furnace. At every temperature the furnace was allowed to stabilize for 8 to 10 hours at a constant power input. Plots of ΔT_r and ΔT_s against isothermal temperatures were made. This procedure was repeated for all the sample materials noted.

The comparison of ΔT_s and $\Delta T_{s'}$ at an isothermal temperature T°C (Figure II.8) for two different samples is a measure of their relative thermal conductivities, provided the heat transfer conditions are identical during the different experimental runs.

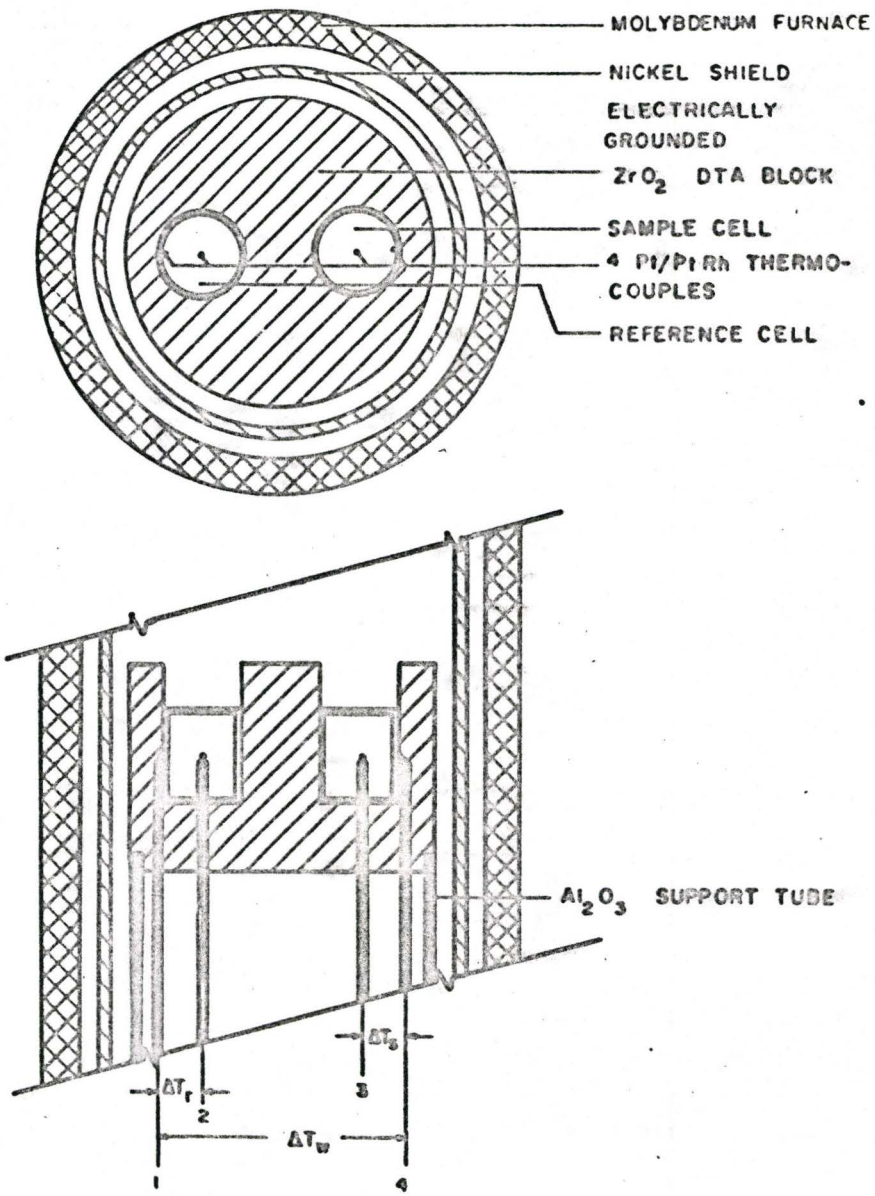

Figure II.9

Thermal Gradient Measurement Set Up

II.7 Heat Losses (ΔT)

The effect of various parameters on the heat losses during DTA experiments as indicated in II.5 were studied. The areas under the DTA peaks obtained were measured with a Polar-Compensating planimeter. Due to the variation of the thermophysical constants before and after the reactions, particularly in reactions involving a loss of weight (the dehydroxylation and carbonate decomposition reactions), the experimental base line drifted. This complicated the area measurements and the method outlined by Mackenzie[17] was used to analyse the thermogram areas.

This method consists of drawing a vertical line from the apex of the DTA peak and extending the base lines on either side of the peak to meet it. The area bounded by the DTA curve and the above lines is considered to define the peak area. The temperature of reaction initiation is defined by the point of intersection of the extended base line and the extension of the straight portion of the initial limb of the reaction peak (see Figure III.7). The reactions investigated were outlined in Section II.5.

The cells were manually loaded with a carefully weighed sample in each case. The loss in weight while loading was at the most 0.35%. Identical masses of sample and reference were used in each case and both powders were compressed equally into the cells using the powder packing stencil. In all the experiments, unless otherwise mentioned, the reference and dilutent substance was Alcoa A-5 calcined alumina.

To investigate the effect of the change of block geometry on the heat distribution between the cell walls and the central thermocouples during an enthalpic effect, two DTA block designs were studied.

The first design had a cell size of ½" diameter by 3/4" deep and was platinum lined to a height of ½". All powders were packed into the cells to a height of ½". Two circular foils of platinum were used to cover the samples and the rest of the cell height was filled with stabilized zirconia powder. Both the reference and the sample cells were packed in a similar fashion. This design had an effective cell height to diameter ratio of unity. The second DTA block design had cells of ¼" diameter by 11/16" deep, which were platinum foil lined up to a height of ½" giving an effective height to diameter ratio of 2. The two block designs are shown in Figure II.5.

CHAPTER III

EXPERIMENTAL RESULTS

III.1 Appraisal of Modified DTA Apparatus for Thermal Conductivity Measurements

In Figure III.1 is shown a plot of the temperature gradient across the reference cell (ΔT_r) as a function of the isothermal furnace temperature for different experimental conditions. All the points fall on the same curve emphasizing the reproducibility of the heat transfer conditions. The temperature drop across the cell increases with increasing temperature.

A plot of the furnace characteristics is shown in Figure III.1(a). This data aided the choice of power input requisite for particular isothermal temperature conditions.

Figure III.2 compares the thermal gradients for Al_2O_3, live kaolinite, semi-dead burnt kaolinite and dead burnt kaolinite in the sample cell. During the dehydration of clays, mineral agglomerates tend to break up and the evolved water vapour and change in particle size may affect the overall effective thermal conductivity of the sample. To check this effect kaolinite was tested in three different states. The semi-dead burnt material was in the meta-kaolinite state, i.e., kaolinite after loss of structural water (700°C). The dead burnt material was prepared by preheating the powder beyond the exotherm (1100°C) before introducing it into the DTA apparatus.

The steady state thermal gradients increase with increasing temperatures. Beyond 1100°C the clay samples begin to sinter. This increases the

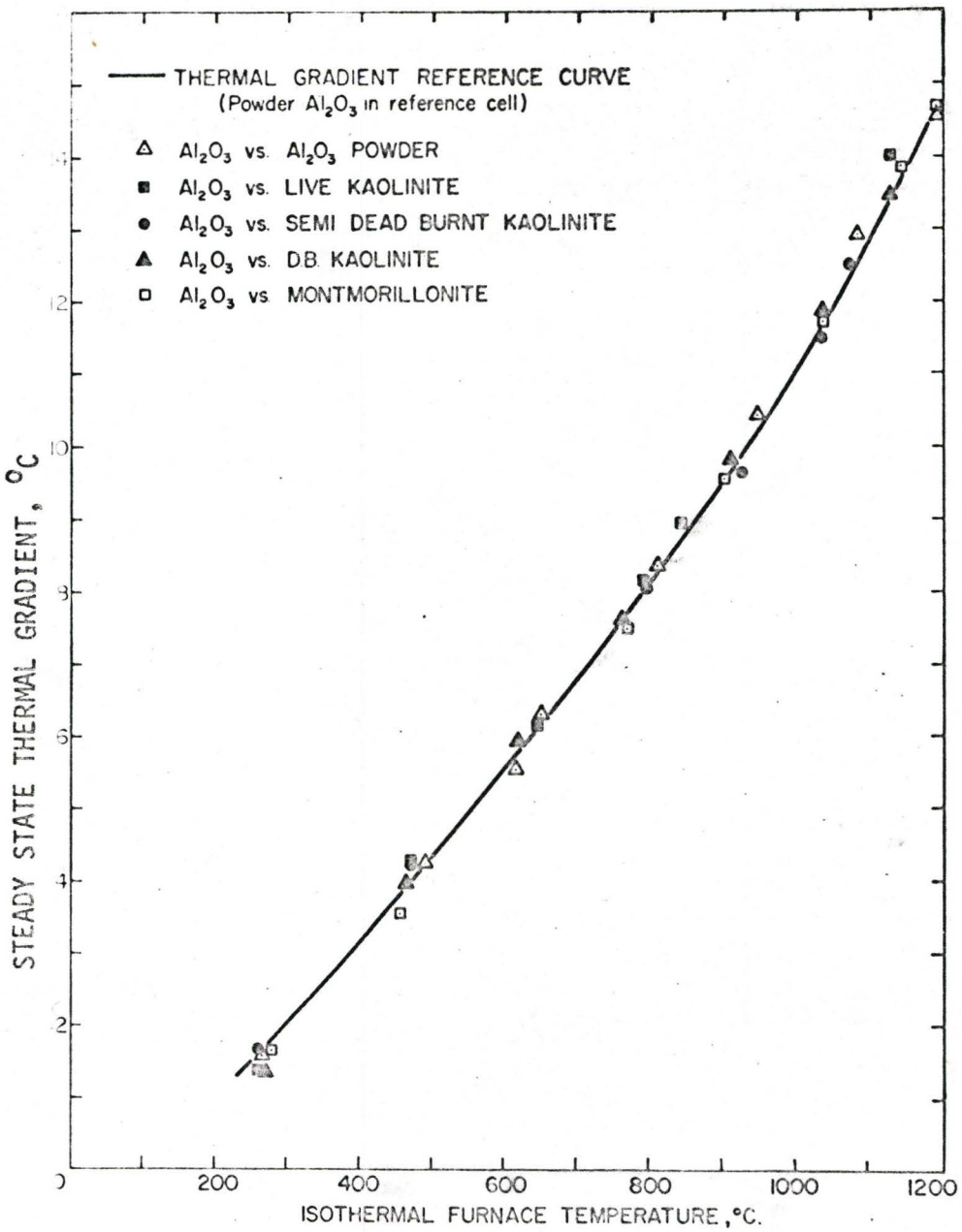

Figure III.1

Thermal Gradient Reference Plot

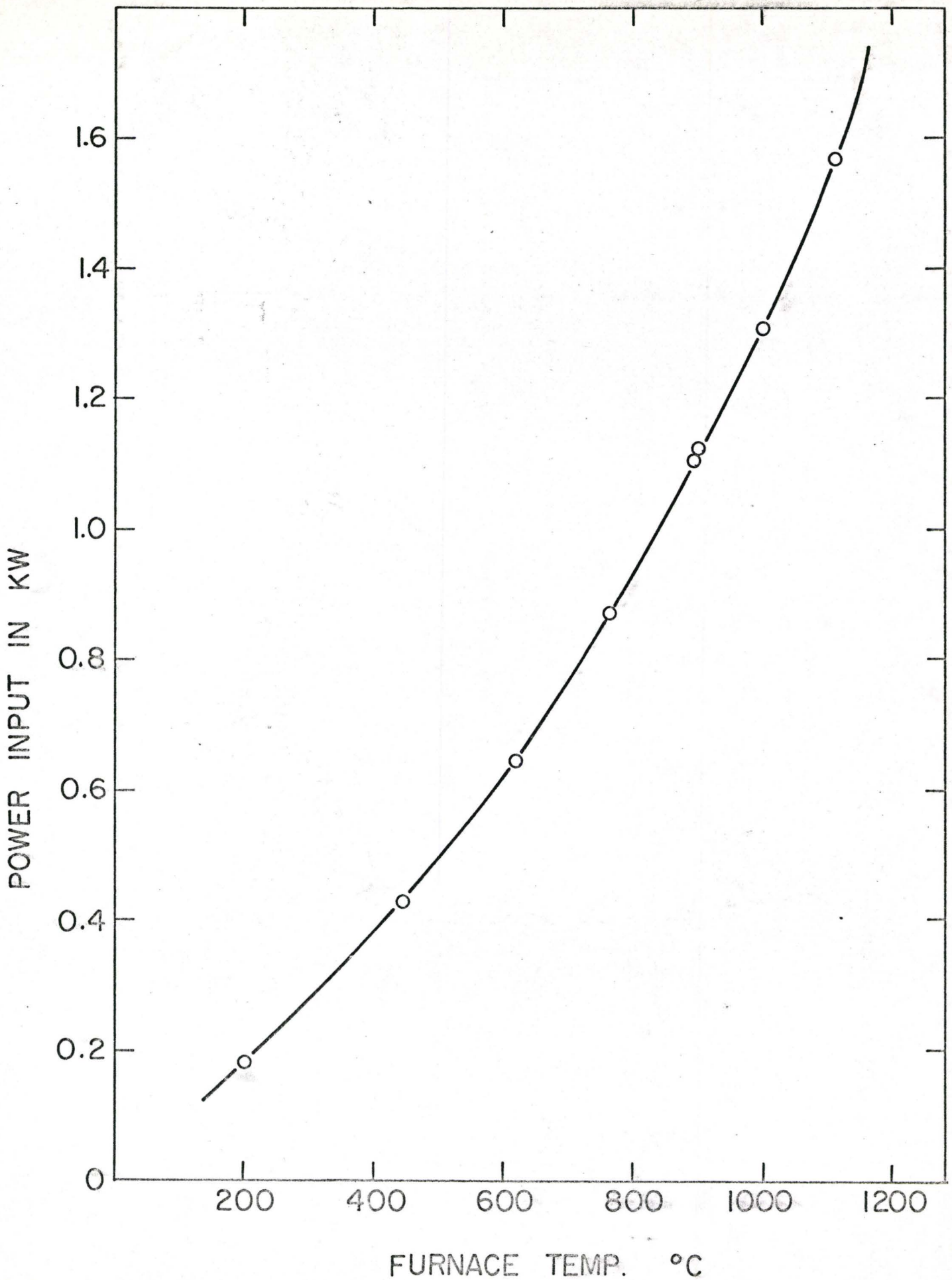

Figure III.1(a) Steady State Furnace Characteristics

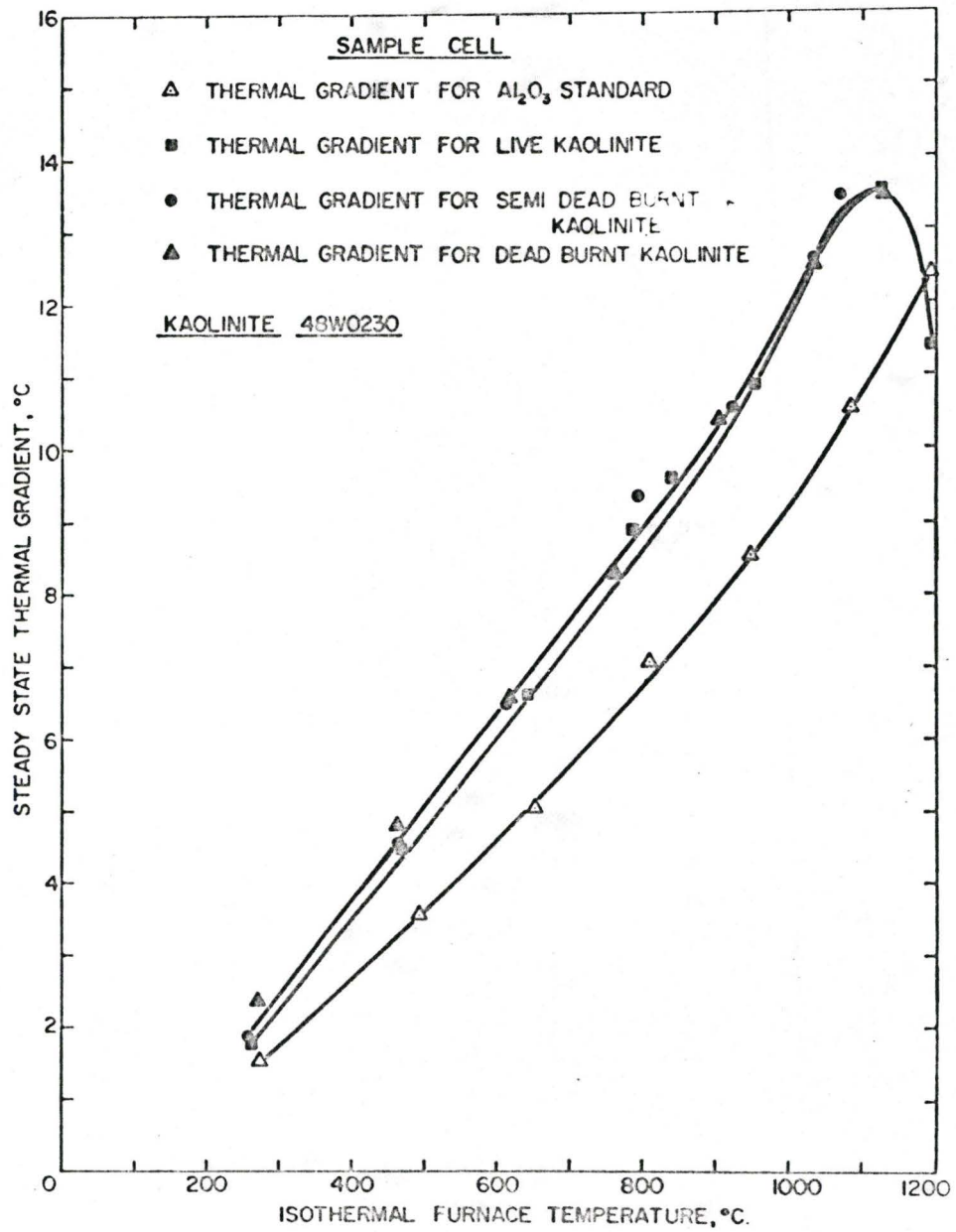

Figure III.2

Kaolinite Thermal Gradient Plot

solid-solid contact area within the sample. Furthermore, the samples begin to shrink away from the cell walls, producing an associated air gap. These two factors increase the overall heat transfer across the cell so decreasing the thermal gradient across it. The dead-burnt material data and that of the semi-dead-burnt material fall along the same curve. The curve for live kaolin shows slightly lower thermal gradients, but the curve for Al_2O_3 shows considerably lower thermal gradients, meaning that effective thermal conductivity for Al_2O_3 is higher than that of kaolinite.

Figure III.3 is a plot of the thermal gradients for the Al_2O_3 standard and live and dead-burnt montmorillonites. The points for live and dead-burnt montmorillonite fall on the same curve. The Al_2O_3 values are a little lower than the montmorillonite values. The montmorillonite curve indicates the commencement of sintering at 1000^{o}C.

Figure III.4 is a plot of the temperature gradient in μV across the sample cell of DTA block design II with (-160 mesh) Al_2O_3 powder in it. The static curve represents thermal gradients across the cell in isothermal conditions, i.e., the furnace was controlled at the observation temperature on the set point mode for a considerable time before a measurement. The dynamic curve corresponds to the quasi-steady state condition, i.e., a heating rate of 2.06^{o}C/min, was imposed on the system and the temperature differential (across the same cell filled with (-160 mesh) Al_2O_3) was measured at different furnace temperatures without interrupting the heating cycle. The dynamic-condition curve plots above that of the static condition, indicating the influence of constantly rising temperature on the heat transfer conditions.

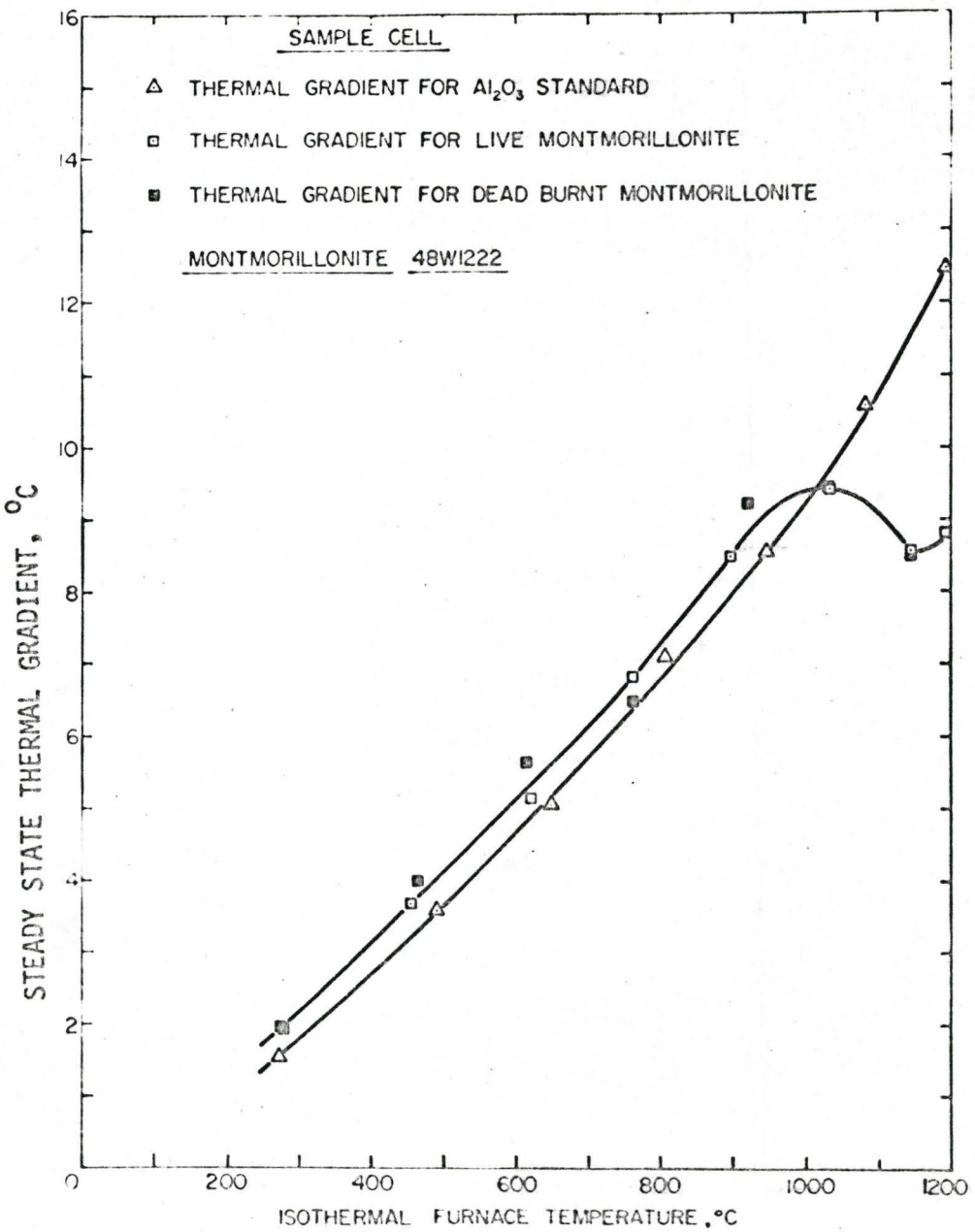

Figure III.3

Montmorillonite Thermal Gradient Plot

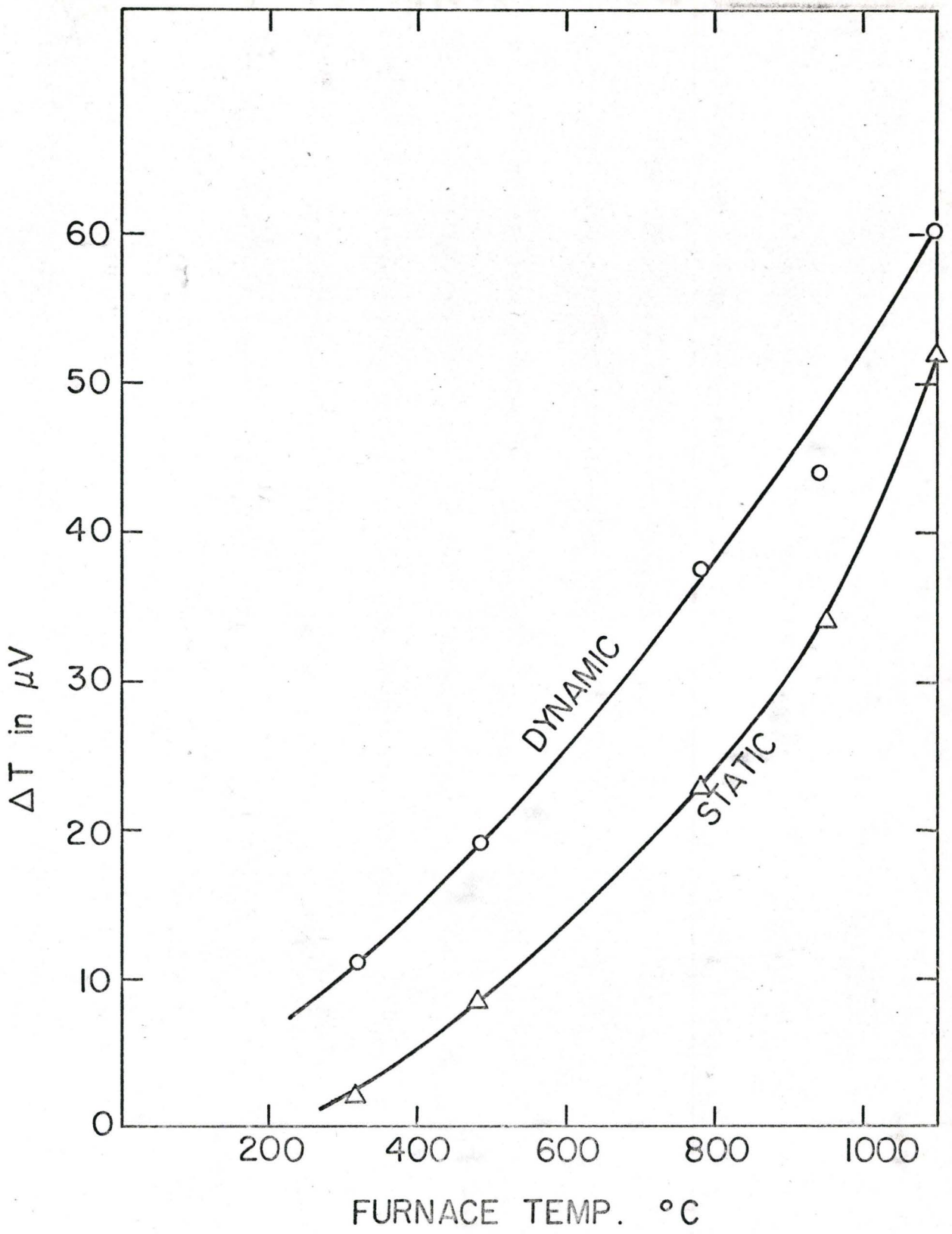

Figure III.4 Thermal Gradients Across Al_2O_3 Loaded Sample Cell for Static and Dynamic Conditions

III.2(a) Heat Loss (ΔT); Influence of Reaction Type

The experimental results in this section conclusively prove the hypothesis proposed in Section I.4(d), i.e., during an endothermic process, heat is gained from the DTA block and during an exothermic reaction heat is lost to the block.

A linear heating rate of 2.06^{o}C/min was used (Figure III.5) and Figures III.6 to III.9 are reproductions of thermograms obtained for different substances in the modified DTA apparatus. The differential signals measured in micro volts (μV) are plotted against time in minutes from the start of the experiment. All the experiments were started at room temperature. O_b and O_w mark the initial positions of the base line for the base and wall differential thermocouples respectively on these figures. The smaller peaks are the ones registered by the wall differential couple and the larger ones correspond to the base (or centre) differential couple. The reference-cell wall and base temperatures were measured intermittently to check the linearity of the heating rate and to obtain accurate reaction-initiation temperatures on the wall and base differential temperature peaks respectively.

Figure III.6 shows the endotherm caused by the rhombic $\rightleftharpoons$ trigonal inversion of $SrCO_3$. The reaction starts at the perifery of the cell, and hence the wall differential couple senses the reaction earlier than the base thermocouple on the time axis. The areas under the two peaks and the sample mass (active component) are shown in Table III.1. The shape of these peaks is slightly distorted as this polymorphic transformation temperature is close to that of the carbonate decomposition. The observed initiation temperatures are well in agreement with literature values[17].

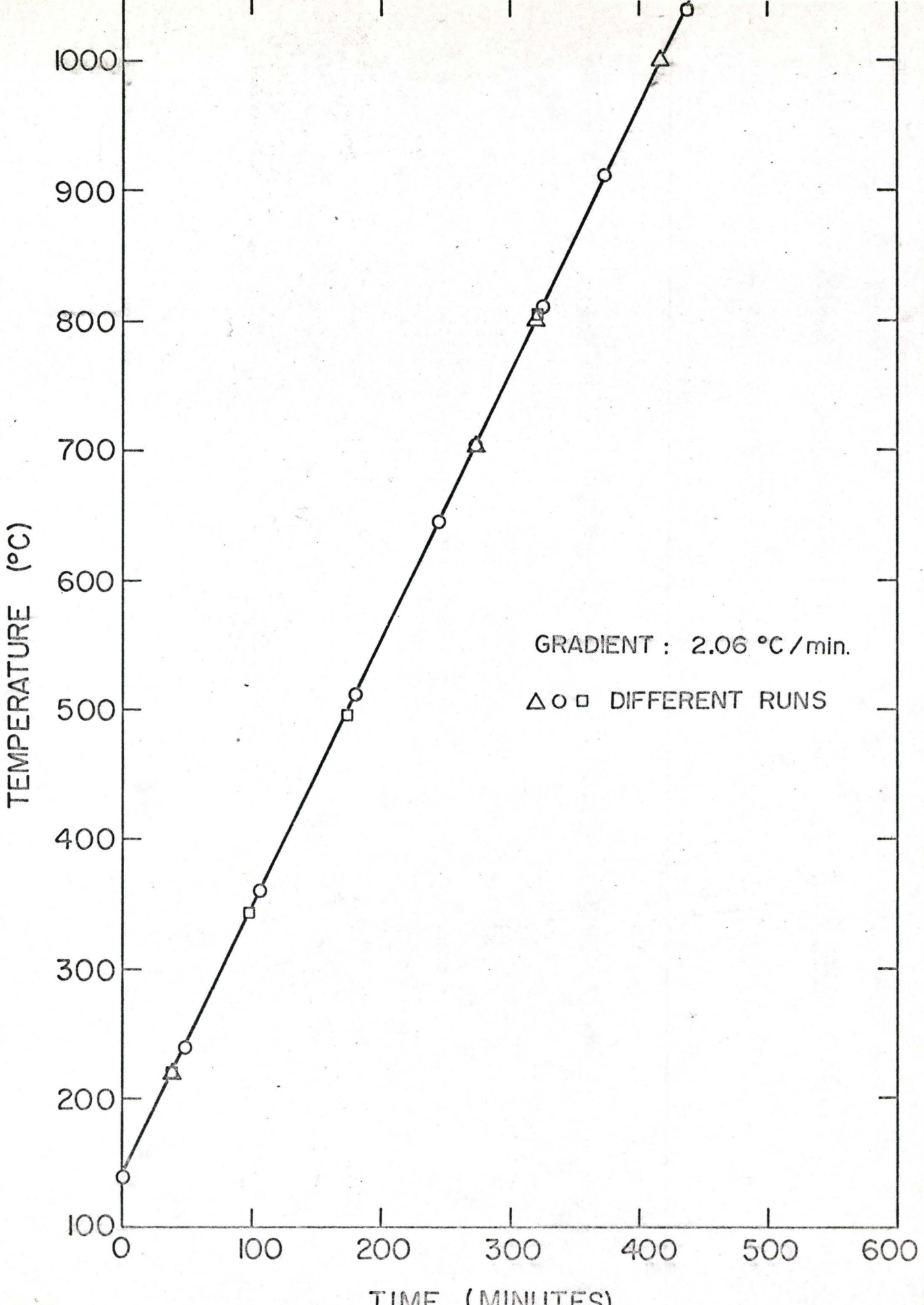

Figure III.5 Heating Rate for DTA Experiments

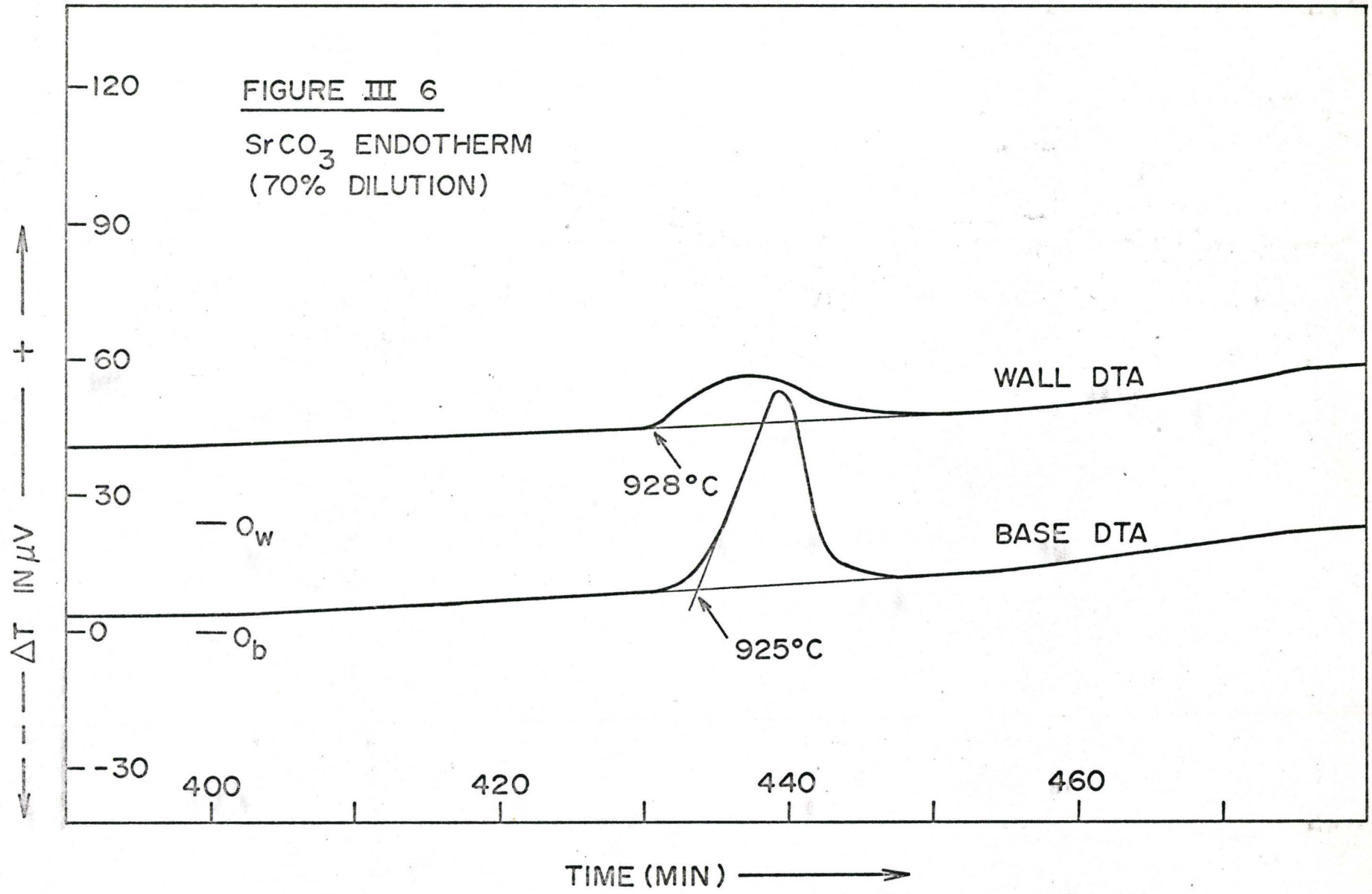
FIGURE III 6
SrCO3 ENDOTHERM
(70% DILUTION)
120
90
60
30
0
-30
ΔT IN μV
+
-
WALL DTA
BASE DTA
928°C
925°C
Ow
Ob
400
420
440
460
TIME (MIN)

The peak corresponding to the exothermic reaction in kaolinite is shown in Figure III.7. The exotherm is believed to be the result of the crystallization of amorphous silica into β-quartz[73].

Figure III.8 is the endothermic trace produced by dehydroxylation of kaolinite.

The 700°C $CaCO_3$ decomposition endotherm is shown in Figure III.9.

The data obtained for the various reactions studied is summarised in Table III.1. The final column of this table indicates the percentage of the heat effect which eludes the single-couple DTA systems.

TABLE III.1

Heat Loss (ΔT): Type of Reactions

Reaction	Active mass of sample in grams	DTA peak areas in square inches		[w/(w+b)] % heat lost/ gained to/from DTA block
		Base (b)	Wall (w)	
$SrCO_3$	0.54	0.78	0.372	32.1
Kaolinite Exotherm	0.652	1.209	0.394	24.8
Kaolinite Endotherm	0.652	5.61	2.34	29.4
$CaCO_3$	0.489	8.45	5.31	39.1

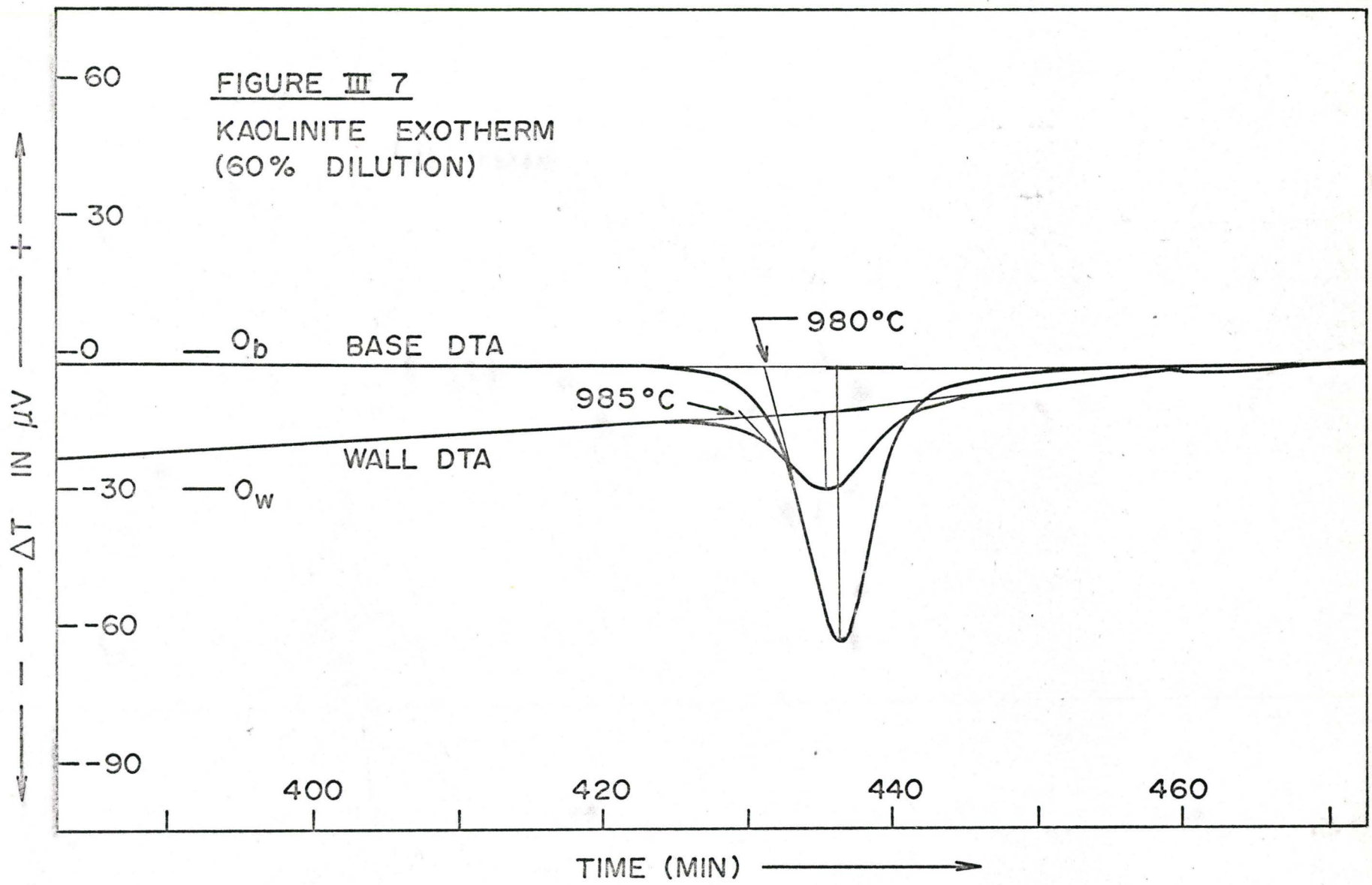
FIGURE III 7
KAOLINITE EXOTHERM
(60% DILUTION)
60
30
0
-30
-60
-90
O_b
BASE DTA
980°C
985°C
WALL DTA
O_w
400
420
440
460
TIME (MIN)
ΔT IN μV
+
-

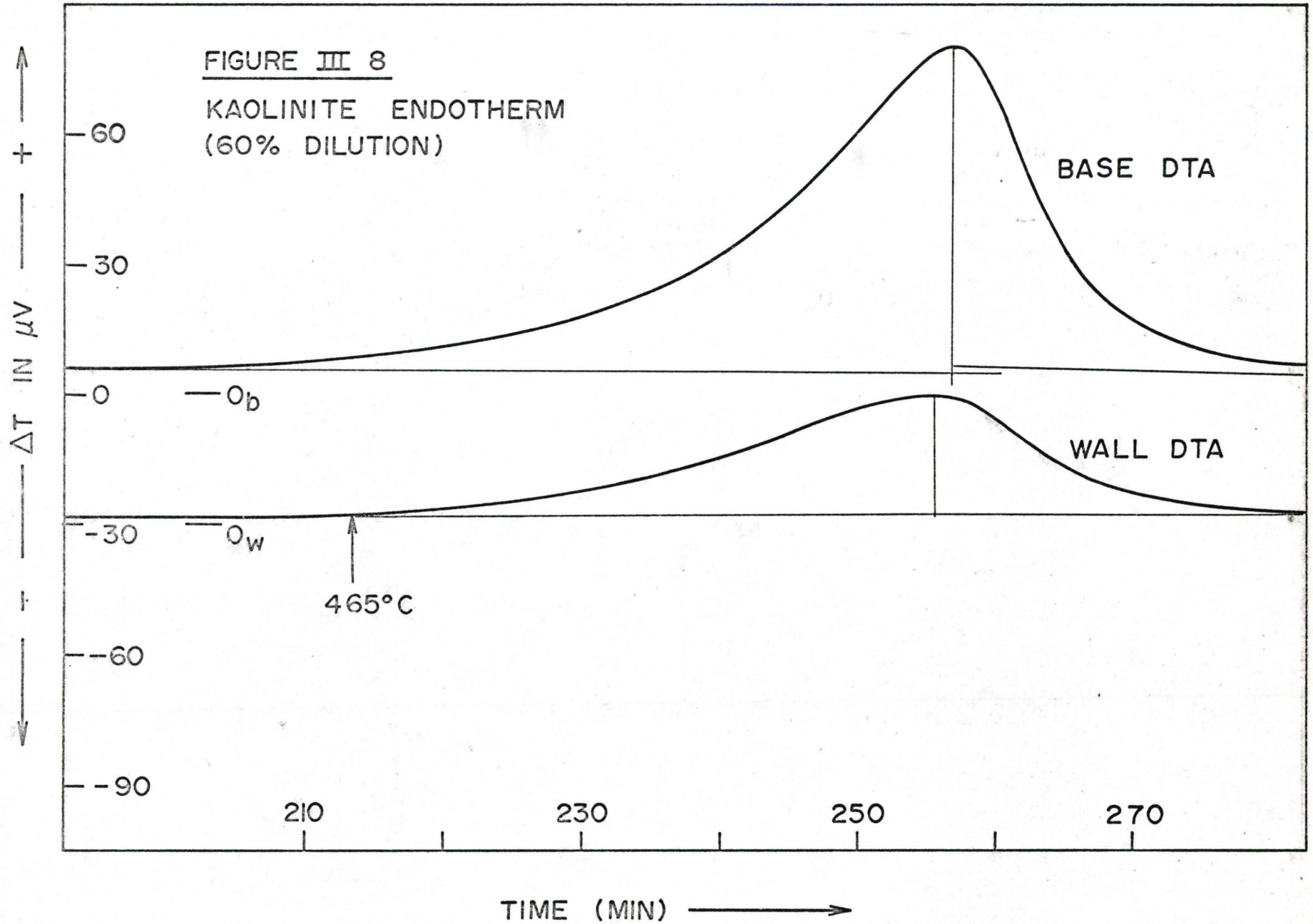
FIGURE III 8
KAOLINITE ENDOTHERM
(60% DILUTION)
BASE DTA
WALL DTA
60
30
0
0_b
-30
0_w
465°C
--60
--90
210
230
250
270
TIME (MIN)
ΔT IN μV
+
-

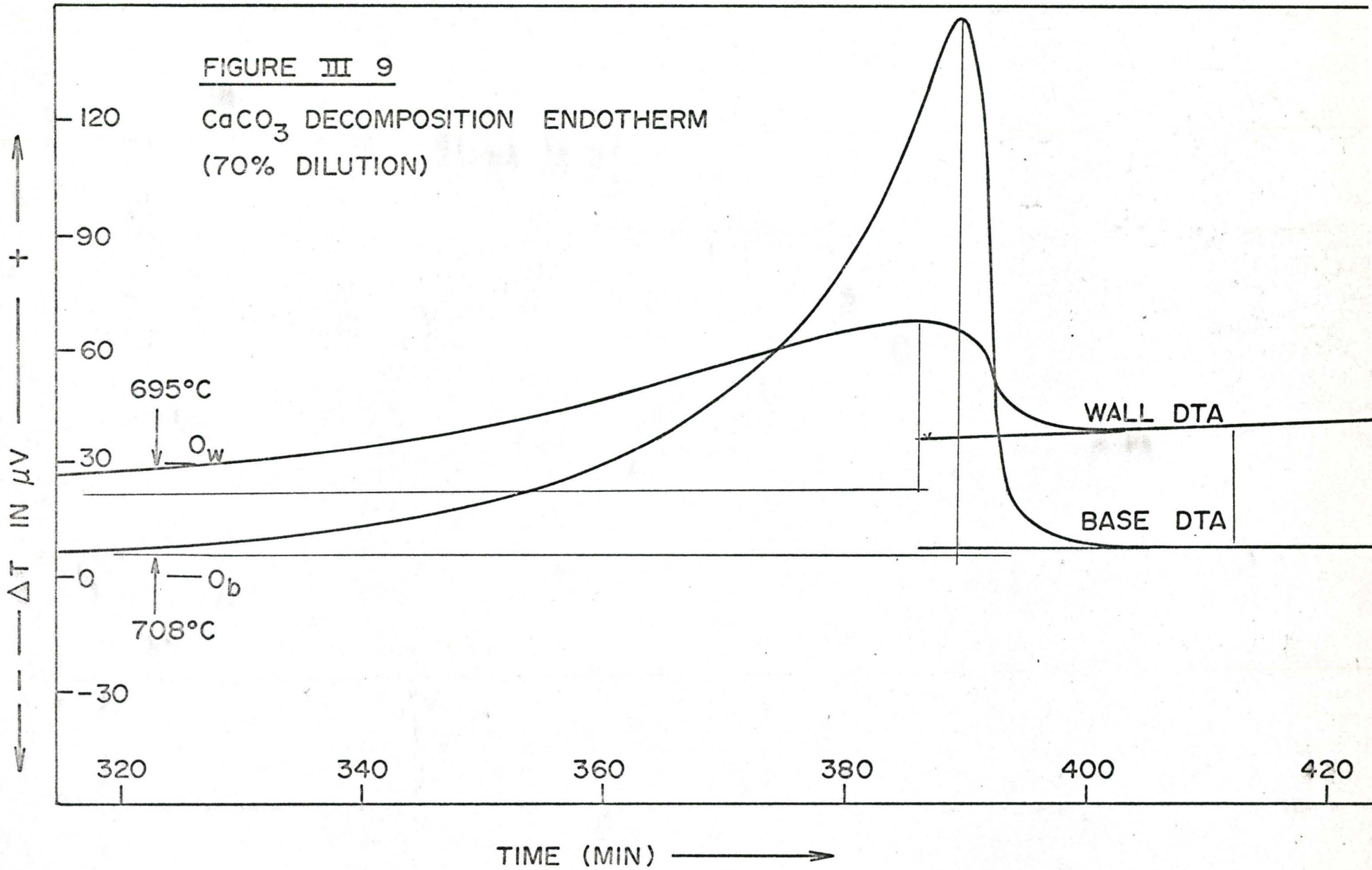
FIGURE III 9
$CaCO_3$ DECOMPOSITION ENDOTHERM
(70% DILUTION)
120
90
60
30
0
-30
695°C
O_w
708°C
O_b
WALL DTA
BASE DTA
320
340
360
380
400
420
TIME (MIN)
ΔT IN μV — — — — + —

III.2(b) Heat Loss (ΔT); Influence of Degree of Dilution

DTA runs were made on kaolinite samples diluted with different percentages of Al_2O_3 powder. The purpose of this investigation series was to study thermogram peak-area/mass relationships for the base and wall DTA's. The results are tabulated in Table III.2.

In Figure III.10 is plotted the base DTA peak areas vs. the % active component for the endothermic and the exothermic reactions of kaolinite. The points at the 60% active component level are low and this was probably due to an error in the weighing or mixing of the samples. The slopes for the two plots are dictated by the size of the heat effects. A reasonably linear plot was obtained in both cases indicating the validity of the dilution technique. The non-origin intercept observed in some cases is interesting and will be considered later.

III.2(c) Heat Loss (ΔT); Influence of Change of Reference Substance

DTA runs were made on kaolinite samples diluted with dead burnt kaolinite powder and utilising dead burnt kaolinite as the reference material. The results obtained are summarised in Table III.3.

In Figure III.11(a), the kaolinite endothermic peak areas for kaolinite-Al_2O_3 and kaolinite-D.B. kaolinite DTA systems are plotted for the wall, base and (wall + base) DTA's. These data are also summarised in Tables III.2 and III.3. It is interesting to note that the peak area/dilution relationship appears independent of the two dilutents for this reaction but the plots do not pass through the origin but indicate a zero peak area for approximately 6% active component level.

Figure III.11(b) is a similar plot of peak areas for kaolinite-Al_2O_3,

TABLE III.2

Kaolinite -Al_2O_3 DTA System

Reaction	% Kaolinite in sample cell	Area under DTA peaks in square inches			% heat lost/gained from DTA block	Mean % heat lost/gained from DTA block
		Base (b)	Wall (w)	(b)+(w)		
ENDOTHERM	20	2.575	.98	3.555	27.6	
	40	5.61	2.34	7.95	29.4	
	60	7.27	3.18	10.45	30.4	28.4
	80	12.9	4.82	17.72	27.2	
	100*	15.68	6.00	21.68	27.6	
EXOTHERM	20	.509	.1525	.6615	23.0	
	40	1.209	.394	1.603	24.6	
	60	1.652	.525	2.177	24.3	23.3
	80	2.75	.763	3.513	21.0	
	100*	3.475	1.068	4.543	23.4	

* 100% sample = 1.63 gms of kaolinite

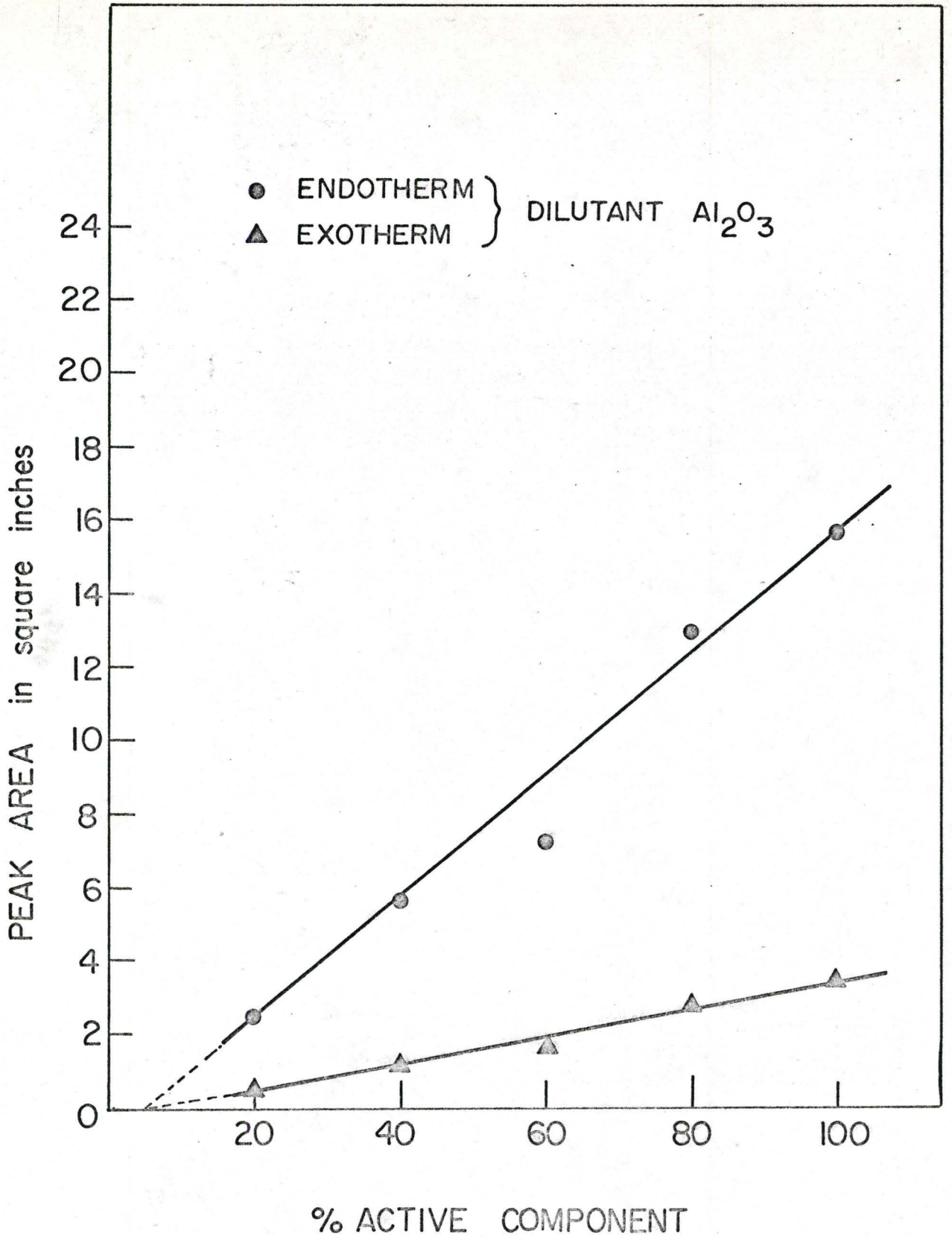

Figure III.10 Peak (base DTA only) Area vs. % Active Component (Kaolinite)

TABLE III.3

Kaolinite-Dead Burnt Kaolinite DTA System

Reaction	% Kaolinite in sample cell	Area under DTA peaks in square inches			% heat lost/gained from DTA block	Mean % heat lost/gained from DTA block
		Base (b)	Wall (w)	(b)+(w)		
ENDOTHERM	20	2.71	1.13	3.84	29.4	
	35	5.27	1.982	7.252	27.3	28.2
	100*	15.61	6.07	21.68	28.0	
EXOTHERM	20	.675	.209	.884	23.6	
	35	1.25	.40	1.65	24.3	24.1
	100*	3.63	1.164	4.794	24.3	

* 100% sample = 1.63 gms kaolinite

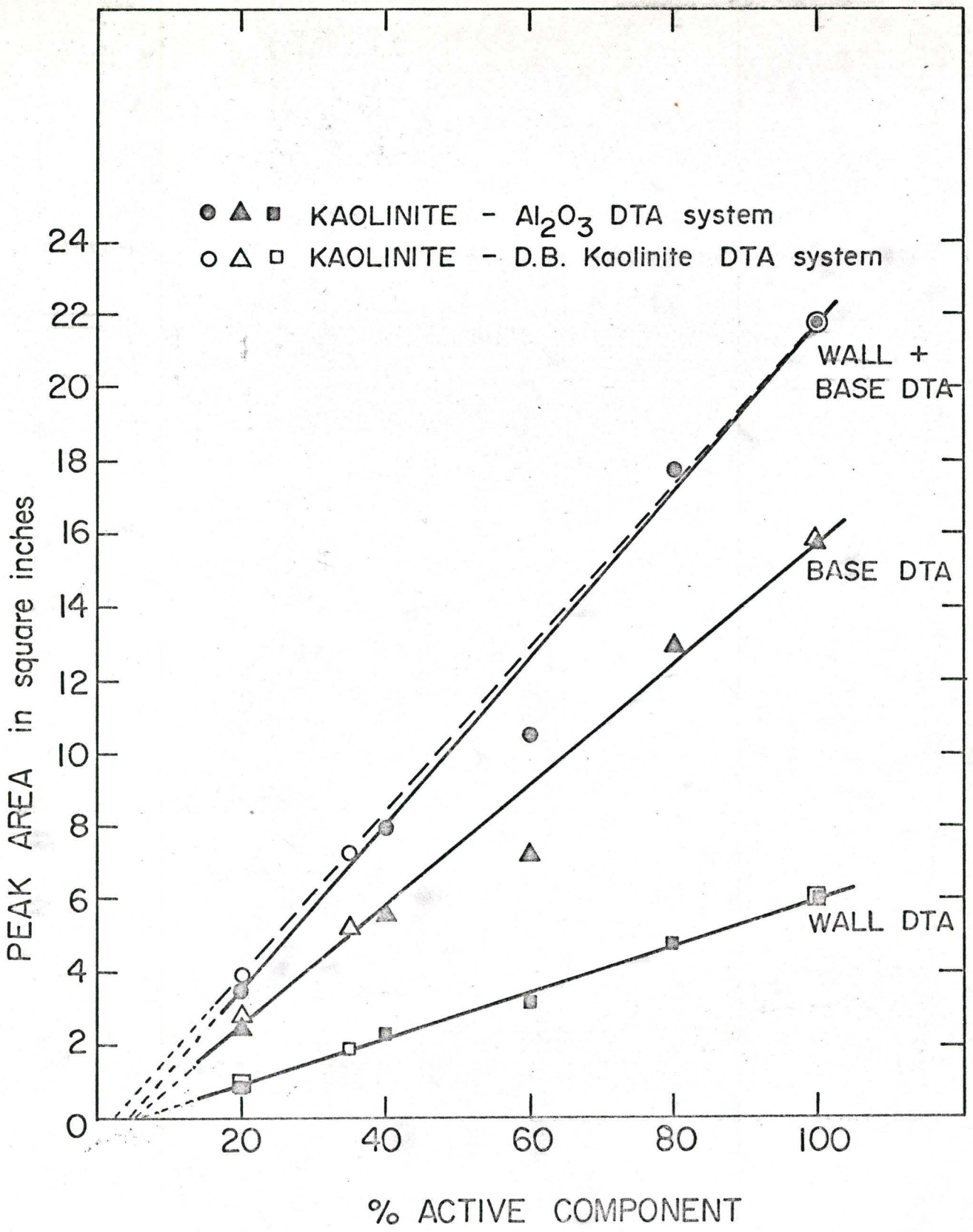

Figure III.11(a) Effect of Change of Reference and Dilutent Substance on Peak Area (Kaolin Endotherm)

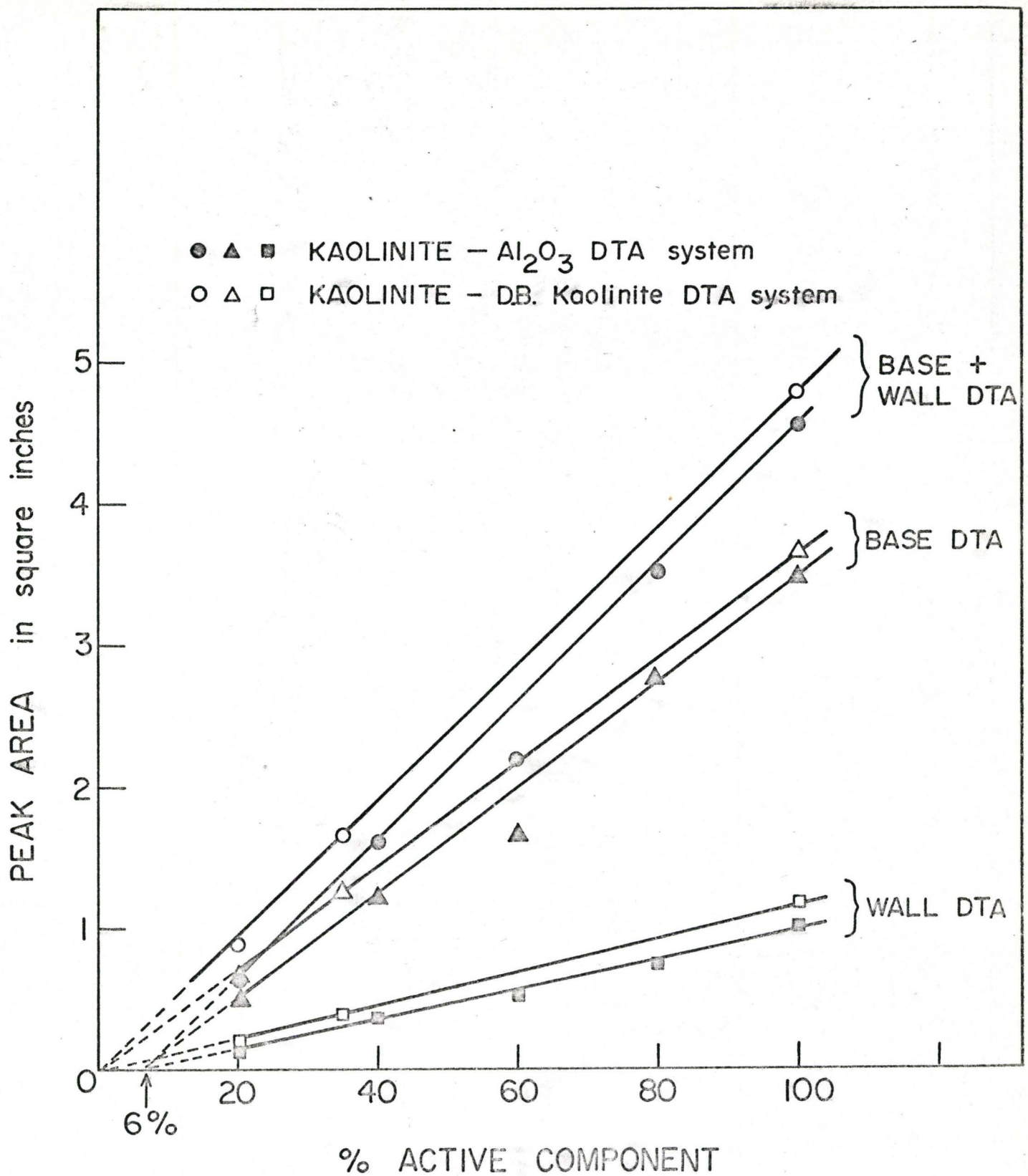

Figure III.11(b) Effect of Change of Reference and Dilutent Substance on Peak Area (Kaolinite Exotherm)

kaolinite-D.B. kaolinite DTA systems in the case of the kaolinite exotherm. In this case the nature of the dilutent appears to play a significant role. A non-zero intercept is again noted for the kaolinite-Al_2O_3 system but not for the kaolinite-D.B. kaolinite system in this case.

A careful study was made of the base line drift of the kaolinite base and wall DTA. The instruments were warmed up for a considerable time to eliminate electronic drifting and the measurements then taken. The drift was studied as a function of the degree of dilution and the reference substance and the results are tabulated in Table III.4

TABLE III.4

Results on Drift

DTA system	Drift measured in μV between 400 - 1000°C			
	Base DTA		Wall DTA	
% Dilution	60%	80%	60%	80%
Kaolinite-Al_2O_3	3	2.5	12	6
Kaolinite-D.B. kaolinite	0	0	7	4

III.2(d) Influence of the Cell Geometry

Kaolinite DTA's undertaken in designs 1 and 2 are shown in Figures III.12 through III.15. The same terminology has been used as in earlier figures. The heating rate in both the cases was the same, i.e., 2.06^{o}C/min and a 300 μV scale was used to record the differential temperature, except in Figure III.14 where 1 mV scale was used. Identical samples of 100% kaolinite were investigated in both DTA block designs. Alumina powder of the same size distribution (-160 + 200 mesh) was used as a reference and compacted to the same density in both investigations. Hence, except for the geometry, all operating parameters were maintained constant. The cell length to diameter ratios in design #1 and #2 were one and two respectively.

Figure III.12 and III.13 are the kaolinite endotherms and Figures III.14 and III.15 are the kaolinite exotherms for both designs.

The base and wall DTA areas for the two designs for the kaolinite endotherm and exotherm are recorded in Table III.5.

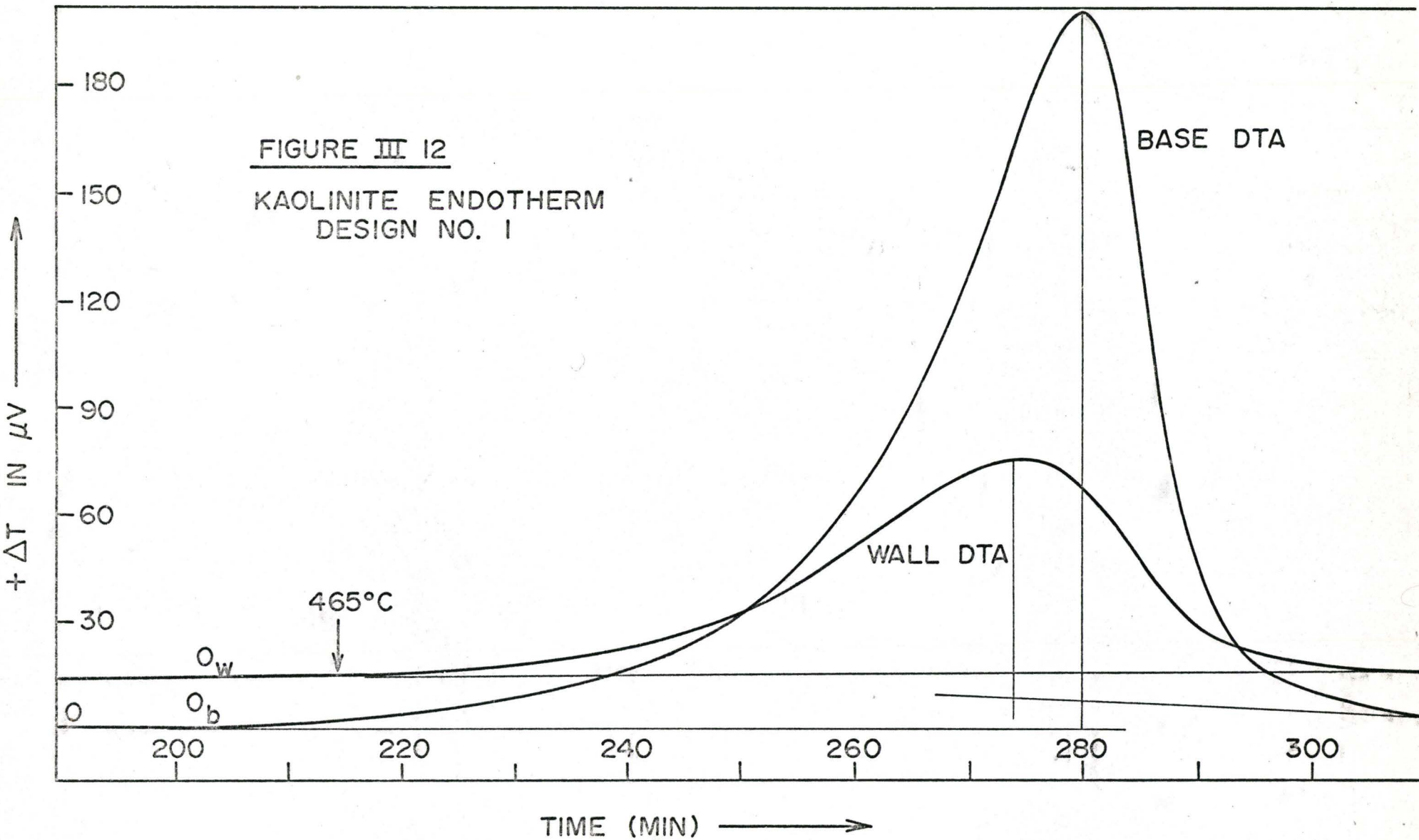
FIGURE III 12
KAOLINITE ENDOTHERM
DESIGN NO. 1
BASE DTA
WALL DTA
465°C
O_w
O_b
O
180
150
120
90
60
30
200
220
240
260
280
300
+ ΔT IN μV
TIME (MIN)

FIGURE III 13

KAOLINITE ENDOTHERM
DESIGN NO. 2

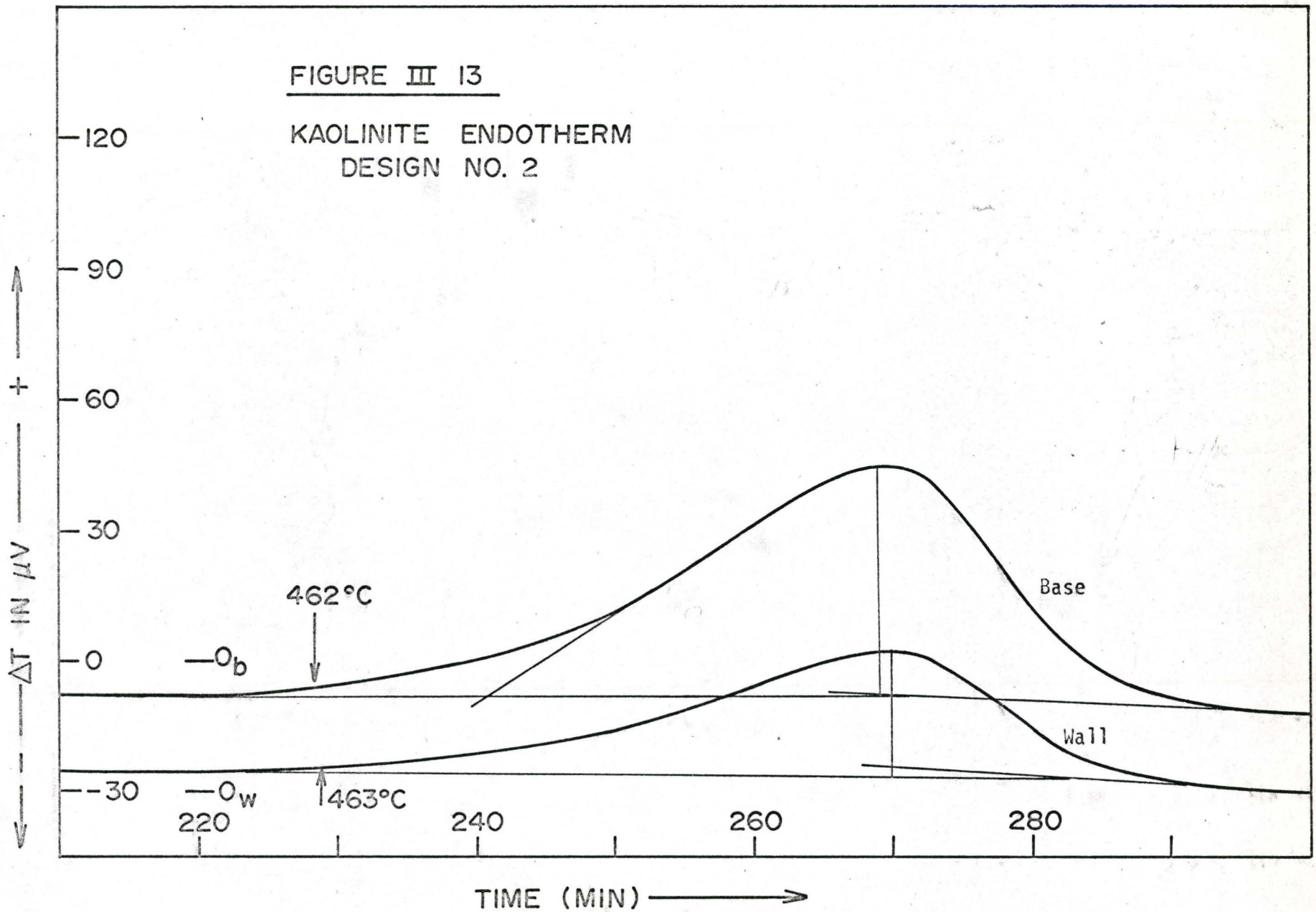

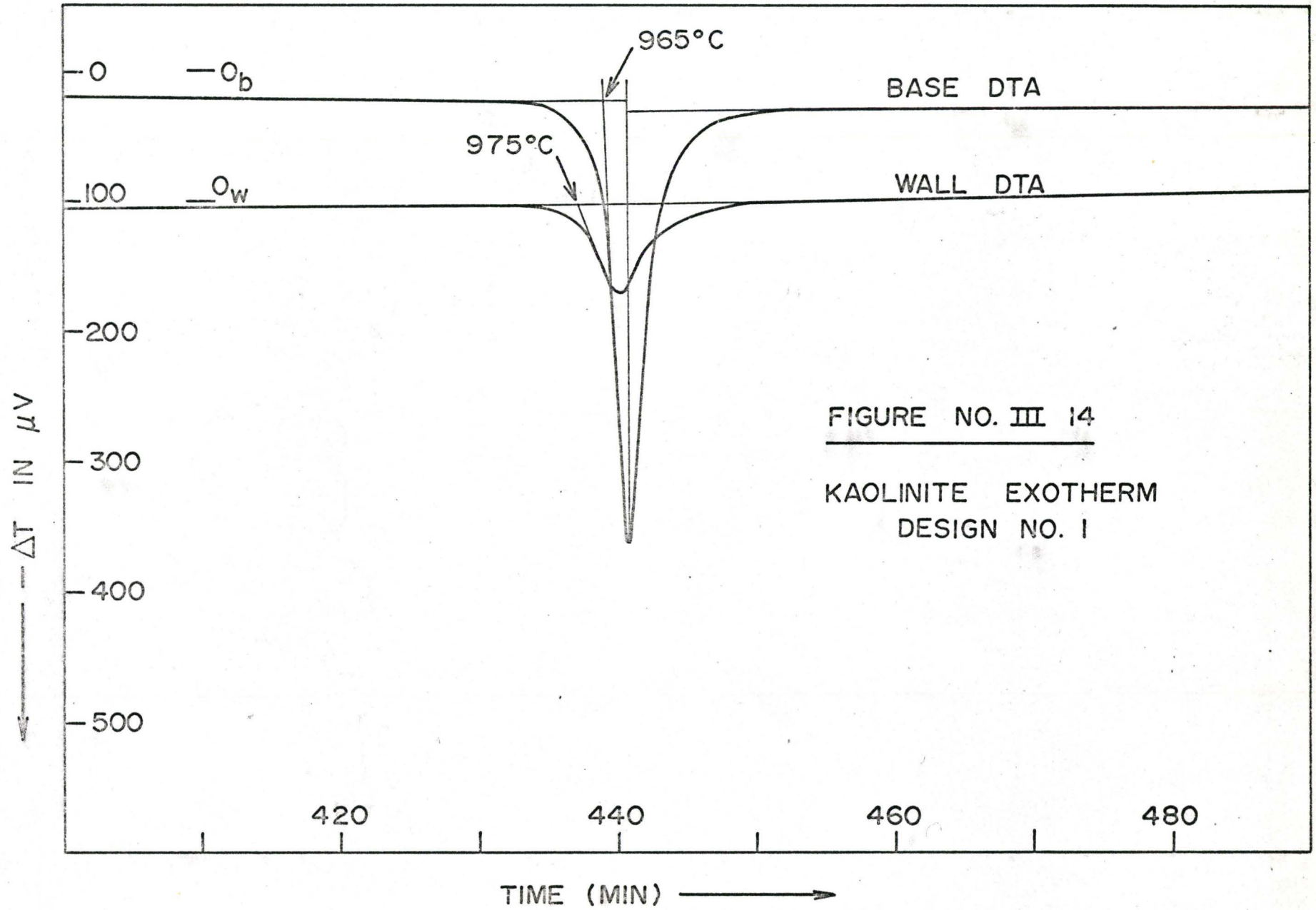

FIGURE NO. III 14

KAOLINITE EXOTHERM
DESIGN NO. 1

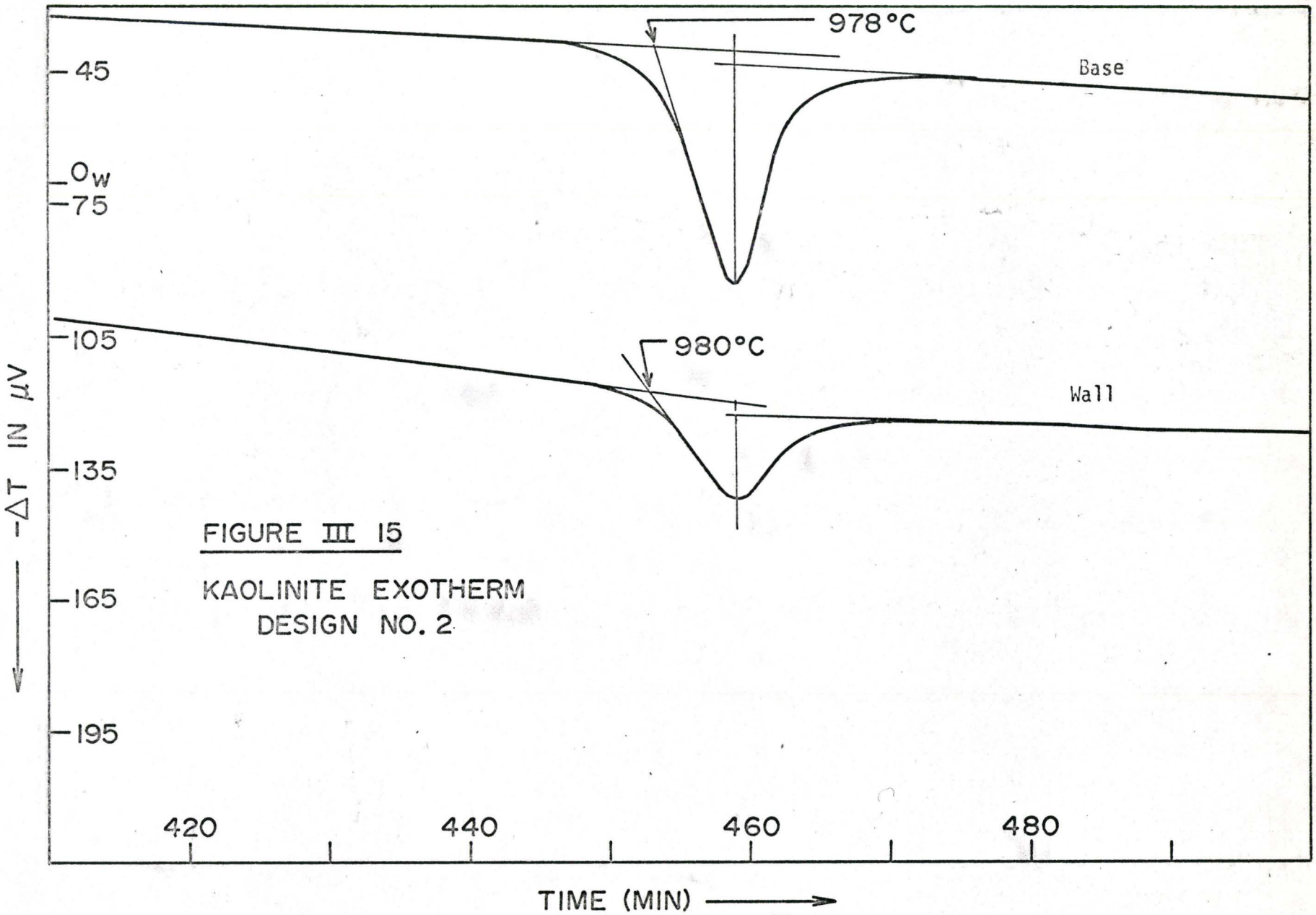

FIGURE III 15

KAOLINITE EXOTHERM
DESIGN NO. 2

TABLE III.5

Effect of Change of Cell Geometry on Peak Area

Kaolinite Endotherm			
Design Number		1 (L/D=1)	2 (L/D=2)
Mass of kaolinite in gms.		1.63	0.37145
	Base (b)	15.61	4.74
	Wall (w)	6.07	2.416
% Heat gained from DTA block (%w/w+b)		28%	34%
Kaolinite Exotherm			
Design Number		1	2
Mass of Kaolinite in gms.		1.63	0.37145
	Base (b)	3.6	1.12
	Wall (w)	1.164	0.484
% Heat lost to the DTA block (%w/w+b)		25%	30%

III.3 Comparison Between Modified DTA and Commercial DTA Equipment

To compare the performance of the experimental DTA with a commercial DTA, kaolinite and $SrCO_3$ thermograms were obtained on a Dupont 900 Thermal Analyser, employing a heating rate of $50^{o}C$/min. This rate is considerably higher than the experimental DTA heating rate of $2.06^{o}C$/min. Al_2O_3 powder was used as a reference material with undiluted samples.

The kaolinite DTA curves obtained in the commerical unit are reproduced in Figure III.16 and those of $SrCO_3$ in Figure III.17. The area under the differential temperature peaks for these investigations are listed in Table III.6.

FIGURE III 16

KAOLINITE DTA ON DUPONT THERMAL ANALYSER THERMOCOUPLE : Pt/Pt-13% Rh

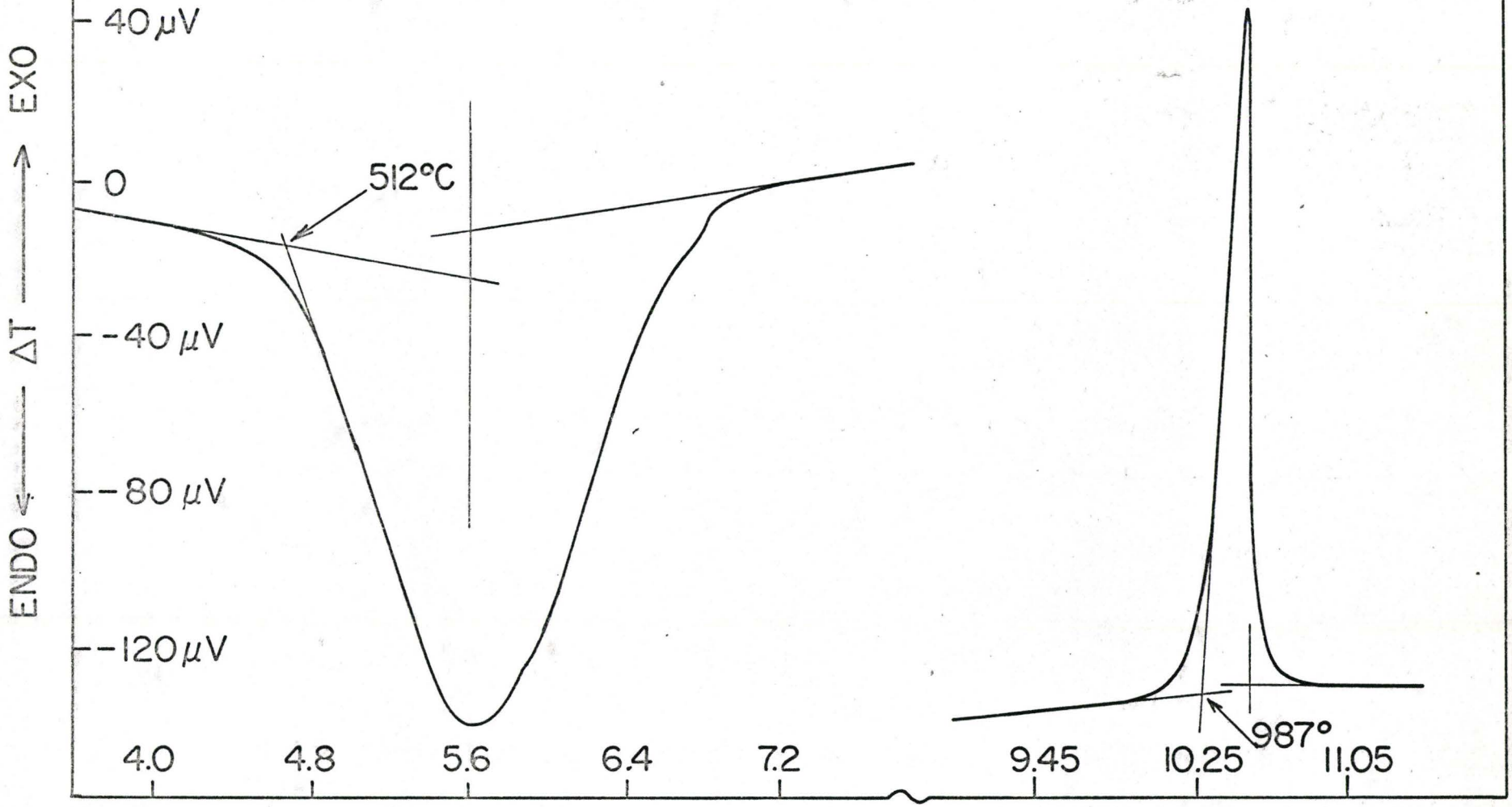

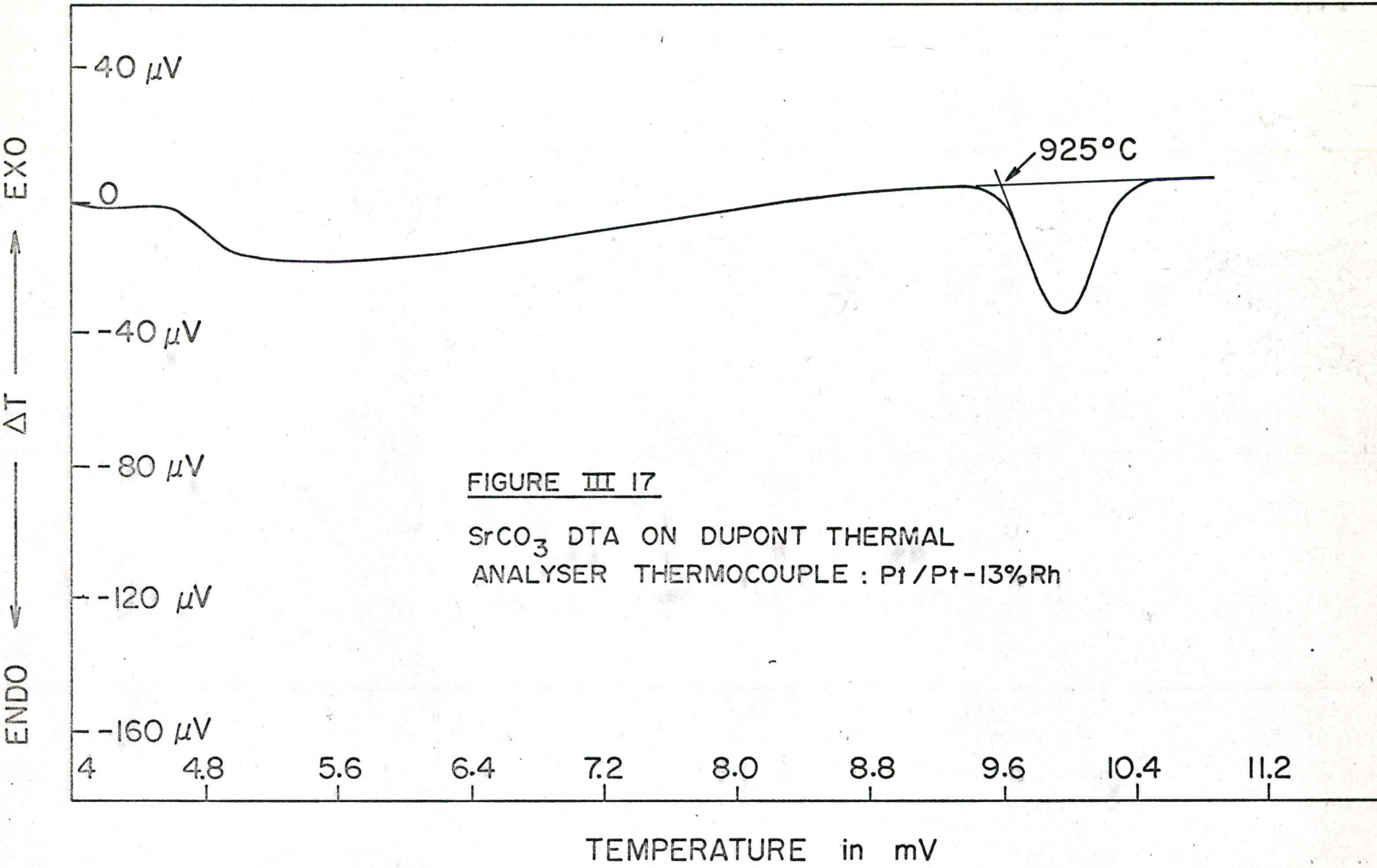

FIGURE III 17

$SrCO_3$ DTA ON DUPONT THERMAL ANALYSER THERMOCOUPLE : Pt / Pt-13%Rh

TABLE III.6

Dupont 900 Thermal Analyser Results

Substance	Mass in gms.	Peak area in Sq. In.
Kaolinite Endotherm	0.0385	4.75
Kaolinite Exotherm	0.0385	0.952
$SrCO_3$	0.0435	0.585

CHAPTER IV

DISCUSSION

IV.1 Thermal Conductivity Measurements

Heat transfer in a particulate medium is complex. The packed powder contains particles touching each other and interstitial voids. Heat transfer occurs between particles by conduction through point contacts, conduction and convection in the gas medium filling the pores and radiation between particles seeing each other directly. With increasing temperature, particularly beyond 500°C, radiation heat transfer and gas conduction predominate, for convection is minimal in a static gas phase and solid conduction is limited by the solid point contacts. Consequently, the heat transfer coefficient, or the effective powder thermal conductivity, should increase with increasing temperature, i.e., the temperature gradient across the medium should decrease with increasing temperature. A temperature gradient change would result if the gas filling the pores is changed. If such a gaseous species change is accompanied by a change from static to dynamic conditions of gas flow the influence of the temperature gradient will be even more marked. Such thermal gradients vs. temperature for alumina powders are shown in Figure IV.1[74].

In contrast to the orthodox ΔT behaviour as a function of increasing temperature, as in Figure IV.1, the thermal gradients across the DTA cells increase with increasing temperature (Figures III.1 to III.3). This behaviour

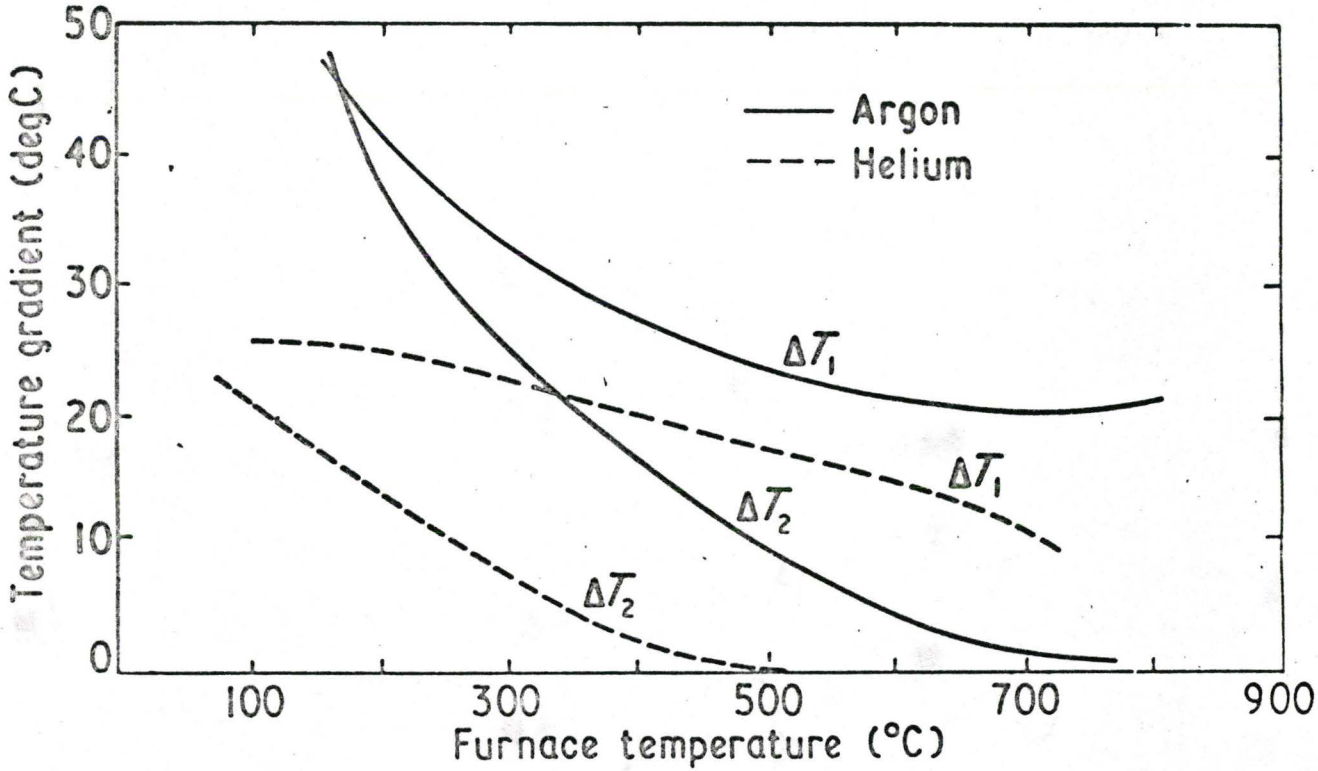

Figure IV.1 Thermal Gradients For Al_2O_3

is a result of the peculiar design of the DTA apparatus. The conventional relative thermal conductivity measurement apparatii make thermal gradient measurements across samples interposed between a heat source and a heat sink. All the heat is constrained to flow in the direction along which thermal gradients are being measured, by adequate thermal lagging. Furthermore, the heat sinks are infinite, or in other words the heat sink temperature is not perturbed from its normal value, no matter what quantity of heat is pumped into it.

In a DTA apparatus, on the other hand, under steady-state conditions, the heat arriving at the perifery of the DTA block (q) is split up into two parts. One part travels through the block, q_{block}, and the other part, q_{cell}, travels across the cell giving

$$q = q_{block} + q_{cell} \qquad (20)$$

The heat travelling across the cell, q_{cell}, sees as the only sink in the neighbourhood the thermocouple placed in the centre of the cell. This sink is however not infinite. The greater the heat supplied, the less efficient is this thermocouple sink and a consequent rise in the cell temperature gradient ensues.

An approximate calculation of the quantity of heat flowing into the block may be made from the furnace characteristic curve (Figure III.1(a).) A power of about 1.2 KW is necessary to maintain a furnace temperature of ~ 870°C. If approximately 70% of this travels to the work load in the furnace tube, then heat dissipated per inch of the 11-inch winding would be: $1.2 \times 10^3 \times .7/11$ watts/inch. If the DTA block is 1½" thick and the heat lost in heating the ambient atmosphere is 30%, then the approximate net heat arriving at the

perifery of the DTA block would be 80 watts or 19.1 cals/sec (q_{total}).

The heat conducted along the platinum thermocouple wires, when the temperature is at about 870°C, would be approximately

$$2 \times [\ \pi D^2/4 \times K_{pt} \times \Delta T/\ell\ ]$$

where D = thermocouple diameter (.008" x 2.54) cms

K_{pt} = platinum thermal conductivity = 0.21 cals/°K.cm.sec.

ΔT = 870 - room temperature (25) = 845°K

ℓ = length of thermocouples = 1 foot = (12 x 2.54) cms.

Substituting values, heat transferred along the thermocouple is 38.2×10^{-4} cals/sec.

Since this heat sink is finite and can only handle the above quantity of heat, only that quantity of heat will flow into the cell and it would be a reasonable assumption to take this quantity of heat as q_{cell}. The deficit between the q_{total} and q_{cell} travels to a sink via the DTA block. The pumping of more heat into the block may therefore increase the value of q_{cell} only marginally in comparison to q_{total}. The deficit would thus go to heat the block. Since the cell wall thermocouples measure the block temperature, they would register higher temperatures in comparison to the central thermocouple. This is a possible explanation of the observed DTA ΔT-T relationships.

This situation can be expressed by electrical analogues as in Figure IV.2. The upper figure represents the situation for the conventional thermal conductivity apparatus, and the lower for the DTA module. In both cases, heat reaches the work surface from the source across a resistor R_r (radiation/convection resistance to heat flow across the gaseous envelope around the DTA

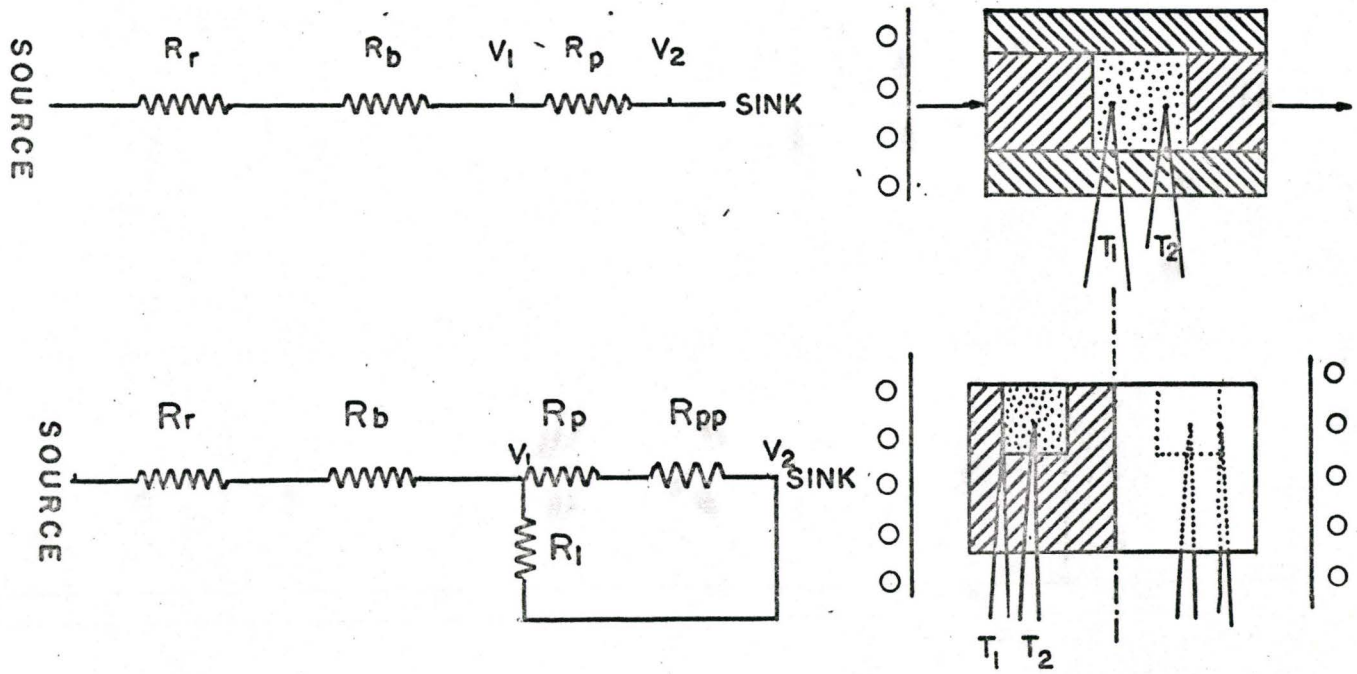

Figure IV.2 DTA Heat flow electrical analogue.

block). From this surface heat flows through the apparatus walls, the powder (R_p) and so into the sink. The two thermocouples therefore register temperatures T_1 and T_2 corresponding to potentials V_1 and V_2, i.e., their difference corresponds to the thermal drop across the powder sample. In the conventional apparatus, heat is constrained to flow in one direction (along the directions of the arrows) by thermal lagging and guard heaters, such that under steady state the heat input (q) is equal to the heat output. Thus, if q is known, the thermal conductivity can be calculated.

The DTA module is different, in that the wall thermocouple (T_1) corresponding to the voltage V_1, represents the surface, where the incoming heat q splits into two parts, q_{cell} and q_{block} (equation 20). The q_{block} heat factor is not constrained to flow in any specific direction (due to the design geometry). This resistance to heat flow may be lumped into a resistance R_1. Since the cell walls are platinum lined, it is reasonable to assume that heat will flow more quickly along the platinum foil than through the sample powder or the zirconia DTA block. Since all the surfaces within the cell are lined with platinum, and the centre thermocouple (T_2) is the one extending out to room temperature, it may be reasonable to assume that q_{cell} is constrained to exit via this thermocouple. The thermocouple wire dimensions limit the heat carrying capacity of this sink. This resistance to heat flow may be regarded as R_{pp}.

This limited sink generates pseudo-gradients across the DTA cells thereby rendering absolute thermal conductivity calculation based on steady-state analysis meaningless. However, given reproducible heat transfer conditions, relative thermal conductivity data may be obtained.

Figure III.1 indicates the reproducibility of the experimental conditions.

Figure III.2, in which steady state thermal gradients vs. isothermal furnace temperature in ^{o}C are plotted for live, semi-dead-burnt and dead burnt kaolinite with Al_2O_3 standard, indicates that Al_2O_3 powder has a higher thermal conductivity than kaolinite. Dead burnt, semi-dead-burnt and live kaolinite fall along the same curve and these powders sinter beyond 1050^{o}C. In the steady state condition, the semi-dead-burnt material does not show a marked difference in its thermal conductivity due to dehydroxylation or subsequent particle size reduction.

Figure III.3 shows that the thermal conductivity of montmorillonite is slightly lower than that of Al_2O_3. The dead burnt and the live materials have identical thermal conductivities.

It is evident therefore that the dead burnt material would be a better reference material with respect to the same live sample material. Such practice may reduce the base-line drift during DTA, so allowing more accurate location of the differential temperature peaks. More will be said on this matter when the dilution results are discussed.

The effect of heating rate on the thermal gradient across the sample cell as a function of the temperature of the furnace is shown in Figure III.4. During these tests the #2 design of DTA block was utilised. The general behaviour of increasing thermal gradients across the sample cell with increasing temperature conforms with observations in the previous experiments. This indicates that this type of behaviour is common to apparatii having a similar geometry. It is also apparent from this figure that imposition of higher heating rates increases the temperature drop across the cell. This is a logical extension of the limited-heat-sink hypothesis in that the imposition of the higher heating rate increases the q_{block} factor more rapidly than the

q_{cell} factor. In effect, therefore, increasing the heating rate produces the same result as decreasing the sample thermal conductivity.

Yagfarov[68] suggests an apparatus of essentially the same geometry (Figure I.4) as used in this investigation to measure thermal gradients and proposes that thermal conductivity (λ) values can be obtained directly from such measurements as a function of the heat rate (v). If this were the case, the thermal gradients across the DTA cells should decrease rather than increase with the heating rate imposition as he suggests that thermal conductivity is directly proportional to the heating rate. Yagfarov presents no experimental data to supplement his formulation.

IV.2a Heat Loss (ΔT), Type of Reactions

The plot shown in Figure III.5 demonstrates that a constant and reproducible heating rate was accurately maintained during the DTA runs. During the cooling cycle, the rate of cooling was controlled accurately until about 300°C.

Figures III.6 to III.9 are DTA's of different substances undergoing different types of reactions. These results clearly indicate that part of the reaction heat evolved or absorbed by the sample during a conventional DTA run is never sensed by the recording single differential thermocouple. At least two such thermocouples are required to record the temperature effect associated with the total reaction heat. In exothermic reactions (Figures III.6 and III.7) some of the reaction heat is transferred to the DTA block and is sensed by the differential thermocouple on the cell wall. During endothermic reactions (Figures III.8 and III.9) heat is absorbed from the DTA block as

well as from the sample and is also sensed in the cell wall differential couple. These results verify the hypothesis proposed in Section I.4d.

In Table III.1 the results obtained are summarised. The last column of the table expresses % (w/b+w) where b is the area under the base DTA and w is the area under the wall DTA. This ratio in effect expresses the percentage inefficiency of the single thermocouple system in detecting the entire heat effect. In quantitative DTA this ratio should ideally be constant for any type of reaction. If such were the case the calibration technique (eq. 18, pg. 19) could be applied with confidence to extract accurate heat effect values associated with unknown reactions. This ratio is not constant and this suggests that more care should be taken when utilising such calibrating techniques.

The last column of Table III.1 is reproduced below:

Sample Material	Reaction Type	% heat lost/gained from DTA block %(w/b+w)
$SrCO_3$	Endothermic (polymorphic change)	32.2
Kaolinite	Exotherm (crystallisation)	24.8
Kaolinite	Endotherm (dehydroxylation)	29.4
$CaCO_3$	Endotherm (decomposition)	39.1

The variation of %(w/b+w) with different types of reactions can be explained qualitatively by the following model shown in Figure IV.3.

Considering the heat flow in the DTA system before the occurrence of

a reaction in the sample and assume for the sake of argument that the temperature gradients in the block and samples are the same. As the sample is hottest at the cell wall periphery, a sample reaction would start at this location. A portion of the heat involved in an exothermic reaction will flow into the DTA block (w) and into the cell material (b). The progressive enthalpic contributions from the successive sample increments as the reaction front advances towards the cell centre determine the cumulative w and b recorded as peak areas by the cell wall and base differential thermocouples respectively. The quantities involved and the temperature peaks generated are shown schematically in Figure IV 3. From the geometry of the temperature profiles in the figure it can be seen that the base differential couples should sense more of the heat generated in an exothermic reaction than the wall couples.

The major heat source in the system is the furnace and the temperature gradient it imposes on the system is such as to limit the amount of sample reaction heat which flows into the DTA block during an exotherm. This is further limited by the progress of the reaction front towards the sample centre for the reaction heat source is moving away from the cell wall boundary. A larger portion of the evolved heat will thus be sensed by the base thermocouple. On the other hand, during an endothermic process the main source of heat is the DTA block (which is at a higher temperature than the sample). Even as the reaction front advances, the sample will gather more heat from its reacted component (and so from the block) than from its unreacted portion. Thus it might be expected that:

$$\underset{\text{(endothermic)}}{\%\,[w'/(b'+w')]} > \underset{\text{(exothermic)}}{\%\,[w/(b+w)]}\,.$$

The $SrCO_3$ polymorphic change endothermic enthalpy and the kaolinite exothermic enthalpy are numerically approximately equal and the postulated (w/w+b) ratio is observed (see table, pg. 58). This is also

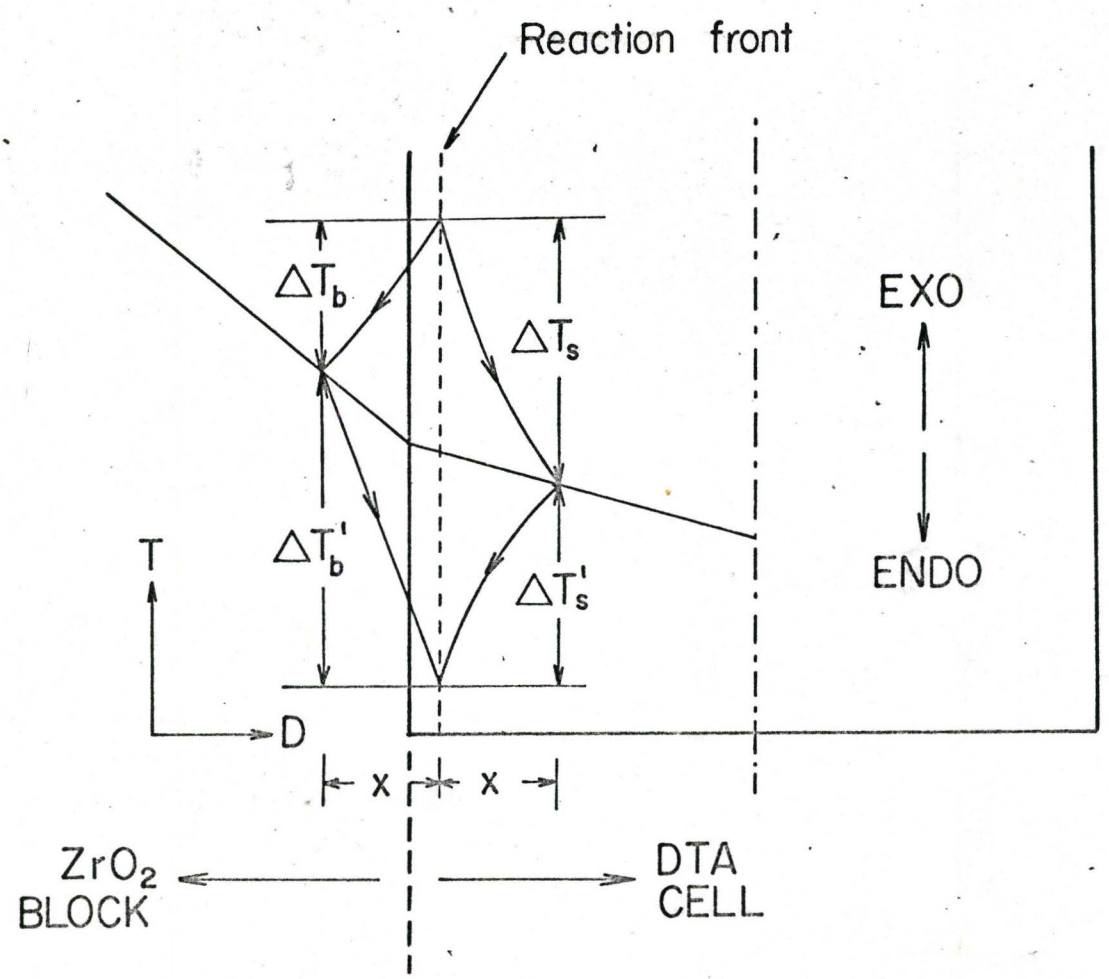

LEGEND

T	=	TEMPERATURE
D	=	DISTANCE
$W(\propto \Delta T_b)$	=	HEAT LOSS TO WALL
$B(\propto \Delta T_s)$	=	HEAT LOSS TO SAMPLE
$W'(\propto \Delta T_b')$	=	HEAT GAIN FROM WALL
$B'(\propto \Delta T_s')$	=	HEAT GAIN FROM SAMPLE

Figure IV.3 Endothermic and Exothermic Reaction Temperature Profile Development in a DTA System

true for the kaolinite endotherm and exotherm comparison although in this case other complicating factors associated with the gaseous evolution in the endotherm case could influence the issue.

The kinetics of the reaction can also influence the (w/w+b) ratio. The endothermic decomposition of $CaCO_3$ (Figure III.8) and the endothermic dehydroxylation of kaolinite (Figure III.9) involve similar enthalpies (39 and 40 kcals/mole respectively). In the carbonate case the reaction slowly builds up to a maximum and then ceases abruptly. The loss of water by kaolinite on the other hand terminates in a less abrupt fashion. In the carbonate decomposition therefore a large part of the required heat is quickly extracted from the DTA block giving:

$$\% \ (w/b+w)_{CaCO_3} > \% \ (w/b+w)_{kaolinite}$$

The evolution of a gas during a reaction will markedly influence the heat transfer characteristics in the sample. This is brought about in two ways, namely the gaseous-phase-conductivity change associated with the species change and the removal of heat from the system in the form of the evolved-gas heat content as it leaves the sample. Both of these processes result in a change in the temperature gradient across the cell and can therefore be considered in terms of the change of overall sample heat transfer coefficient. The relative contribution of the two processes can be tested by comparison of the measured heat transfer coefficients for given reacting systems at the same temperature and the calculated heat-content ratios for the two gases involved. The quantitative DTA relationships (equation 11, Chapter I) indicate that

$$\text{peak area } (A) = \frac{\Delta H . m}{gK}$$

and if A, ΔH, m and g are known then the heat transfer coefficient (K) values for the two reactions can be compared. In these studies two reactions were investigated involving the evolution of a gas, namely the decomposition of $CaCO_3$ (CO_2) and the dehydroxylation of kaolinite (H_2O). These two reactions occur in approximately the same range of temperature. Comparison of the K value ratios obtained and the heat content ratios for the two gases at these temperatures are shown in Table IV.1. To construct this table, the base peak areas and sample masses were measured, the geometric factor was assumed constant and corrections were made for the non-linearity of the thermocouple output (mVs) with temperature. The following literature enthalpy values were also assumed:

$$\Delta H\ (CaCO_3 \rightarrow CaO + CO_2) = 40.38 \text{ kcals/mole } (1000^{o}K)$$

$$\Delta H_{(\text{kaolinite} \rightarrow \text{metakaolin} + H_2O)} = 39.0 \text{ kcals/mole } (900^{o}K)$$

These results would tend to indicate that the change in heat transfer conditions in the reacting sample could in large measure be explained by the loss of the evolved gas and its heat content from the sample.

The influence of the evolved gaseous phase on the heat transfer characteristics in the DTA system is important when the calibration technique of quantitative DTA is used. The calibrant reaction should, if possible, evolve the same gaseous species as the unknown sample reaction of interest if a true calibration is to result.

TABLE IV.1

$\frac{K_{CaCO_3}}{K_{\text{kaolinite endotherm}}}$ (calculated)	1.35
$\frac{\text{Heat content of } CO_2 \ (1000^oK)}{\text{Heat content of } H_2O \ (900^oK)}$	1.34

IV.2(b) Heat Loss (ΔT); Degree of Dilution

The quantitative relationship between the DTA peak area and the mass

of active component suggests a linear relationship between these two variables. The results tabulated in Table III.2 and plotted in Figure III.10 confirm this prediction. As the slopes of the plots are equal to $\Delta H/gK$ and the value of ΔH and K for the two reactions differ, the two lines have different slopes.

It is interesting to note that these plots do not pass through the origin. More will be said on this point later in this section.

IV.2c Heat Losses (ΔT); Change of Reference Substance

The results in Section III.1 indicate that dead burnt kaolinite and kaolinite have the same heat transfer characteristics. The dead burnt material therefore should be used as the DTA reference material rather than Al_2O_3 powder say, when studying the action of heat on kaolinite by DTA.

The linear relationship between the peak areas and percentage active component is evident in Figures III.11a and III.11b. In Figure III.11a the wall, base and (base + wall) DTA results have been plotted for the kaolinite endothermic reaction with Al_2O_3 as reference and dilutent and dead burnt kaolinite as reference and dilutent. The two systems follow the same pattern and the plots do not pass through the origin. Thus for the kaolinite endotherm at least, the dead burnt kaolinite may not be a better reference material than Al_2O_3.

The results for the kaolinite exothermic reaction, however, show a difference between the dead burnt kaolinite-Al_2O_3 reference systems. Also, the (kaolinite-dead burnt kaolinite) plots pass through the origin. The curves for this system plot above those for the Al_2O_3 reference system, i.e.,

for the same mass of active component the peak areas are larger than those obtained in the Al_2O_3 system. This is consistent with the heat transfer characteristics of the two systems as discussed in Section III.

It is interesting to examine the intercept differences obtained in these dilutent systems keeping in mind the existence of the two heat transfer paths in the DTA system. This availability of alternate paths for heat flow in the DTA system means that modification of the heat transfer conditions for one path could lead to an increase in flow along the other paths. The two major variables influencing intercept results are the type of reaction (endo- or exothermic) and the dilutent material. As the plots in each case are linear with respect to the percentage of dilutent material the intercept value should be independent of this parameter. The results can be summarised as follows:

zero intercept - kaolinite-exotherm for the kaolinite/dead-burnt-kaolinite DTA system.

non-zero intercept - kaolinite endotherm for the kaolinite/dead-burnt-kaolinite and kaolinite/Al_2O_3 DTA system.

- kaolinite exotherm for kaolinite/Al_2O_3 DTA system.

Comparing the nature of the two reactions first, they differ three ways, i.e., one is endothermic and one exothermic, the enthalpy involved in the endothermic reaction is significantly greater and a gas is evolved during the endotherm and no gas produced during the exotherm. The non-origin intercept cases essentially indicate that mixtures containing 6% of active component or less do not produce a differential temperature peak associated with the reaction of this component. The nature of the enthalpic effect and its magnitude should not influence the origin intercept value. It can only be supposed that some modification of heat transfer conditions within the reacting diluted sample occurs associated with the reaction. This modifica-

tion is such as to maintain the temperature gradients within the dilute sample and inert reference sensibly equal, i.e.,

$$(dT/dx)_{sample} = (dT/dx)_{reference} \tag{21}$$

where T defines temperature and x is a distance parameter measured within the sample or reference. If for the sake of simplicity, the simple conductivity equation is assumed then the above relation means that:

$$(q/KA)_{sample} = (q/KA)_{reference} \tag{22}$$

where q is the energy input into each system, K the effective thermal conductivity and A the area across which the heat flows. Considering the energies involved in the two pertinent reactions, assuming the K-values remain constant, then for the endotherm

$$q_{sample} - q_{reaction} = q_{reference} \tag{23}$$

$$\text{i.e., } q_s > q_{ref}$$

and for the exotherm

$$q_{sample} + q_{reaction} = q_{reference} \tag{24}$$

$$\text{i.e., } q_s < q_{ref}$$

for the 6% active component to react unnoticed. For compatability between equation (22) and (23) and (24) it is necessary that

$$K_{sample} > K_{reference} \text{ for the endotherm}$$

and

$$K_{sample} < K_{reference} \text{ for the exotherm}$$

The endothermic "K" inequality could possibly be explained by the replacement of the air in the powder by the evolved water vapour and a possible increase in heat transfer coefficient. It should be pointed out that this will only apply to highly-diluted samples as the escape of water vapour from the system will upset the conditions dictated by equation 21.

The exothermic "K" inequality could be associated with the reduction of the effective thermal conductivity of Al_2O_3 by dilution with a lower thermal conductivity component, i.e., kaolinite. It is possible that the difference between the heat transfer characteristics of the inert reference (100% Al_2O_3) and the sample (94% Al_2O_3) could counteract the extra energy input when the 6% active component reacts. This explanation differs from the endothermic case in that the K inequality will exist throughout the whole DTA run whereas the gas release will be associated with the endothermic reaction only. The major influence of this difference is the possible association of base-line drift with the permanent "K" inequality. Such drift however should be continuous and therefore not mask a reaction differential temperature peak. It should be emphasised that no particular significance is attached to the intercept value of 6% reactive material but rather to the existence of a non-origin intercept in a system which should very definitely always exhibit one.

In summary therefore it is suggested that at high dilution levels the zero peak area observation for non-zero active material compositions may be the result of a trade off between the enthalpy

involved and the change in heat transfer conditions produced. The peak area is a function of both these variables according to

$$\text{peak area} \propto \frac{\Delta H}{K}$$

The availability of alternative heat flow paths and sinks in the system is very important as the energy involved however small must be transferred out of or into the sample in such a way as to avoid upsetting the heat transfer system being monitored. Another way of considering the phenomenon might in fact be with respect to the change in magnitude of the monitored heat pipe with respect to the alternative heat pipes in the system. In any event, the results indicate that choice of the wrong reference material or a gaseous atmosphere different from that produced during a reaction involving gas evolution could lead to an error of at least 6%.

With respect to the heat loss values measured on the wall differential couple, it can be seen by comparison of the last columns of Tables III.2 and III.3 the nature of the reference material did not significantly influence these results.

The data in Table III.4 compares the drift in μV in the 400 to 1000°C temperature range for the kaolinite thermograms with dead-burnt kaolinite and Al_2O_3 as reference materials respectively. As the level of dilution increases, the thermal properties of the sample approach those of the reference substance, thus reducing the drift. The drift on 80% diluted sample is less than that on 60% diluted sample. The drift is further reduced when dead burnt kaolinite is used as a reference and dilutant substance, indicating that the dead burnt material is a better reference material than Al_2O_3 for the differential thermal analysis of

kaolinite.

IV.2(d) The Geometric Factor

Results of Section III.2(d) indicate that reaction initiation temperatures as detected by both designs are essentially the same and for kinetically slow reactions (with large enthalpic effects such as the kaolinite endotherm,) it is difficult to detect the initiation temperature with confidence by the method outlined on page 36. The drift associated with design #2 is higher than that for design #1. As the second design is more sensitive (next section) it may be expected to respond more readily to differences in thermal diffusivities of the reference and sample materials in terms of drift.

Although the wall peak areas in the second design are smaller than the base peak areas as before, the peak area ratio, %(w/w+b) for the second design is higher. Table III.5 indicates the difference in %(w/w+b) for both designs for two different reactions. As the L/D ratio is increased, the wall thermocouple moves towards the central thermocouple and the wall platinum foil contacts more powder area/unit mass of sample. These facts will both increase the proportion of heat sensed by the wall thermocouple. This difference is reflected in higher values for %(w/w+b) for the second design with respect to the first.

IV.3 Quantitative Measurements

The commercial apparatus thermograms obtained for kaolinite and $SrCO_3$ are similar to those obtained in the experimental apparatus. The kaolinite endothermic peak appears symmetrical with a good deal of variation in the base line before and after the reaction. The kaolinite exotherm and the $SrCO_3$ endotherm also appear symmetrical (Figures III.16, III.17).

In Table IV.2 the sensitivities of the three DTA's, i.e., commercial, design # 1 and design # 2, for quantitative analysis are compared for the kaolinite reactions. Designs # 1 and # 2 use the same heating rate; that of the commercial unit was higher. Because of the higher L/D ratio in design # 2, larger areas/unit gm of kaolinite were obtained. The L/D ratio for the commercial apparatus is slightly lower than design # 2, but it employs a heating rate twenty-five times faster than the experimental DTA's. The influence of heating rate on peak areas is well known (equation 14, peak area is directly proportional to heating rate). The observed behaviour is in agreement with the literature.

Although accurate measurement of the effective conductivity prohibits the direct measurement of the reaction enthalpies, it would appear from the foregoing that, with sufficient precautions as to nature of calibration reaction and heat losses, accurate reaction heat measurements should be possible in a calibrated system. The inversion heat for the rhombic $\rightleftarrows$ trigonal transformation in $SrCO_3$ was measured on the experimental DTA and on the commercial apparatus, both of which had been calibrated with the kaolinite exotherm. Each estimation was performed four times and in each case the calibration and experimental runs were carried out in identical DTA systems.

TABLE IV.2

SENSITIVITIES OF DIFFERENT DTA's

Type of Reaction		DTA Sensitivity (area/gm of kaolinite in $^{o}C.sec/gms \times 10^{-3}$)		
		Design # 1	Design # 2	Dupont Commercial DTA
	Length/dia. ratio	1	2	1.5
Endotherm	Base	14.8	19.8	35.9
	(Base+Wall)	20.6	30.7	---
Exotherm	Base	3.0	4.1	7.2
	(Base+Wall)	4.0	5.9	---

TABLE IV.3

QUANTITATIVE ESTIMATION

(A) Calibrant: Kaolinite Exotherm
(B) Calibrant: Kaolinite Endotherm
(C) Calibrant: $CaCO_3$ Endotherm

Type of DTA	Heat Effect for $SrCO_3$ Rhombic $\rightleftarrows$ Trigonal Inversion (kcals/mole) ($\pm$ 5%)
Dupont thermal analyser (A)	2.83
Design #1 (this work) (A) Peak area: - central DTA	4.16
Design #1 (A) Peak area: - (central+wall) DTA	4.63
Literature values for $SrCO_3$ inversion	4.7
Design #1 (B) Peak area: - (central+wall) DTA	3.46
Design #1 (C) Peak area: - (central+wall) DTA	4.29

Neither reaction involves a gaseous product and both occur at roughly the same temperature (930°C and 975°C respectively). The results, together with the accepted literature value[75,76] are shown in Table IV.3. Also included in this table are the estimated enthalpies for the inversion based on the kaolinite and calcium carbonate endothermic reactions as calibrants. Both these results are for the double-thermocouple DTA design. The commercial apparatus utilised a much higher heating rate (50°C/minute) giving it a high sensitivity to the detection of changes but little quantitative accuracy. The accuracy of the double-differential thermococuple DTA technique is evident. These results also show the influence of the non-identity of the calibrant and investigated reaction types (the endothermic calibrant reactions involve gaseous evolution and occur at different temperatures) and the errors involved indicate the importance of the choice of the proper calibrant reaction.

IV.4 Comparison with Quantitative Measurements on Herold and Planje Type Apparatus

This type of DTA consists of two platinum cells interconnected by a platinum wire. On the outside of each cell a Pt-10% Rh wire is welded, such that the differential across these two wires and the wire connecting the two cells constitutes a differential thermocouple.

Honeybourne and Sewell are of the opinion that results obtained on such an apparatus will be independent of sample thermal conductivity. In this case, then, DTA peak area should yield better quantitative data and any calibrant reaction should be valid. The experimental wall-DTA has a similar geometry. Basing calculations on the $CaCO_3$ endotherm, quantitative heat effect values for the kaolinite endotherm, exotherm and $SrCO_3$ inversion were calculated and are presented in Table IV.4. The values so calculated do not agree with the literature data indicating that the sample and calibrant reactant thermal conductivities and nature of reactions cannot be ignored.

TABLE IV.4

QUANTITATIVE CALCULATIONS FOR HEROLD-PLANJE TYPE APPARATUS

Reaction	Literature Value	Herold and Planje apparatus results
Kaolinite endotherm	39.0 Kcals/mole	34.2
Kaolinite exotherm	9.1 Kcals/mole	5.75
$SrCO_3$ (inversion)	4.7 Kcals/mole	3.763

CHAPTER V

CONCLUSIONS AND SUGGESTIONS FOR FUTURE WORK

As a result of the investigations here reported the following conclusions can be made:

(1) Absolute thermal conductivity data cannot be measured in DTA apparatii as the very reason for their design (high sensitivity to small heat effects in terms of the associated temperature changes - a result of the utilisation of limited heat sinks) militates against thermal conductivity measurements which require infinite heat sinks.

(2) Relative effective thermal conductivity values as a function of temperature can be checked on a DTA apparatus. The results obtained indicate that values for alumina powder are greater than for kaolinite and the values for kaolinite, semi-dead burnt kaolinite and dead burnt kaolinite are sensibly equal. Results also indicated that the effective thermal conductivity values as a function of temperature for montmorillonite and alumina were the same. It can be concluded, based on these results, that the dead burnt material constitutes a better DTA reference than any other inert material.

(3) Dynamic relative thermal conductivity measurements made on the DTA apparatus indicate that increasing the heating rate is equivalent to decreasing the effective thermal conductivity of the system.

(4) It has been demonstrated that a substantial portion of the enthalpy produced in the reacting sample in a single thermocouple differential thermal analyser escapes detection and constitutes a major error in quantitative DTA estimations.

(5) The percentage heat loss associated with the escape of heat is not constant and varies with the type of reaction concerned, the reaction temperature and the reaction products. For valid results based on calibration techniques, therefore, the calibrant reaction should be physically identical to the reaction being investigated.

(6) Heat losses mentioned in the last two points can be substantially reduced by the incorporation of a second differential thermocouple in the DTA system and the assumption that the ΔT effects are additive. The relative proportions of the ΔT effects experienced by the "base" and "wall" thermocouples for endo- and exothermic reactions are explained by the geometry of the DTA system. This ratio is also influenced by the kinetics of the reaction involved and the gaseous species (if produced) evolved.

(7) As an evolved gas species leaves the reacting system it removes its heat content from the system. This energy removal influences temperature

gradients in the system and it is suggested that the effect can be treated as a drop in the heat transfer coefficient value in the reacting system. Some evidence suports this analogy in that the calculated effective conductivity ratios for two reactions involving different gas product species is similar to the ratio of the gas heat content values at the reaction temperatures.

(8) Certain dilution techniques appear to give valid results but care should be taken that the dilutant has the same effective thermal conductivity as the diluted species. It was shown that a possible 6% error can be introduced by diluting procedures and it is suggested with evidence, that these errors are associated with heat transfer conditions.

(9) The "base" and "wall" enthalpic effect ratio is influenced by the DTA cell geometry.

(10) It was demonstrated that the correctly calibrated double-couple DTA technique gave more accurate results than the correctly calibrated single-couple technique and the commercial apparatus.

(11) Neglect of the relative thermal conductivity and reaction natures of both sample and calibrant materials, as proposed in the Herold-Planje analysis leads to erroneous results.

Absolute quantitative thermal analysis requires precise knowledge of the sample thermal conductivity during any reaction. This thermal conductivity may be calculated from results obtained on apparatus such as shown in Figure V.1. This apparatus consists of an adequately supported test capsule with an internal heater around which the test sample powder is compacted. Two thermocouples are spot welded to the test capsule tubes and measure the thermal gradient across the test sample. The test capsule is surrounded with ZrO_2 powder held within a nickel tube over which a furnace has been wound. At any temperature the power within the small heater is so maintained that temperature-wise, thermocouple (2) reads higher than thermocouple (3). A knowledge of power input into the small heater and thermal drop across thermocouples (1) and (2) enables the powder effective thermal conductivity to be calculated under static conditions. The ZrO_2 powder effectively acts as a controlling heat sink between the two power sources. Such a heat flow control design was developed in the Nicholson-Fulrath differential calorimeter apparatus[74]. Similarly, by employing a uniform heating rate on the external booster furnace, dynamic effective thermal conductivity data could be gathered.

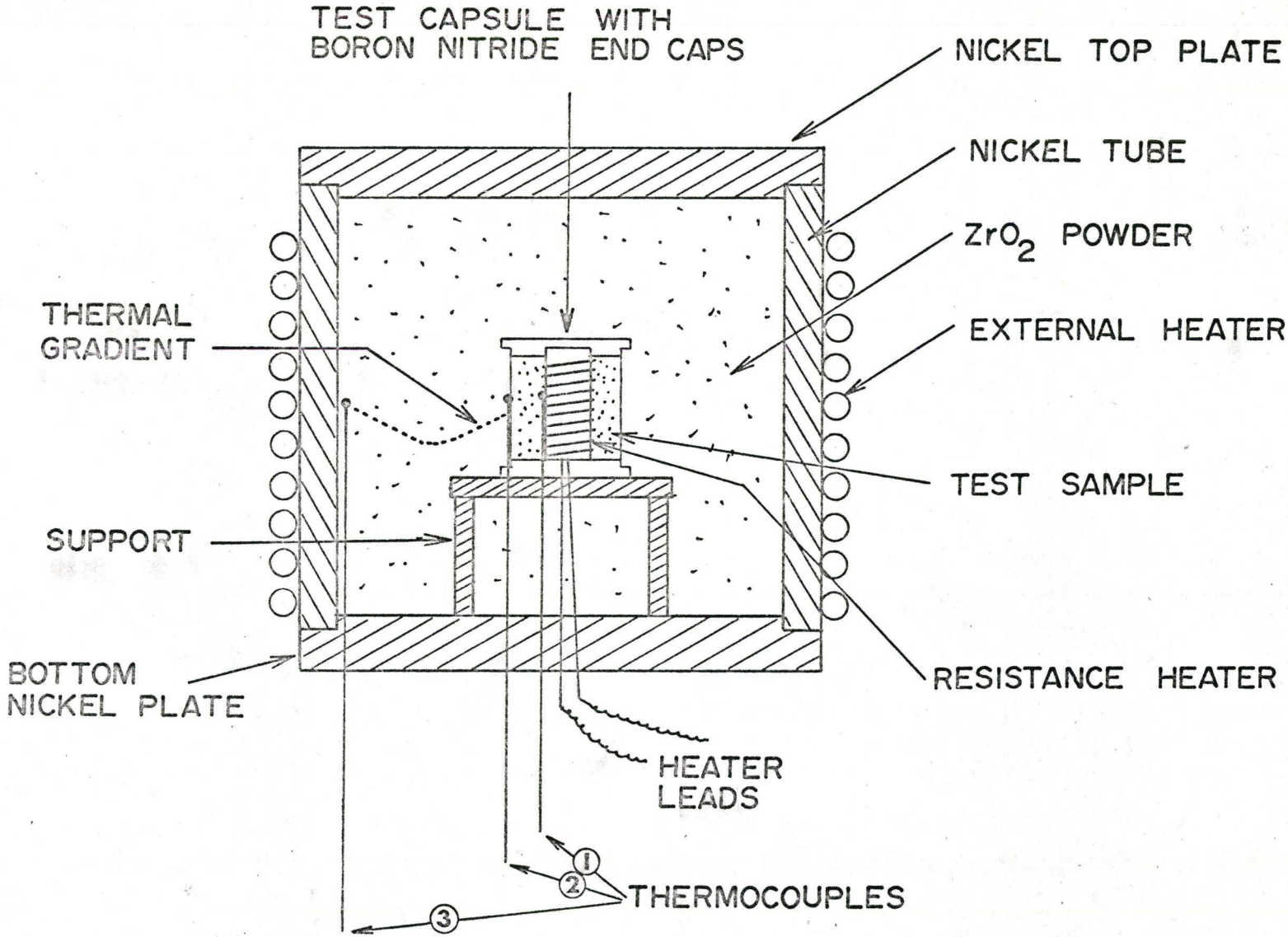

Figure V.1 Thermal Conductivity Measurement Apparatus

REFERENCES

1. T. J. Seebeck, Annln. Phys., 6 (1826) 130-148, 253-257.
2. A. C. Becquerel, Annln. Chin. Phys., 31 (1826) 371-392.
3. H. LeChatelier, C.r. hebd. Seanc. Acad. Sci., Paris, 102 (1886) 819-822.
4. W. Ramsay, J. Chem. Soc., 32 (1877) 395-399.
5. H. LeChatelier, C.r. hebd. Seanc. Acad. Sci., Paris, 104 (1887) 1443-1446.
6. W. C. Roberts-Austen, Proc. Instn. Mech. Engrs., (1899) 35-102.
7. N. S. Kurnakov, Zh. russk. fiz-khim., Obshch, 36 (1904) 841-856.
8. L. G. Berg, Izd. Akad. Nauk. SSSR, Moscow, "Vvedenie v Termografiyu" (Introduction to Thermal Analysis), (1961a).
9. F. C. Kracek, J. Phys. Chem., Ithaca, 33 (1929) 1286-1308.
10. F. H. Norton, J. Am. Ceram. Soc., "Analysis of High-Al_2O_3 Clays by the Thermal Method", 22 (1939) 54-68.
11. L. G. Berg, I. N. Lepeshkov and N. Y. Bodaleva, Dokl. Akad. Nauk SSSR, 31 (1941) 577-580.
12. S. Speil, Tech. Pap. Bur. Mines, Washington, No. 664 (1945) 1-37.
13. V. P. Ivanova, Zap. vses. miner. obshch., 90 (1961) 50-90.
14. R. C. MacKenzie and B. D. Mitchell, Analyst, Lond, "Effect of Soil Forming Factors on Clay Genesis", 87 (1962) 420-434.
15. R. C. MacKenzie, "'Scifax' Differential Thermal Analysis Data Index", First suppliment, MacMillan, Lond (1964).
16. Sadtler Research Labs, Inc., (1965), "DTA Reference Thermograms", Sadtler Research Labs, Inc., Philadelphia.
17. R. C. MacKenzie, "Differential Thermal Analysis", Vol. 1, Academic Press, London and New York (1970) 503.

18. B. Ke, "Application of Differential Thermal Analysis to High Polymers" in "Organic Analysis", Vol. IV (J. Mitchell, I.M. Kolthoff, E. S. Proskauer and A. Weissberger, eds.) Interscience, New York (1960) 361-93.

19. H. E. Kissinger and S. B. Newman, "Analytical Chemistry of Polymers, Part III", "Analysis of Molecular Structure and Chemical Groups", (G. M. Kline, ed.) Interscience, New York (1962) 159-179.

20. J. J. Keavney and E. C. Eberlin, "The Determination of Glass Transition Temperature by Differential Thermal Analysis", J. Applied Polymer Science, 3 (1960) 47-53.

21. B. Ke, "Characterization of Polyolefins by 'DTA'", J. Polymer Science, 62 (1960) 15-23.

22. R. C. Hontz, "Orlon Acrylic Fibre: Chemistry and Properties", Textile Res. J., 20 (1950) 786.

23. E. V. Thompson, "Dependence of the Glass-Transition Temperature of Poly (Methyl methacrylate) on Tacticity and Molecular Weight", J. of Polymer Science, Part A-12, 4 (1966) 199.

24. D. E. German, B. H. Clampitt and J. R. Galli, "Polymerization of Triallyl Cyanurate", J. Polymer Science, 38 (1959) 433-440.

25. P. H. Cless, D. H. Percival and R. R. Miron, J. Polymer Science, B2 (1964) 133-137.

26. F. W. Wilburn and C. V. Thomasson, "Application of Differential Thermal Analysis to the Study of Reactions Between Glass Making Materials, III. The Calcium Carbonate-Silica System", Phys. Chem. Glasses, 2 (1961) 126-131.

27. Taro Moriya, Terrio Sakaino, Hiroshi Saino, and Masacki Eudo, "Devitroceram of the System Mica-Spodumene", Yogy Kyokai Shi, 68 (1960) 44-49.

28. J. A. Hill, R. E. Rippere and C. B. Murphy, "Soldering Analysis of Soldering Flux Components", Insulation, Feb. (1963) 31-32.

29. W. A. Oates and D. D. Todd, "Kinetics of Reduction of Oxides", J. Australian Institute of Metals, 7 (1962) 109-114.

30. H. J. Dichtl, Berg-Huettenmaenn, Monatsh, 111 (1966) 430.

31. A. R. Spencer and W. M. Spurgeon, Paper 670081, Society of Automotive Engrs. Congr., Detroit, Mich., Jan. (1967) 9-13.

32. R. E. Grim and W. D. Johns, "Clay Minerals in the Northern Gulf of Mexico", Clays and Clay Minerals, Proc. 2nd National Conf., 1953, National Academy of Science - National Research Council Publication 327: 81-103 (1954).

33. R. R. West, "Solving Ceramic Problems with Differential Thermal Methods", 72 (37:14-16:42) (1958), Ceramic Abstr. 1961: 127.

34. V. S. Ramachandran and N. C. Majumdar, "Differential Thermal Analysis as Applied to Study of Thermal Efficiency of Kilns", J. Am. Ceram. Soc., 42 (1961) 96.

35. M. Kantzer, "The Glass Phase in Refractories", Silicates Ins., 23 (1958) 185-190, C.A. 52:20967.

36. W. J. Smothers and Y. Chang, "Handbook of Differential Thermal Analysis", Chemical Publishing Co., Inc., New York (1966), 177.

37. K. T. Greene, "Early Hydration Reactions of Portland Cement", Chemistry of Cement, Vol. 1, Proc. Fourth Int. Symposium, Washington D.C., 1960, National Bur. Stds., Monograph 43:359-85 (1962).

38. H. G. Midgley, "The Mineralogical Examination of Set Portland Cement", in "Chemistry of Cement, Vol. 1", Proc. Fourth Int. Symposium, Washington D.C., (1960), National Bur. Stds. Monograph 43:479-90 (1962).

39. P. G. Rivette and E. D. Besser, "Differential Thermal Analysis as a Research Tool in Characterizing New Propulsion Systems", U.S. Dept. of Com., Office. Tech. Serv., AD 264 748, 22 pp. (1961).

40. A. G. Keenan, "Differential Thermal Analysis of Thermal Decomposition of Ammonium Nitrate", J. Am. Chem. Soc., 77 (1955) 1379-80.

41. J. L. Eades and R. E. Grim, "Reactions of Hydrated Lime with Pure Clay Minerals in Soil Stabilization", Natl. Acad. Sci. - Natl. Research Council, Publication 771: (1960) 51-63.

42. S. K. Bhattacharyya and V. S. Ramchandran, "Differential Thermal Analysis of Catalyst Powders III. Differential Thermal Analysis of ZrO-Cr_2O_3 Mixtures", J. Sci. Ind. Research (India) 11B (1952) 550-551.

43. C. E. Locke and H. F. Rase, "Differential Thermal Analysis, Rapid Definition of Catalyst Characteristics", Ind. Eng. Chem., 52 (6) (1960) 515-516.

44. J. N. Stephens, Fuel. Lond., 42 (1963) 179-181.

45. S. Warne St. J., J. Inst. Fuel, 38 (1965) 207-217.

46. L. H. King and W. L. Whitehead, "Vacuum Differential Thermal Analysis of Coal", Econ. Geol., 50 (1955) 22-41.

47. J. L. Kulp, H. L. Volchock and H. D. Holland, "Age from Metamict Minerals", Am. Mineralogist, 37 (1952) 709-18.

48. Y. P. Castille and V. Stannett, J. Polym. Sci., Part A-1, 4 (1966) 2063-2079.

49. G. Hardy, K. Nyitrai, J. Varga, G. Kovacs, N. Fedorova, "Radiation Induced Solid State Polymerization", J. Polymerization", J. Polym. Sci., C4 (1964) 923-934.

50. C. B. Murphy and J. A. Hill, "Detection of Irradiation Effects by DTA", Nucleonics, 18 (1960) 78-79.

51. A. A. Krawetz, T. Tovnog, "DTA for Estimation of the Relative Thermal Stability of Lubricants", Ind. Eng. Chem. Prod. Res. Develop., 5 (1966) 191.

52. L. M. Brancone, H. J. Ferrari, "Application of DTA in the Examinations of Synthetic Organic Compounds", Microchem. J., 10 (1966) 370.

53. R. Reubke, J. A. Mollica Jr., J. Pharm. Sci., 57 (1967) 822.

54. B. D. Mitchell, A. C. Birnie and J. K. Syers, Analyst, 91 (1966) 783.

55. G. Liptay, M. Berenyi, L. Erdey, A. Babics, Orv. Hetilap, 107 (1966) 155.

56. L. Soule, "Quantitative Interpretation of Differential Thermal Analysis", J. Phys. Radium, 13 (1952) 516-520.

57. S. L. Boersma, "A Theory of Differential Thermal Analysis and New Methods of Measurement and Interpretation", J. Am. Ceram. Soc., 38 (1955) 281-284.

58. E. C. Sewell and D. B. Honeybourne, in "The Differential Thermal Investigation of Clays", R. C. Mackenzie, ed.) Mineralogical Society, London, (1957) 65-97.

59. L. G. Berg and V. P. Egunov, "Quantitative Thermal Analysis I", Journal of Thermal Analysis, 1 (1969) 5-13.

60. K. Nagasawa, "DTA Studies on the High-Low Inversion of Vein Quartz in Japan", Journal of Earth Sciences, 1 (1953) 156-176.

61. V. Kostoinaroff and M. Rey, Silic. Ind., 28 (1963) 9-17.

62. N. L. Silaktorskii and L. S. Arkhangelskaya (1958) in "Trudy Pyatogo Soveshchaniya po Ek sperimentalnoi i Tekhnicheskoi Mineralogii i Petrografii" (Transactions of the Fifth Confierence on Experimental and Technical Mineralogy and Petrography).

63. L. G. Berg and V. P. Egunov, "Quantitative Thermal Analysis III - Effect of Experimental Factors in Quantitative Analysis", J. Thermal Analysis, 2 (1970) 53-64.

64. M. J. Laubitz, "Thermal Conductivities of Powders", Cdn. J. of Physics, 37 (1959)

65. M. J. Vold, "Differential Thermal Analysis", Anal. Chern., 21 (1949) 683-688.

66. H. S. Carslaw and J. C. Jaeger, "Conduction of Heat in Solids", Clarendon Press, Oxford (1947) pp. 88 (4), 202 (7) and 203 (11).

67. P. Murray and D. White, "Kinetics of Clay and Dehydration", Clay Min. Bull. 2 (1955b) 255-264.

68. M. Sh. Yagfarov, "A New Method of Quantitative Thermography", Russian J. of Inorganic Chem., 6 (11) (1961) 1236-1237.

69. F. W. Wilburn, J. R. Hesford and J. R. Flower, Analyt. Chem., 40 (1968) 777-788.

70. G. deJosselin de Jong, "Verification of Use of Peak Area for Quantitative Differential Thermal Analysis", J. Am. Ceram. Soc., 40 (1957) 42-49.

71. R. Kronig and F. Snoodijk, "Determination of Heats of Transformation in Ceramic Materials", Appl. Sci. Research, A3 (1) (1951) 27-30.

72. P. G. Herold and T. J. Planje, "Modified DTA Apparatus", J. Amer. Cer. Soc., 31 (1948) 20-22.

73. P. S. Nicholson and R. M. Fulrath, "Differential Thermal Calorimetric Determination of the Thermodynamic Properties of Kaolinite", J. Amer. Ceram. Soc., 53 (1970) 237-240.

74. P. S. Nicholson and R. M. Fulrath, "The Design and Calibration of a High

Temperature Differential Thermal Calorimeter", 3 (1970) 351-355.

75. J. J. Lander, J. Amer. Chem. Soc., 73 (1951) 5794.

76. Metallurgical Thermochemistry by O. Kubaschewski, E. Evans and C. Alcock, Pergamon Press, 4th Edition (1967).